Manipulation and elucidation of intracellular signaling through periodic stimulation using microfluidics

by

Andreja Jovic

A dissertation submitted in partial fulfillment
of the requirements for the degree of
Doctor of Philosophy
(Biomedical Engineering)
in the University of Michigan
2010

Doctoral Committee:

Associate Professor Shuichi Takayama, Chair
Professor Jennifer J. Linderman
Professor Richard R. Neubig
Associate Professor Michael Mayer

Dedication

This dissertation is dedicated to my parents Srboljub and Natasha, my sister Aleksandra, my aunt Bojana, and my grandparents Radmila, Dragoslav, and Darinka.

Their love and encouragement have been an enlightening force that I am immensely grateful for, and have felt from my days as a baby to the present, even when great distances separated us.

Acknowledgements

With a great deal of gratitude, I would like to acknowledge my advisor Prof. Shuichi Takayama. Reflecting upon on my interactions with him, I realize that he possessed many admirable traits that guided and nurtured my growth both as a researcher and a person: enthusiasm, optimism, big-picture thinking, risk-taking, analytical thinking, and friendliness. Some of my favorite moments during these last five years came from discussions with Prof. Takayama, as I observed him deconstruct an idea and transform it into something grandiose. Not only were the resulting ideas awe-inspiring, but also the analytical process itself.

While I was not officially her student, I would like to acknowledge and profoundly thank Prof. Jennifer Linderman for her guidance and treating me as one of her own students. I always looked forward to meetings with her, not only because I always left her office feeling more assured of our ideas and approaches, but also because the discussions were so engaging and insightful. It was a pleasure interacting with someone who approached problems with such care and meticulousness. These traits of hers superbly complemented Prof. Takayama's and mine.

It was through Prof. Linderman's suggestion that I met Prof. Richard Neubig, whom I would like to gratefully acknowledge. His insight and attention to detail helped shape the projects presented here; Prof. Neubig kindly allowed me to use his lab facilities and equipment, oftentimes with thoughtful assistance from members of his lab (from whom I learned a great deal about biochemical techniques).

I would like to graciously acknowledge Prof. Mayer for his insight and the interesting "Biomembranes" class he taught during my first year of graduate school.

These four wonderful individuals comprised my Dissertation Committee, and were instrumental in guiding me through my graduate studies.

Lastly, I would like to acknowledge and deeply thank my friends, who led me to the realization that a person can feel at home anywhere, as long as he is surrounded by the right people.

Table of Contents

List of Figures

Figure

Abstract

Orchestration of cellular operations often requires faithful conversion of chemical signals from the environment into intracellular messages that cells must decipher with their internal protein machinery. Intracellular messages are conveyed by chemical messengers, such as calcium. Signals from the environment and chemical messengers are regularly frequency-encoded: biological information is stored in the periodicity, not just the amplitude, of signals. Despite the wealth of mathematical models available for predicting and interpreting the mechanisms mediating the conversion of extracellular signals into messenger signals, there is a paucity of experimental setups enabling manipulation and further elucidation of this crucial conversion process. These limitations were overcome by developing a microfluidic platform able to deliver periodic extracellular chemical signals to mammalian cells and amenable to real-time imaging of messenger signal dynamics.

While microfluidic-mediated periodic chemical stimulation afforded greater control over the timing of calcium messenger signals, compared to continuous chemical stimulation, fidelity was compromised; however, this deficiency was surmounted to a degree by modulating periodic stimulation parameters. These results provided concrete strategies for effectively manipulating intracellular calcium signals, using physiologically-relevant stimulant concentrations and periodicities. Our theoretical results predicted that small changes in cellular components could yield precipitous changes in calcium response fidelity, showing that fidelity can be highly sensitive to both stimulation and intrinsic parameters. By demonstrating experimentally that these cellular components can dramatically modulate the fidelity of intracellular signals, these studies provide insight into how the body achieves high fidelity control of signaling.

Compromised fidelity of intracellular signals, while potentially harmful, provided valuable insight into the chemical mechanisms mediating the conversion of extracellular

signals into calcium signals. limitations, nor predict the effects of altering periodic stimulation parameters on the calcium response fidelity. Simple revisions to model mechanisms were able to account for all our experimental results, demonstrating that this approach is powerful for evaluating models and elucidating signaling mechanisms. Collectively, this thesis research delineated that by theoretically and experimentally analyzing cells' abilities to convert periodic chemical signals into intracellular chemical messengers, manipulation and elucidation of cellular signaling mechanisms was achieved.

Chapter I.

Introduction

It is not only the magnitude of a chemical stimulus that determines cellular response; it is becoming increasingly clear that the timing of stimuli is very important as well. Currently there is a paucity of data regarding cell behavior under dynamic stimulation conditions that are representative of what occurs *in vivo*. This is, at least in part, attributed to the lack of appropriate tools for generating time-varying stimulatory signals in highly diverse patterns. Fluidics on the macro and micro scale has provided a practical platform for dynamically stimulating cells in a highly controllable manner at physiological and supra-physiological time scales (seconds to a few hours). These fluidic systems have contributed substantially to our understanding of how cells process and react to dynamic stimulatory environments.

The chemical environment of a cell is highly dynamic, as manifested in hormonal regulation and neuronal signaling (Brabant *et al,* 1992; Goldbeter 1996; Laurent 2002). In order to survive and prosper in such an environment a cell must be able to appropriately interpret these chemical cues and react accordingly (Goldbeter 2008; Knobil 1981a). While the magnitudes of these chemical stimuli provide important information to a cell, the temporal patterns of the stimuli are equally if not more significant for the orchestration and coordination of cellular processes (Knobil 1981a; Li and Goldbeter 1989). Information is stored in the frequency of the chemical signals, and cells utilize their external and internal machinery to aptly decode the meaning of these stimuli (Brabant *et al,* 1992; Goldbeter 1996, 2008; Schofl *et al,* 1994).

Aside from several canonical hormone cycles, however, relatively little is known about cellular responses under diverse patterns of chemical stimulation on physiological timescales (Brabant *et al,* 1992). With recent advances in chemistry and genetic engineering, there is a relative abundance of real-time readouts for assessing cellular

responses (Zhang *et al,* 2002) compared to the number of uses of such readouts in dynamic flow systems. A major limiting factor is the lack of technologies for generating well-controlled temporal patterns of chemical stimuli. Conventional techniques for assessing cellular responses under dynamic conditions are deficient in the diversity of chemical patterns that can be created, reproducibility, and potential for high-throughput. These techniques entail adding known amounts of chemicals to a culture of cells growing in culture dishes or on glass slides, effectively exposing cells only to step increases in stimulant concentration (Paliwal *et al,* 2008); this setup is straightforward, but is labor-intensive and not amenable to quick and reproducible stimulus patterns. Perfusion chambers represent a step up in terms of reproducibility, but lack versatility and scalability (King *et al,* 2008). Herein lies the opportunity to utilize microfluidic technologies to provide versatile and precise temporal controls in a robust and user-friendly format to enhance our understanding and control of biochemical timing and rhythm (Fig. I.1). Early macrofluidic setups for analyzing cellular responses under dynamic patterns of stimuli were used to assess the physiological role that pulsatile chemical patterns played in certain cellular systems, such as liver cells (Schofl *et al,* 1991; Schofl *et al,* 1993; Weigle *et al,* 1984) and lens tissue (Brewitt and Clark 1988). Once certain differences in cellular response were observed between dynamic and constant chemical stimulatory conditions (such as the quantity of glucose released, the amplitude and frequency of calcium transients, the induction of transparency in lens tissue) and real-time readouts improved, the focus shifted from the physiological relevance of these chemical pulses to the mechanisms by which the external and internal cellular machinery interpret temporal patterns. While these were bulky systems that consumed large quantities of reagent, macrofluidics provided a platform for making key observations of cellular and molecular responses (such as the levels of intracellular second messengers like calcium (Schofl *et al,* 1993), cAMP (Schofl *et al,* 1991), or Chloride (Verkman *et al,* 1992)) under dynamic conditions and motivated the development of microfluidic technologies for similar types of studies. The findings enabled by the macrofluidic technology portrayed that there were substantial reasons for analyzing biological systems in this manner: there were clear differences between pulsatile chemical delivery compared to continuous delivery on the whole cell level

[slime mold behavior (Robertson *et al,* 1972), bacterial movement (Block *et al,* 1982), glucose release (Weigle *et al,* 1983), lens tissue development (Brewitt and Clark 1988)] and the intracellular level [calcium levels (Schofl *et al,* 1993), cAMP levels (Schofl *et al,* 1991)]. These observations indicate that pulsatile delivery is potentially very physiologically relevant and can be used to probe cellular processing properties.

The advent of microfluidics has provided a platform that not only minimizes reagent and cell consumption, but also harnesses the physical properties of fluids on the micro and nano scale for creating highly controllable, repeatable, and versatile chemical patterns for cellular stimulation (Beebe *et al,* 2002; Melin and Quake 2007; Shim J *et al,* 2003; Whitesides *et al,* 2001); Whitesides *et al* (2001) provides a thorough overview of the application of soft-lithography for biology and biochemistry applications, as well as microfluidic device fabrication. These microfluidic setups, combined with mathematical and computer modeling, have resulted in key findings in terms of determining the architecture and dynamics of internal and external cellular machinery (Bennett *et al,* 2008; Hersen *et al,* 2008, Mettetal *et al,* 2008). In these most recent cases, yeast cells were used; platforms will need to be developed that can support more delicate and complex mammalian cells as well as real-time imaging and endpoint assessment of the state of their cellular machinery. In addition, microfluidic setups will need to be developed that have capabilities for high-throughput screening of the effects of versatile patterns of stimulation with frequencies over the range of seconds to hours, along with the ability to image in real-time. Ultimately, this is an exciting time for studying temporal dynamics on these time scales in cellular systems, because many read-outs are readily available, and also because microfluidic technology provides an ideal platform for regulating the timing of stimulation of cells (Fig. I.2). By providing an overview of the macrofluidic setups that led up to the development of current microfluidic setups (Fig. I.2), I show the importance and the impact that research with these systems has had on our understanding of temporal dynamics in cell biology.

I.1 Macrofluidics in Physiology

As early as 1972, researchers used fluidics to analyze temporal dynamics and control cellular behavior, providing the impetus for studying these crucial biological properties

(Fig. I.2). In this case the target system was slime mold (*Dictyostelium discoideum*) (Robertson *et al,* 1972); using well-controlled, external pulses of stimulant, Robertson and colleagues were able to control aggregation and migration of these cells. The discovery of its unique behavior in the face of rhythmic stimulation set off a wave of important theoretical analyses (Barkai and Leibler 2000; Li and Goldbeter 1992; Martiel and Goldbeter 1987; Novak and Tyson 1993; Tolic *et al,* 2000) and ushered further investigation into the rhythmic patterns of signaling in mammals (Brabant *et al,* 1992; Brewitt and Clark 1988; Dalkin *et al,* 1989; Knobil 1981b, Norstedt and Palmiter 1984; Steiner *et al,* 1982; Wildt *et al,* 1981). Just recently, a different form of slime mold was discovered to have "learning" capabilities when subjected to temporal patterns of temperature and humidity shocks (Saigusa *et al,* 2008).

In order to study the effects of temporal patterns of chemical stimulation on human cellular systems, researchers required setups that could reliably and repeatedly generate pulsatile patterns of chemical stimulation, while also providing an appropriate environment for cells. The first prominent example of the application of macrofluidics for the study of cell biology on mammalian cells was by Weigle and colleagues (1984), who developed a system for analyzing the effect of pulsatile and continuous application of glucagon on glucose production in packed beds containing liver cells. The setup consisted of two 10-cc plastic syringes clamped vertically with a 105 μm membrane at the bottom. Polyacrylimide gel beads were then deposited and allowed to settle, followed by liver cells. A peristaltic pump was used to deliver glucagon to the respective columns and integrated glucose production was assessed over a 90 minute period (continuous glucagon stimulation vs. 6 consecutive 3-minute pulses). It was found that liver cells had a significantly higher glucose production rate under pulsatile stimulation conditions versus continuous stimulation conditions over a physiological range of glucagon concentrations. This study illustrated early on that the timing of stimulation was very important in human cellular systems and demonstrated that fluidics coupled with end-point readouts (glucose) could be used to assess the cellular responses in an important physiological system. Liver cells, in particular, need a very specific environment to grow; microfluidics can provide proper microenvironments for cells, and can be custom made for particular cellular systems so that temporal dynamics can be properly assessed.

In a seminal study of lens development, Brewitt and Clark (1988) used a perfusion chamber to demonstrate that pulsed delivery of platelet derived growth factor (PDGF) led to the growth and transparency of lens tissue, whereas continuous administration of PDGF led to lens opacity, reduced protein content, and reduced weight.

Using a similar setup to that of Weigle *et al* (1984), Schofl and colleagues (1993) created a superfusion chamber to study the temporal dynamics of liver cells, but on the molecular scale. The authors analyzed how square-wave pulses of stimulation at different frequencies affected cellular calcium levels in real-time, using aequorin as a readout. Since cellular calcium controls a number of important cellular functions, it is critical to assess how it is regulated through external chemical stimulation. This study revealed many significant properties regarding receptor control of the amplitude and frequency of calcium spikes. Applying this type of analysis also allowed the researchers to extract important kinetic parameters (such as time constants associated with calcium amplitude and response lag time), which are valuable for mathematical and computer models used to recapitulate molecular pathways. Ultimately, this demonstrates that a straightforward setup can be implemented to analyze the dynamics of internal and external cellular machinery as well as cellular behavior.

Other seminal studies were conducted with the use of simple, programmable fluidic setups such as the previous examples. Dolmetsch *et al* (1998) discovered that the frequency of intracellular calcium signaling controlled the expression of certain genes in T cells. In this study, cells were exposed to different frequencies of square-wave pulses of extracellular calcium; the cells' calcium stores were emptied prior to experiments, thereby enabling the extracellular calcium concentration to dictate the intracellular concentration. While providing a great deal of control over the intracellular concentration in a population of cells, the technique bypasses the cells' natural machinery for calcium signaling. For this study, the temporal patterns were generated through the use of a computer-controlled solenoid valve that selectively pumped from two reservoirs (one containing calcium, the other a calcium chelator) (Fig. I.3). In order to assess gene expression, cells were collected and analyzed separately, in an endpoint manner. A slightly modified version of this setup was utilized to assess the effect of calcium patterns

on cellular pathways implicated in cellular growth and cancer (Ras and ERK signaling) (Kupzig *et al*, 2005). Again, in this case, pulses of calcium were applied to cells and endpoint measurements were taken of the activation state of the cellular pathway components. It was found that over a particular time-average calcium concentration, pulses of stimulation were more effective than continuous stimulation in inducing component activation. This was yet another example of a biological study in which a simple fluidic premise was employed to make a substantial biological finding.

These setups, while providing key biological findings, are a bit difficult to construct and are bulky, meaning that they expend a great deal of reagents. For example, studies using expensive growth factors and cytokines in a flowing system could cost thousands of dollars or more per experiment if not scaled down. Researchers would benefit from the development of microfluidic systems that could perform similar functions with less volume, are easy to setup, and also generate more elaborate patterns to provide further insight into cellular and molecular behaviors.

I.2 Microfluidic Setups

Recently developed microfluidic setups have overcome the limitations of the aforementioned macrofluidic setups by not only reducing the level of reagent consumption, but also by enhancing the breadth of stimulation patterns possible for probing of temporal dynamics in cells. To this end, Olofsson and colleagues (2005) developed a "chemical waveform synthesizer" (Fig. I.4). In this microfluidic system, single cells are held fixed above an open microfluidic chamber possessing multiple laminar flow streams containing various cellular stimulants. The individual cells are then dipped into the laminar flow streams, and a moveable x-y stage is then used to precisely and rapidly expose the cell to a new flow stream or to another area of the same flow stream (where the concentration of the stimulant in that flow stream is different). The result is one of the most versatile setups for stimulant pattern generation. Swift switching between streams and precise positioning result in exquisite temporal and spatial resolution for cellular studies. However, the method currently is limited to electrical activity readouts through the patch-clamping technique, which might preclude any real-time imaging capabilities. In addition, the patch-clamp technique is difficult to setup and

the method is amenable currently to the study of single cells, and in that regard is not high-throughput (Chiu and Orwar 2004). It may be possible, however, to combine this setup with that developed by Estes *et al* (2008) and others (Fertig *et al,* 2002; Huang *et al,* 2006; Pihl *et al,* 2005; Schmidt et al 2000) to facilitate patch-clamp analysis of a greater number of cells.

An elegant solution to the throughput limitations of the "chemical waveform synthesizer" was realized with the "flow-encoded switching" setup developed by King *et al* (2008) (Fig. I.5). This microfluidic system consisted of two inlets and columns of "experimental" channels, where cells were cultured and stimulated, and "gap" channels, which were positioned in between "experimental" channels in order to properly control the position of flow streams. Manipulation and variation of just one fluidic parameter (either ratio of inlet flow rates, or inlet pressure) resulted in generation of dynamic temporal patterns. This setup is very powerful not only in its fluidic simplicity, but also because it permits a user to test and observe multiple cellular stimulation conditions during one experimental run, on a single chip. These latter properties overcome some of the issues of throughput with microfluidic systems. In addition, the authors show how the setup can be multiplexed, to achieve control of more than one pattern generation parameter (duration, frequency, concentration, etc.). The "Flow-encoded switching" setup cannot create stimulation patterns as diverse as the "chemical waveform synthesizer" and experimental channels cannot be individually addressed. The setup is currently not optimized for rapid switching either; this issue cannot be simply settled by increasing inlet flow rates, because high shear stress levels can harm or detach cells (Lu *et al,* 2004) and can elicit certain cellular signals, like calcium (Ando *et al,* 1990); the previously mentioned microfluidic and macrofluidic examples did not take into consideration shear stress levels induced by fluid flow, despite its pertinence to cell viability and signaling.

Evaporation can pose a tremendous problem for microfluidic setups especially for long-term studies on cells because of harmful osmolality shifts, but the implementation of special membranes can ameliorate this (Heo *et al,* 2006). Cell viability can be further compromised by the presence of bubbles, which can also adversely affect flow streams in

microfluidic setups (Kang *et al,* 2007; Walker *et al,* 2004). Another potentially confounding factor is that cells secrete their own chemicals which can be taken up by their neighbors and influence their behavior; in the "flow-encoded switching" system, experimental channels have cells arranged in series, such that cells downstream can sense chemicals released by cells upstream, which may potentially result in different behaviors. In the study by King and colleagues (2008), the rat hepatoma cell line H35 was used, which is known to release the growth-inducing factor transferrin (Shapiro and Wagner 1989). Ultimately, this latter setup demonstrates great potential and portrays how microfluidic designs can be easily parallelized to enable more efficient investigation of the effects of dynamic chemical stimulation on cells. It also highlights some of the challenges and constraints encountered with developing such microfluidic platforms.

While these aforementioned microfluidic platforms exhibit great potential for biological investigations, the studies were mainly device design oriented. A trio of seminal studies emerged recently in which yeast cells were exposed to dynamic chemical stimulation patterns using microfluidic technology and the resulting behavior of the internal cellular machinery was compared with existing mathematical models, in order to elucidate the mechanisms of cell signaling regulation and to gather important kinetic parameters for these components.

I.3 Systems biology approaches to temporal dynamics

Hersen and colleagues (2008) developed a straightforward microfluidic setup for generating a fast switching microfluidic system for delivering osmotic shocks to yeast cells (Fig. I.6). Reminiscent of the previously mentioned macrofluidic setups, this system consisted of reservoirs with stimulant and neutral media; one could address cells with particular square wave patterns of various frequencies in a programmable manner. Using this setup, the authors monitored the fidelity of internal cellular signals to the frequency of square-wave osmotic shocks; it was found that the internal machinery responsible for controlling the osmo-adaptation response acted as a low-pass filter for this type of stimulation, since the real-time readouts used in this study showed an integrated response and vastly reduced oscillatory amplitude once the frequency of the shocks became too high. In this manner, the bandwidth of this cellular signaling system was deciphered,

thereby providing ranges for important kinetic parameters, such as the rate constants for phosphorylation, nuclear translocation, and deactivation of several HOG1 MAPK pathway components controlling cellular osmotic shock responses. The determination of such parameters serves to enhance mathematical and computer models of the behavior of internal cellular machinery. For this study, mathematical modeling was used to test the accuracy of the postulated network of cellular machinery architecture and make predictions about system behavior under certain altered conditions. This same setup and experimental procedure are potentially amenable to the analysis of other cellular machinery components as well.

The same signaling pathway was analyzed by Mettetal *et al* (2008); in this study, yeast cells were exposed to periodic stimulation at specific frequencies and stimulant concentrations, and the corresponding response amplitudes and phase shifts were captured. These pieces of information enabled the authors to treat the cell as a black box and develop an abstract model of the signaling pathway, which was then compared to what was previously known about the molecular machinery. Differences between the two models led to the discovery of negative feedback loops in the yeast osmo-adaptation response which acted over short and long time scales. Bennett and colleagues (2008) used a slightly more sophisticated setup to study yeast cell metabolic gene regulation under dynamic stimulation conditions (Fig. I.7). Applying mathematical modeling and microfluidics, these researchers discovered previously unreported properties of the internal cellular machinery that regulates metabolic inputs in yeast. This discovery was made upon the observation that their mathematical model of the molecular machinery dynamics did not correspond with their experimental data. Further characterizations of the molecular machinery were made by using a mutant strain of yeast and comparing its behavior to that of normal yeast; interestingly, it was found that under dynamically changing conditions, these cells responded similarly, despite their differing responses under static conditions. This finding implied that the molecular machinery in yeast had evolved "universally" to adapt to fluctuating environments.

These three studies exemplify an important, emerging approach for biological analysis, involving the union of microfluidics, real-time imaging of biochemical cellular responses,

and mathematical and computer modeling, rooted in well-established engineering concepts. The essence of this experimental approach is captured through precise, reproducible delivery of well-controlled patterns of stimulation to cells, real-time imaging of cellular responses, and effectively recapitulating these stimulation patterns in a mathematical model to see how the *in vitro* and *in silico* models compare. Discrepancies reveal missing components in the mathematical model architecture or might be indicative of suspect parameters or mechanisms, all of which can be potentially resolved with microfluidic technology through dynamic probing with different patterns of stimulation (Ingolia and Weissman 2008). The next generation of microfluidic setups for this type of analysis and other applications will need to be optimized for mammalian cells, high-throughput capabilities, and fast-switching, versatile stimulation patterns.

The three aforementioned examples used yeast cells as their model system; these cells are less complex in terms of their signaling pathways and upkeep. Several microfluidic setups have been developed that have taken advantage of this. With their microfluidic setup, Groisman *et al* (2005) demonstrated that bacterial and yeast cells could be grown to high densities under chemostatic and thermostatic conditions from single cells, a feat that is very challenging to achieve using conventional techniques. The authors monitored colony growth from a single cell and analyzed the effect of the addition of an auto-inducer upon the growth response. Repeated transient exposure to exogenous chemical signals was possible with the microfluidic device, however, these temporal dynamics were not explored in this work. Using a similar microfluidic setup, Balaban *et al* (2004) used the system to identify two types of bacterial "persister" types upon transient exposure to antibiotics, a seminal finding and one that would have been difficult to achieve otherwise since single cell analysis is not amenable with conventional lab techniques as opposed to microfluidics. While these two microfluidic setups had a highly flexible design allowing for easy control of colony growth and development, they were optimized for yeast and bacterial cell culture and not mammalian cell culture. Mammalian cells are generally more delicate and challenging to culture compared to yeast and bacteria. Use of non-standard culture surfaces such as PDMS in microfluidic devices as well as changes in volume and flow can significantly add to these challenges, especially cell seeding and long term-culture (Mehta *et al,* 2007; Walker *et al,* 2004). To

this end, Gomez-Sjoberg and colleagues (2007) developed a PDMS-based high-throughput, automated microfluidic cell culture system capable of long-term growth and analysis of mammalian cells (up to several weeks). In this work, transient stimulation exposures (hours to days) were applied in order to observe the effect on cell growth, differentiation, and motility; using human primary mesenchymal stem cells (hMSCs), the authors demonstrated that 96 hours of stimulation with differentiation media was the minimum amount of time needed for cells to differentiate to an osteogenic lineage with their setup; in addition, it was shown that hMSCs stimulated continuously for 9 days with differentiation media exhibited reduced motility compared to previously unstimulated cells when the two groups were incubated with differentiation media after more than 18 hours. Despite the many attractive features this microfluidic setup has for analysis of temporal dynamics in cellular systems, such as full automation of stimulation schedules, high-throughput capabilities, and time-lapse microscopic imaging, there exist several key drawbacks. One major limitation is that it is extremely difficult to fabricate and setup, compared for instance to the "flow-encoded switching" system. While the combination of the fluidic inputs and a multiplexer conveniently facilitated the formulation of individual media compositions that could individually address each of the 96 cell culture chambers, unlike the "flow-encoded switching" setup, the scheme is not very user-friendly or portable. With the flow rate used in this study, the shear stress level was noted to be an order of magnitude smaller than the minimum level required to perturb differentiation or proliferation for the cells used in their study (Kreke *et al,* 2004; Riddle *et al,* 2005), comparable to the shear stress levels used in the "flow-encoded switching" setup; as suggested by King *et al* (2008), to achieve faster media switching through increased flow rates without significantly augmenting shear stress levels, cells could be placed in recessed wells. Even with this design improvement to the setup, the versatility of stimulation patterns that can be generated with the system developed by Gomez-Sjoberg *et al* (2007) is not at the level of the "chemical waveform synthesizer". This setup however portrays that long-term mammalian cell culture is achievable in microfluidic devices in an automated, high-throughput manner. Other setups which have achieved long-term mammalian cell culture include the portable, handheld recirculation system developed by Futai and colleagues (2006), the "airway epithelia on a chip" by Huh *et al*

(2007), "differentiation on a chip" by Tourovskala *et al,* (2005), and the continuous perfusion setup developed by Hung *et al,* (2005).

There exists a great opportunity to analyze mammalian cells under dynamic stimulation so that cellular processing mechanisms can be better understood on a signal pathway level and eventually cellular behavior can be better understood and controlled on a systems or organ level. The caveat is that mammalian cellular processing is generally more complex than that of yeast and this means that more intricate techniques for analysis will be necessitated for analysis (Ingolia and Weissman 2008; Paliwal *et al,* 2008). This potentially means that more complex patterns of stimulation will be necessitated, compared to the sinusoidal or square-wave patterns used in the aforementioned yeast cell studies. In a physiological context, it has already been demonstrated that when certain rhythmic chemical patterns are disrupted in the body, it leads to pathological conditions (Brabant *et al,* 1992; Gambacciani *et al,* 1987; Van Couter and Refetoff 1985). This provides further motivation for investigating temporal dynamics with mammalian cells, in addition to getting a better grasp of how more complex pathways process dynamic chemical information.

I.4 Mathematical modeling of cellular signaling

In order to effectively predict and interpret biological results, the implementation of mathematical models is necessary. Early mathematical models were developed to predict and understand everything from microbial cell growth (Monod 1942) to predator-prey dynamics (Lotka 1925; Volterra 1926). These seminal theoretical studies laid the foundation for the emergence of mathematical biology, and later the advent of synthetic (Benner and Sismour 2005) and systems biology (Kitano 2002). For the two latter fields, there exist a variety of methods for analyzing signal transduction pathways and gene dynamics: differential equations, fuzzy logic, Bayesian networks, and principle component analysis (listed in order from highly specific to abstract). The choice of modeling approach is ultimately determined by several factors, including the type of experimental information available (quantitative, qualitative), how much is known about the interactions between cellular components (mechanisms, kinetic parameters), and what are the goals of the study. As a result of the relative abundance of mechanistic insight,

availability of kinetic parameters, and desire to capture temporal dynamics of individual cellular reactions, ordinary differential equations (ODEs) are frequently used for mathematical models of signal transduction pathways (King *et al,* 2005). Upon solving these ODEs, the dynamics of cellular components can be tracked over time.

A signal transduction pathway that has garnered immense attention in terms of mathematical modeling studies is intracellular calcium signaling, due in part to the discovery of calcium oscillations upon chemical stimulation of cells (Jacob *et al,* 1988; Prentki *et al,* 1988; Woods *et al,* 1986). Another key observation of this dynamic behavior was that the amplitude of the calcium oscillations did not drastically change upon increasing or decreasing the strength of chemical stimulant; it was the frequency of the oscillations that changed for the most part (Cuthbertson and Chay 1991). These observations, along with culling of relevant kinetic parameters, led to the development of several types of oscillatory calcium models, whose mechanisms differ in terms of how oscillations are generated. For the "receptor-controlled" mechanism, calcium oscillations are generated by negative feedback upon receptor or G-protein activation initiated by calcium or calcium precursors (such as IP3 or diacylglycerol) (Chay *et al,* 1995; Cuthbertson and Chay 1991). The other mechanism entails feedback between IP3, Ca2+, and the IP3 receptor (Sneyd 2005) to generate calcium oscillations. For this thesis research, two representative mathematical models of calcium oscillations of each mechanistic type were chosen for making predictions and evaluation, one by Chay et al. (1995), the other by Politi et al (2006).

One instrumental factor that has spurred further development of mathematical modeling of cellular signaling has been the advancements made in real-time imaging of signaling systems. For Ca2+ signaling, dynamics of single cells could be monitored using aequorin (Blinks *et al,* 1982), later Fura-2 (Grynkiewicz *et al,* 1985), and still later YC3.60 (Nagai *et al,* 2004). Monitoring individual cellular signaling dynamics is essential, as demonstrated by the case of the tumor suppressor protein p53 (Lahav *et al,* 2004). Ultimately, the advancement of mathematical modeling of cellular signaling is intimately linked with advancements made in imaging of the same phenomenon.

I.5 Imaging

In order to assess temporal dynamics in cellular systems, appropriate readouts are needed. Compared to the degree to which they are utilized in microfluidic systems, there is a relative abundance of real-time fluorescent readouts that exist for tracking the localization, translocation, appearance, or degradation of target proteins. This development is a consequence of the ability to fuse Green Fluorescent Protein (GFP) (or variants of GFP) to proteins of interest and genetically encode these in cells (Zhang *et al,* 2002). These types of readouts were implemented in the works by Bennett *et al* (2008), Hersen *et al* (2008), and Mettetal *et al* (2008), and represent passive applications of these fluorescent constructs. In their microfluidic setup, King *et al* (2007) created a high-throughput "gene expression living cell array", which employed fluorescently tagged transcription reporters to capture levels of gene expression in real-time under chemical stimulation. These indicators cells are useful for evaluating longer term responses of cells on the timescale of expression and degradation of fluorescent proteins (many hours to days). However, in order to advance our understanding of temporal dynamics in cells and capture key dynamic intracellular parameters on the seconds to hours scale, such as biochemical messenger concentrations (calcium and cAMP for example), protein activity levels, and protein-protein interactions, specialized probes are required. In the aforementioned study by Schofl *et al* (1993), the fluorescent protein aequorin was used to quantify calcium concentrations in liver cells; while this probe has been used successfully in characterizing intracellular calcium levels in real-time, it does not afford high-throughput analysis as a result of its labor-intensive introduction into cells, which involves individual microinjection. Genetically encoded probes are more effective in this manner because they can be introduced to a large pool of cells all at once through various transfection methods. Many fluorescent probes implement the phenomenon known as fluorescence resonance energy transfer (FRET) in order to convey dynamic intracellular information (Miyawaki 2003). FRET is the radiation-less transfer of energy from an excited donor (in this context, usually a GFP variant) to an acceptor (a different GFP variant) (Jares-Erijman and Jovin 2003). These exist either as bimolecular probes, where two different types of proteins are labeled with two different GFP variants and their subsequent interactions lead to FRET signals, or unimolecular probes, where two

different GFP variants are fused to a single macromolecule and subsequent conformational changes of the macromolecule lead to FRET signals. Bimolecular probes have the advantage of being easier to construct, however, quantifications derived from these signals are much more difficult to assess compared to unimolecular biosensors (Jares-Erijman and Jovin 2003). Unimolecular FRET probes are more difficult to construct to ensure viability and functionality, but signal quantitation is much easier compared to bimolecular probes mostly because the donor and acceptor fluorophores are in equimolar quantities (Miyawaki 2003). Several prominent unimolecular FRET biosensors have been developed to probe intracellular pathway dynamics: Cameleon (for intracellular calcium) (Miyawaki *et al*, 1997), Raichu-Ras (measures levels of activated Ras) (Mochizuki *et al*, 2001), Picchu (indirect measure of EGFR and Abl kinase phosphorylation) (Kurokawa *et al*, 2001; Ting *et al*, 2001), cGMP probe (Honda *et al*, 2001; Sato *et al*, 2000), PKA probe (Nagai *et al*, 2000; Zheng *et al*, 2001), cAMP probe (Nikolaev *et al*, 2004), and most recently Rab5 probe (Kitano *et al*, 2008).

While FRET probes have provided tremendous insight into spatial and temporal cellular signaling dynamics, there are always concerns about slow kinetics in the face of dynamically fluctuating signals, low dynamic ranges, and interference that they cause, as with any reporter system (Tay *et al*, 2007). In many cases FRET probes are composed of functional proteins, and their introduction may alter signal dynamics of a target pathway if the probe is expressed in exorbitant quantities (Miyawaki 2003). Similarly, certain probes are designed to capture intracellular components, but if these probes are highly expressed in cells, then they may act as harmful buffers and if the probes compete for intracellular substrates with endogenous proteins, signal levels can be attenuated (Miyawaki 2003). In a study of the FRET biosensor for calcium, Cameleon, a unimolecular and bimolecular version were analyzed (Miyawaki *et al*, 1999). The authors concluded that high concentrations of the endogenous protein greatly affected the sensitivity of the probe to intracellular calcium levels, while the unimolecular version was not affected. Nonetheless, these probes introduce their own "interpretations" of the signaling dynamics, and accordingly need to be deconvolved if precise quantification of the target signal is desired (Gunawardena 2008). To this end, Tay and colleagues (2007) probed the kinetics and reliability of a Troponin-C-based calcium sensor through

15

deconvolution of the transfer function of the biosensor based upon the input signal, which was the fluorescent signal from the calcium dye Indo-1 in this case. The authors concluded that the FRET probe showed quantitative reproducibility, which meant that algorithms could be developed in the future that could overcome the slow kinetics inherent to many current FRET probes. Fluorescent dyes for intracellular signal measurement generally exhibit faster kinetics and higher dynamic ranges compared to genetically encoded probes; however, the dyes can leak out of cells and thereby do not afford long-term temporal dynamics characterizations.

To date, only one study has utilized FRET-based probes to measure intracellular signal dynamics in a microfluidic chip (Sawano *et al,* 2002). In this study, cells loaded with various probes were locally stimulated through coupled laminar flow streams and the resulting spatial dynamics were captured through the resulting FRET signals; the authors discovered that the degree of propagation of stimulus across a cell was dependent upon the density of receptors expressed on its surface. This result has tremendous implications for cancer biology, since certain receptors are over-expressed in many forms of cancer (Hynes and Lane 2005). As FRET-based biosensors improve and diversify, there will be a tremendous opportunity to implement them with microfluidics so that effective assessments of temporal dynamics of pathway components can be made.

One caveat of microfluidics, however, is that continuous real-time imaging can be a challenge. Some actuation systems, such as the programmable Braille display (Wu *et al,* 2004), are not transparent and are difficult to access by a microscope. Even with actuation setups that are amenable to real-time imaging by microscope, we have observed that PDMS-based microfluidic devices can be suboptimal for phase imaging due to unevenness or inconsistencies in device thickness or shape; oil-immersion imaging can be problematic due to PDMS absorption of the oil. In addition, microfluidic actuation can cause vibrations and unwanted movements that can render long-term imaging of temporal dynamics challenging. In this regard, future microfluidic setups will need to take into consideration these requirements for improving real-time microscopy for studies of temporal dynamics in cellular systems.

I.6 Motivations and Research Objectives:

For decades fluidics has played a vital role in elucidating the effect of temporal stimulation dynamics on cellular systems, from simple organisms such as slime molds (Robertson *et al,* 1972) and yeast (Bennett *et al,* 2008; Hersen *et al,* 2008, Mettetal *et al,* 2008) to more complex systems such as liver cells (Schofl *et al,* 1991; Schofl *et al,* 1993; Weigle *et al,* 1984) and lens tissue (Brewitt and Clark 1988). The ability to dynamically stimulate cells has provided a means of investigating how cells process and interpret information on the molecular level as well as on a multi-cellular level. Seminal studies have effectively demonstrated the importance that non-static stimulation of cellular systems has in our understanding of temporal dynamics and the timing involved in biological systems; in this manner, fluidics overcomes the limitations of conventional static techniques used in biology labs. Several prominent examples were provided where simple fluidic setups were employed to deliver well-controlled, reproducible pulses of chemical stimulant to cells; these simple studies resulted in some of the most important biological discoveries (Balaban *et al,* 2004; Bennett *et al,* 2008; Brewitt and Clark 1988; Dolmetsch *et al,* 1998; Hersen *et al,* 2008; Kupzig *et al,* 2005; Mettetal *et al,* 2008; Robertson *et al,* 1972; Weigle *et al,* 1984). Recent efforts have resulted in the development of microfluidic platforms with rapid pattern switching for single cell studies ("chemical waveform synthesizer" (Olofsson *et al,* 2005)) or slower pattern switching for higher throughput characterizations ("flow-encoded switching" (King *et al,* 2008)); the setup developed by Gomez-Sjoberg and colleagues (2007) provided a means for long-term maintenance of mammalian cell cultures (up to several weeks) in an automated, high-throughput fashion. An emerging field for microfluidics in biological investigations has been for testing cellular network architectures under dynamic stimulation conditions, providing an optimal platform for scrutinizing existing mathematical and computer models of cellular signaling pathways to a greater degree, compared to conventional methods (Bennett *et al,* 2008; Hersen *et al,* 2008, Mettetal *et al,* 2008). These latter examples again portray that the simple principle of being able to deliver well-timed pulses of stimulant in combination with mathematical modeling can lead to vital biological discoveries. It is important to note that these studies were conducted on yeast cells, organisms which are much simpler than mammalian cells. In addition, despite

knowing many of the components of a cellular signaling pathway, the way that these components interact is very complex and needs elucidation (Brabant *et al,* 1992). This provides the motivation for the development of next generation microfluidic platforms for investigation of temporal dynamics, since dynamic stimulation patterns can be used to probe signaling mechanisms in ways that static systems cannot (Ingolia and Weissman 2008; Paliwal *et al,* 2008). The results of such studies hold enormous physiological and therapeutic importance, since many times disruption of the intrinsic rhythms of these systems leads to pathological conditions (Brabant *et al,* 1992; Gambacciani *et al,* 1987; Van Couter and Refetoff 1985) and knowing the signaling mechanisms can help with drug development (Linderman 2008; Persidis 1998). As read-outs for the state of cellular machinery improve and expand, this will provide an exceptional opportunity for the development of the next generation of microfluidic devices. It will be necessary for these devices to be amenable to real-time imaging, operate at suitable shear stress levels, and be optimized for supporting cells with complex microenvironments. Ultimately, the microenvironment must be sufficiently recapitulated so that measurements have a proper physiological meaning (Griffith and Naughton 2002, Khetani and Bhatia 2006, Tsang and Bhatia 2006). In addition, future setups will need to combine the versatility of stimulation pattern generation (media switching on the order of seconds to hours) of the "chemical waveform synthesizer" with high-throughput characteristics (preferably 384 or more parallel assays) and the ability to test multiple conditions on a single chip; this latter property was demonstrated by the user-friendly "flow encoded switching" setup and the fully automated setup developed by Gomez-Sjoberg *et al,* (2007). Although a large variety of pumps and valves have been developed, even performing simple two-fluid switching with seconds to hours periods over 96 or larger cell culture wells/channels is still a huge challenge; commercially available microfluidic perfusion setups do exist for mammalian and cell culture, but these are generally not tailored for temporal dynamics studies. Other challenges of adapting microfluidics for characterizing temporal dynamics include difficulties with long-term real-time imaging, cell seeding, controlling shear stress levels that may affect cell signaling and viability, and lack of accessibility to non-engineers. Ultimately, the idea is to have a straightforward microfluidic platform that can be accessible by both engineers and biologists, fostering greater collaboration between

these two groups. The timing is right for microfluidic engineers to make a larger impact on the field of temporal dynamics in biology.

In that spirit, the objective of this thesis research was to develop a microfluidic system enabling dynamic manipulation and elucidation of cellular signaling mechanisms. The studies are focused upon the M3 muscarinic receptor signaling pathway, a G-protein coupled receptor; upon receptor activation by chemical stimulants (such as acetylcholine), cells release calcium into the cytoplasm, triggering a variety of vital cellular operations. In addition to garnering increasing attention as a therapeutic target (Iversen 1997; Maresca and Supuran 2008; Song *et al,* 2003), the M3 receptor is highly expressed in organs that are exposed to fluctuating chemical environments, such as the brain (Gautam *et al, 2009*) and the pancreas (Gautam *et al,* 2006). For these reasons, the M3 receptor-mediated calcium signaling pathway presents an important physiological system for both manipulation and for more profound understanding of its signaling mechanisms. The microfluidic system described in Chapter II enabled enhanced control of the intracellular calcium levels in mammalian cells through periodic exposure to M3 receptor ligands, compared to continuous exposure. However, these studies revealed that the fidelity of calcium responses to periodic chemical stimulation was compromised in a percentage of cells in a population, a finding that had not been previously explored experimentally. In Chapters II and III, guided by mathematical models of intracellular calcium signaling, the effect of periodic stimulation parameters and intrinsic cellular parameters (such as M3 receptor density and RGS concentration) on calcium response fidelity were characterized; fidelity was quantified two ways: 1) by calculating the percentage of cells in a population that responded to every stimulation event, 2) the phase-locking ratio (number of calcium responses/number of stimulation events).

These studies provided concrete strategies for manipulation of intracellular signaling mechanisms and insight into cellular regulation of fidelity, facets unattainable with conventional methods. In addition in Chapter III, the potential downstream consequences of compromised calcium response fidelity are explored theoretically, providing key insight into elusive aspects of temporal dynamics in physiological systems and inciting future studies in this crucial field of research. Harnessing the fidelity limitations

uncovered in Chapter II through periodic chemical stimulation, previously published mathematical models of intracellular calcium signaling were analyzed to observe whether these limitations were manifested theoretically, as described in Chapter IV. None of the models tested was able to account for our experimental observations, necessitating model revisions. Model revisions resulted in correct prediction of these limitations, serving as a readout for signaling mechanism elucidation, complementing conventional techniques. Collectively, these studies enhance the tools and approaches available for probing temporal dynamics of cellular systems and further narrow the gap between engineering analysis and understanding biological phenomena.
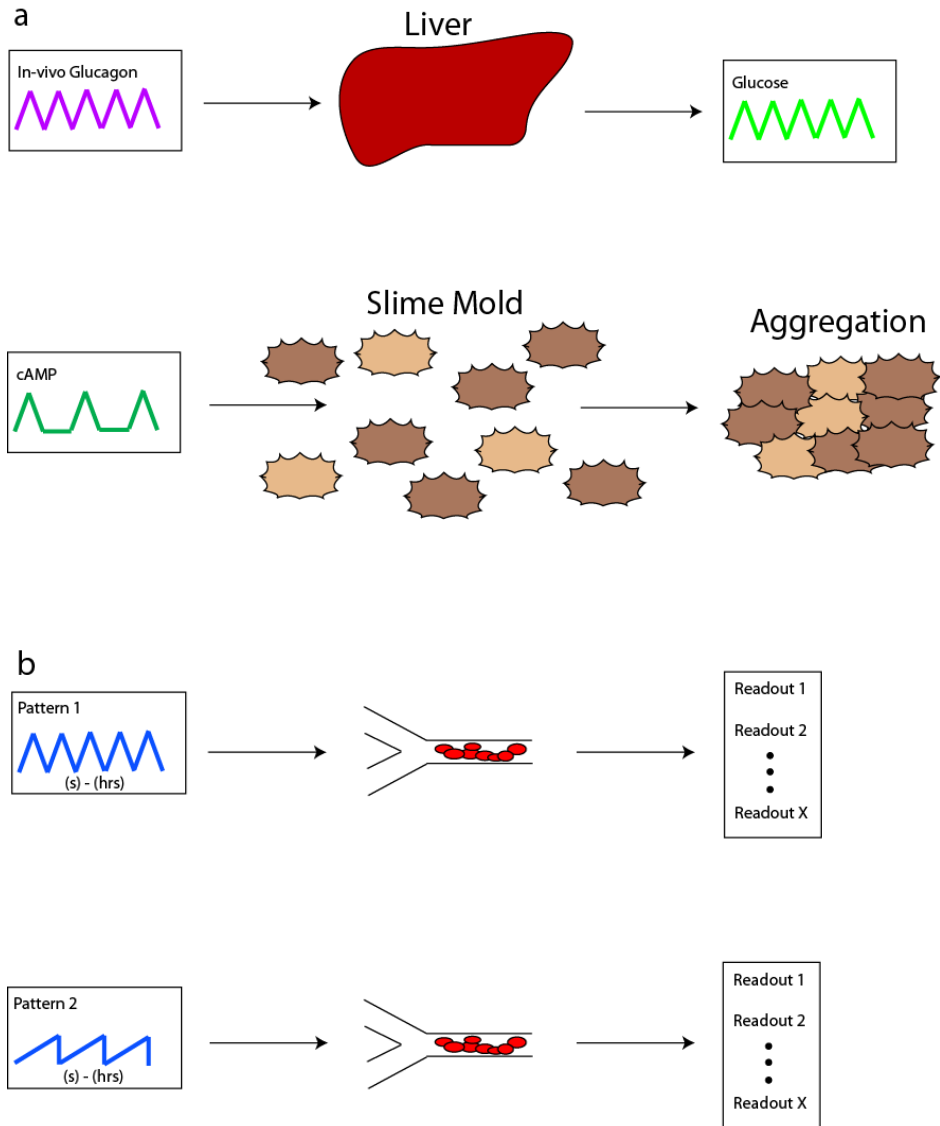
Fig. I.1 Temporal dynamics in nature and how microfluidics can be used to analyze this phenomenon. **a** Examples of naturally occurring time-varying chemical patterns in nature: pulsatile glucagon stimulates liver cells to produce higher levels of glucose compared to continuous stimulation (Weigle *et al*, 1984); slime mold naturally release the chemical cAMP in a pulsatile fashion when starved and aggregate as a result. Results have shown that the frequency of this chemical release is crucial to the aggregation process (Robertson *et al*, 1972). **b** Microfluidics provides an ideal platform for studying physiologically relevant temporal dynamics in cellular systems. Various methods have been developed to create time-varying (seconds to hours) chemical patterns for cellular stimulation, and there are a multitude of both real-time and endpoint readouts available to assess cellular responses.
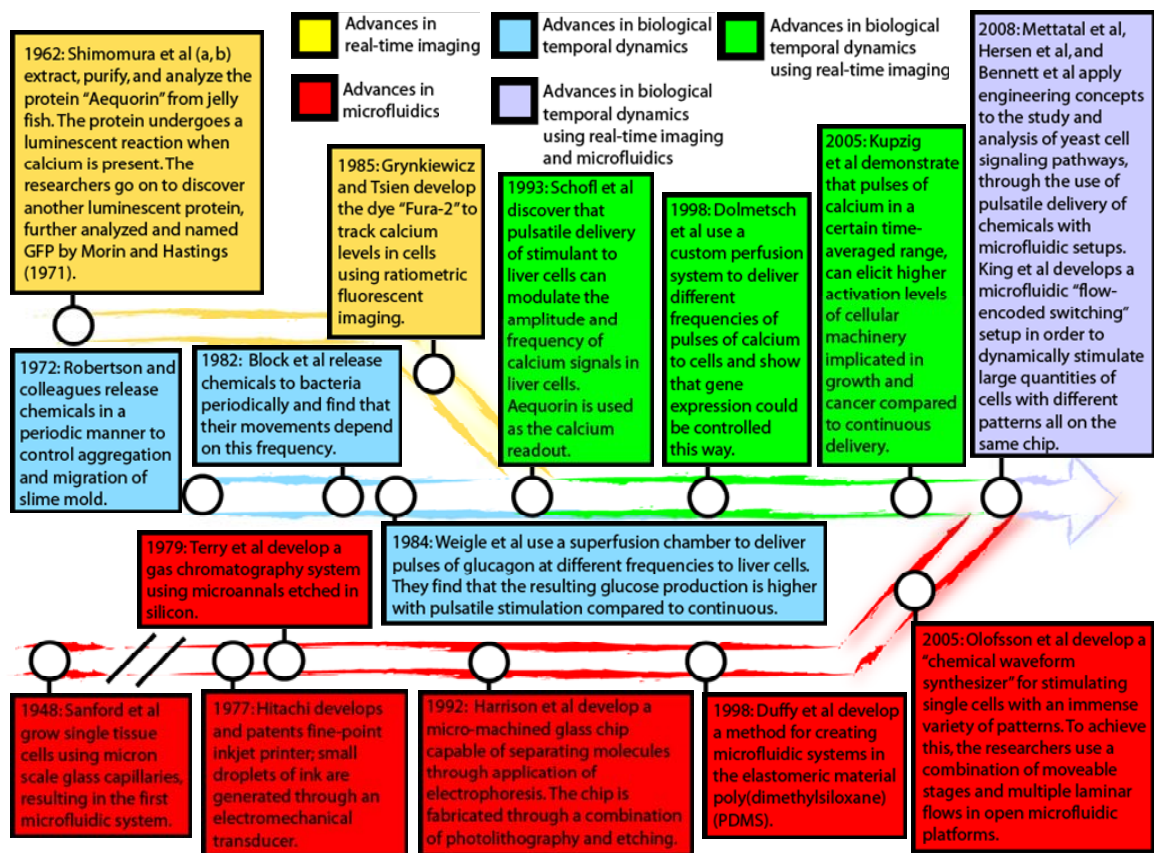
Fig. I.2 Timeline: Timeline with select examples, of important advances in the areas of real-time imaging, microfluidics, and temporal dynamics in biology, as well as seminal research where these fields converged, resulting in key biological discoveries.
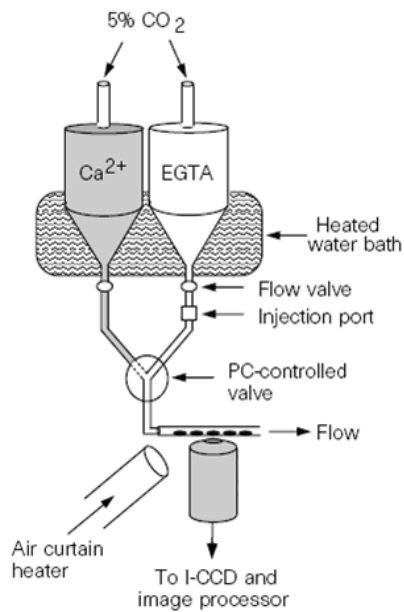
Fig. I.3 The calcium clamp setup. It was developed to control calcium levels inside cells, in order to analyze the effect that the frequency of the calcium signals had on gene expression and activation of cellular machinery implicated in growth and cancer (Ras and ERK proteins). A computer-controlled solenoid valve was used to switch between two reservoirs (one containing calcium, the other containing EGTA, a calcium chelator). Real-time imaging was used to monitor the calcium levels, while endpoint readouts were used to quantify gene expression and Ras and ERK activation. Figure from Dolmetsch *et al* (1998).
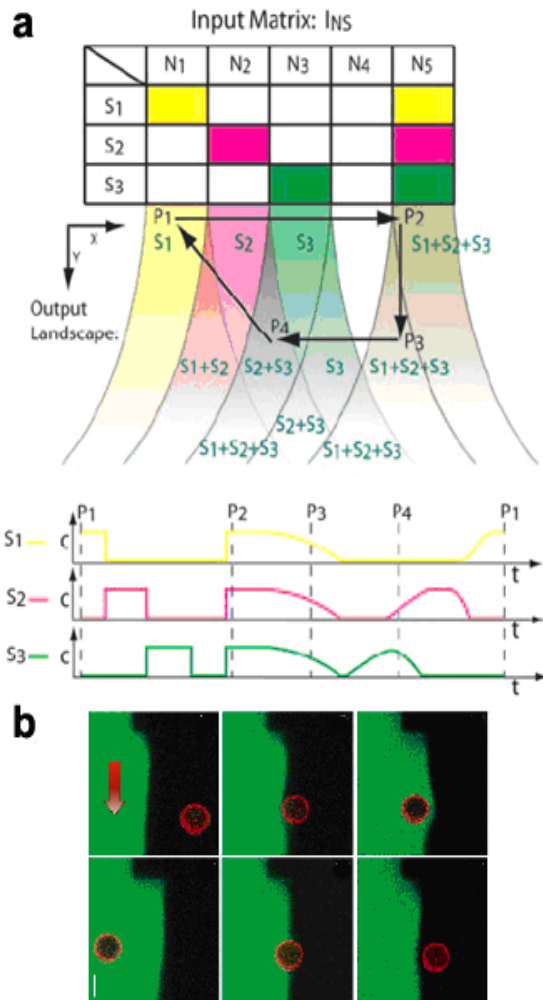
Fig. I.4 The setup of the "chemical waveform synthesizer". **a** For this example, there are five laminar flow streams (N1-N5) containing three different stimulants S1-S3. The stage is moved along the paths P1-P4 depicted below the "Input Matrix", creating the stimulation patterns portrayed in the graphs. It can be seen that three different stimulation patterns with the three different stimulants are obtained during one run. Figure from Olofsson J *et al* (2005) **b** A cell (in red) is moved between two laminar flow streams (green and black) to expose it to varying chemical environments. The red arrow indicates the direction of flow. The scale bar represents 10 microns. Figure from Olofsson J *et al* (2004).
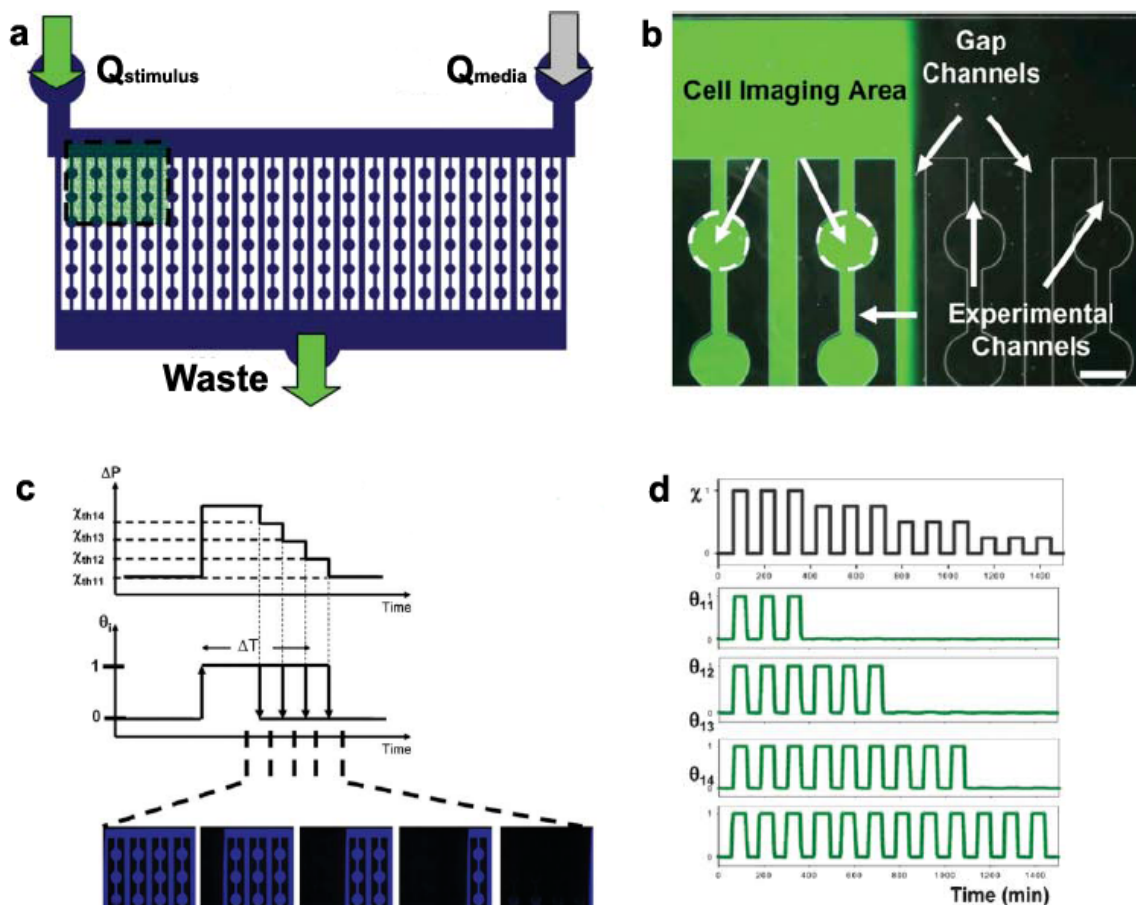
Fig. I.5 The "Flow Encoded Switching" setup. **a** Schematic of the microfluidic device, with two inlet flow inputs, Qstimulus and Qmedium, controlling the patterns of stimulation addressing the experimental channels. **b** The device is composed of "gap" channels and "experimental" channels. The "experimental channels" contain cells and convey the desired stimulation patterns to the cells; the "gap" channels provide a means of properly positioning the flow streams between "experimental channels". **c** The duration of stimulation of individual "experimental" channels can be controlled by modulating one fluidic parameter, the inlet flow ratio in this case. As depicted this ratio is initially increased and then progressively reduced, resulting in different time spans of stimulation for the depicted "experimental" channels. **d** Fluorescence measurement of stimulation profile where pulse train duration is varied across several "experimental" channels. Figure from King *et al* (2008).
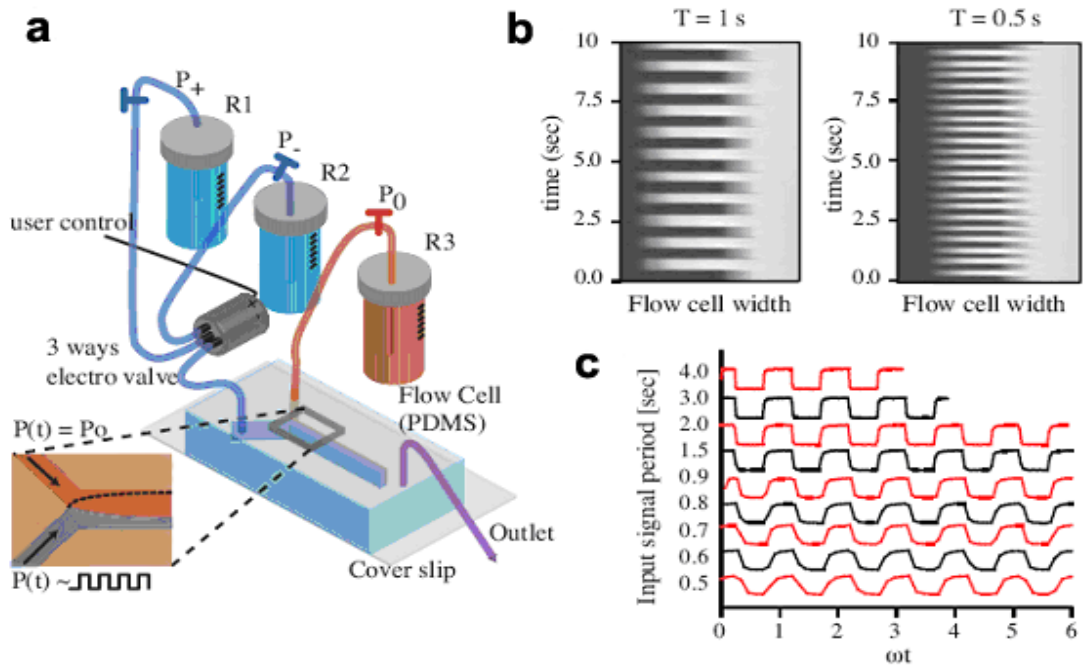
Fig. I.6 Rapid pulse generation setup used to study frequency response in yeast cells. **a** Schematic of microfluidic setup, where inlet pressures are manipulated to generate pulses of different periods as depicted in **b** and **c**. When reservoir R2 is chosen, through the user-controlled 3-way valve, then the contents of R3 fill the microchannel; when reservoir R1 is chosen, its contents fill the microchannel. Figure from Hersen *et al* (2008).
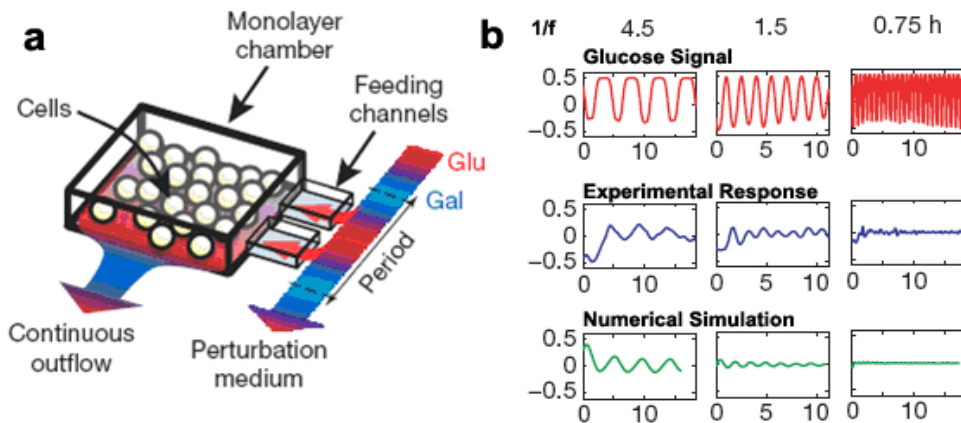
Fig. I.7 Microfluidic setup used for analysis of metabolic gene regulation in yeast cells. **a** Yeast cells grown in a monolayer are addressed with different stimulation patterns of glucose which are created by a waveform generator and conveyed to the cells through the feeding channels. **b** Cellular responses to different frequencies of glucose stimulation were measured using real-time readouts, and mathematical models were developed in order to test the postulated signal pathway architectures. As depicted in the graphs below, as the period of the glucose pulses diminished, the cellular response attenuated and eventually did not respond, which was predicted by numerical simulations; this indicated that this was a low-pass filter system. Figure from Bennett *et al* (2008).

I.7 References:

Ando J, Ohtsuka A, Katayama Y, Araya S, Kamiya A (1990) Fluid shear stress effects on intracellular calcium concentrations in cultured vascular endothelial cells. *Resp Circ* **38**:1107-1113.

Barkai N, Leibler S (2000) Biological rhythms – Circadian clocks limited by noise. *Nature* **403**:267-268.

Beebe DJ, Mensing GA, Walker GM (2002) Physics and applications of microfluidics in biology. *Annu Rev Biomed Eng* **4**:261-286.

Bennett MR, Pang WL, Ostroff NA, Baumgartner BL, Nayak S, Tsimring LS, Hasty J (2008) Metabolic gene regulation in a dynamically changing environment. *Nature* **454**:1119-1122.

Brabant G, Prank K, Schofl C (1992) Pulsatile patterns in hormone secretion. *Trends Endocrinol Metabol* **3**:183-190.

Brewitt B, Clark JI (1988) Growth and transparency in the lens, an epithelial tissue, stimulated by pulses of PDGF. *Science* **242**:777-779.

Block SM, Segall JE, Berg HC (1982) Impulse responses in bacterial chemotaxis. *Cell* **31**:215-226.

Chay TR, Lee YS, Fan YS (1995) Appearance of phase-locked Wenckebach-like rhythms, devil's staircase and unviersality in intracellular calcium spikes in nonexcitable cell models. *J Theor Biol* **174:** 21-44.

Chiu DT, Orwar O (2004) Functional cell-based high-throughput drug screening. *Drug Disc World* **5**:45-51.

Cuthbertson KSR, Chay TR (1991) Modeling receptor-controlled intracellular calcium oscillators. *Cell Calcium* **12:** 97-109.

Dalkin AC, Haisenleder DJ, Ortolano GA, Ellis TR, Marshall JC (1989) The frequency of gonadotropin releasing hormone stimulation differentially regulates gonadotropin subunit messenger ribonucleic acid expression. *Endocrinol* **125**:917-924.

Dolmetsch RE, Xu, KL, Lewis RS (1998) Calcium oscillations increase the efficiency and specificity of gene expression. *Nature* **392**:933-936.

Duffy DC, McDonald JC, Schueller OJA, Whitesides GM (1998) Rapid prototyping of microfluidic systems in poly(dimetheylsiloxane). *Anal Chem* **70**:4974-4984.

Estes DJ, Memarsadeghi S, Lundy SK, Marti F, Mikol DD, Fox DA, Mayer M (2008) High-throughput profiling of ion channel activity in primary human lympochytes. *Anal Chem* **80**:3728-3735.

Fertig N, Blick RH, Behrends JC (2002) Whole cell patch clamp recording performed on a planar glass chip. *Biophys J* **6**:3056-3062.

Futai N, Gu W, Song JW, Takayama S (2006) Handheld recirculation system and customized media for microfluidic cell culture. *Lab Chip* **6**:149-154.

Gambacciani M, Liu JH, Swartz WH, Teuros VS, Yen SSC, Rasmussen DD (1987) Intrinsic pulsatility of luteinizing-hormone release from the human pituitary in-vitro. *Neuroendocrinol* **25**:402-406.

Gautam D, Jeon J, Starost MF, Han SJ, Hamdan FF, Cui YH, Parlow AF, Gavrilova O, Szalayova I, Mezey E, Wess J (2009) Neuronal M3 muscarinic acetylcholine receptors are essential for somatotroph proliferation and normal somatic growth. *Proc Natl Acad Sci USA* **106**:6398-6403.

Gautam D, Han SJ, Hamdan FF, Jeon J, Li B, Li JH, Cui YH, Mears D, Lu HY, Deng CX, Heard T, Wess J (2006) A critical role for beta cell M3 muscarinic acetylcholine receptors in regulating insulin release and blood glucose homeostasis in-vivo. *Cell Metabol* **3**:449-461.

Goldbeter A (1996) Biochemical Oscillations and Cellular Rhythms. The Molecular Bases of Periodic and Chaotic Behaviour. Cambridge Univ. Press, Cambridge, UK.

Goldbeter A (2002) Computational approaches to cellular rhythms. *Nature* **420**:238-45.

Goldbeter A (2008) Biological rhythms: Clocks for all times. Curr Biol **18**: R751-R753.

Griffith LG, Naughton G (2002) Tissue engineering – current challenges and expanding opportunities. *Science* **295**:1009-1016.

Grynkiewicz G, Poenie M, Tsien RY (1985) A new generation of Ca-2+ indicators with greatly improved fluorescence properties. *J Biol Chem* **260**:3440-3450.

Gu W, Zhu X, Futai N, Cho BS, Takayama S (2004) Computerized microfluidic cell culture using elastomeric channels and Braille displays. *Proc Natl Acad Sci USA* **101**: 15861-15866.

Gunawardena J (2008) Signals and systems: Towards a systems biology of signal transduction. *Proc IEEE* **96**: 1386-1397.

Harrison DJ, Manz A, Fan ZH, Ludi H, Widmer HM (1992) Capillary electrophoresis and sample injection systems integrated on a planar glass chip. *Anal Chem* **64**:1926-1932.

Heo YS, Cabrera LM, Song JW, Futai N, Tung YC, Smith GD, Takayama S (2006) Characterization and resolution of evaporation- mediated osmolality shifts that constrain microfluidic cell culture in poly(dimethylsiloxane) devices. *Anal Chem* **79**:1126-1134.

Hersen P, McClean MN, Mahadevan L, Ramanathan S (2008) Signal Processing by the HOG MAP kinase pathway. *Proc Natl Acad Sci USA* 105:7165-7170.

Honda A, Adams SR, Sawyer CL, Lev-Ram V, Tsien RY, Dostmann WR (2001). Spatiotemporal dynamics of guanosine 3-5-cyclic monophosphate revealed by a genetically encoded, fluorescent indicator. *Proc Natl Acad Sci USA* **98**:2437–2442.

Huang CJ, Harootunian A, Maher MP, Quan C, Raj CD, McCormack K, Numann R, Negulescu PA, Gonzalez JE (2006) Characterization of voltage-gated sodium-channel blockers by electrical stimulation and fluorescence detection of membrane potential. *Nature Biotechnol* **4**:439-446.

Huh D, Fujioka H, Tung YC, Futai N, Paine R, Grotberg JB, Takayama S (2007) Acoustically detectable cellular-level lung injury induced by fluid mechanical stresses in microfluidic airway systems. *Proc Natl Acad Sci USA* **104**:18886-18891.

Hung PJ, Lee PJ, Sabounchi P, Lin R, Lee LP (2005) Continuous perfusion microfluidic cell culture array for high-throughput cell-based assays. *Biotechnol and Bioeng* **89**:1-8.

Hynes NE, Lane HA (2005) ERBB receptors and cancer: the complexity of targeted inhibitors. *Nature Rev Cancer* **5**:341-354.

Ingolia NT, Weissman JS (2008) Systems biology- reverse engineering the cell. *Nature* **454**:1059-1062.

Iversen SD (1997) Behavioural evaluation of cholinergic drugs. *Life Sci* **60**:1145-1152.

Jacob R, Merritt JE, Hallam TJ, Rink TJ (1988) Repetitive spikes in cytoplasmic calcium evoked by histamine in human endothelial cells. *Nature* **335:** 40-45.

Jares-Erijman EA, Jovin TM (2003) FRET imaging. *Nat Biotechnol* **21**:1387-1395.

Kang JH, Kim YC, Park JK (2007) Analysis of pressure-driven air bubble elimination in a microfluidic device. *Lab Chip* **8**:176-178.

Kermack W, McKendrick AG (1927) A contribution to the theory of epidemics. *Proc Roy Soc A* **115**:700–721.

Khetani SR, Bhatia SN (2006) Engineering tissues for *in vitro* applications. *Curr Opin Biotech* **17**:524-531.

King KR, Wang SH, Irimia D, Jayaraman A, Toner M, Yarmush ML (2007) A high-throughput microfluidic real-time gene expression living cell array. *Lab Chip* 7:77-85.

King KR, Wang S, Jayaraman A , Yarmush ML, Toner M (2008) Microfluidic flow-encoded switching for parallel control of dynamic cellular microenvironments. *Lab Chip* **8**:107-116.

King RD, Garrett SM, Coghill GM (2005) On the use of qualitative reasoning to simulate and identify metabolic pathways. *Bioinformatics* **21:** 2017-2026.

Kitano H (2002) Systems biology: A brief overview. *Science* **295:** 1662-1664.

Kitano M, Nakaya M, Nakamura T, Nagata S, Matsuda M (2008) Imaging of Rab5 activity identifies essential regulators of phagosome maturation. *Nature* **453**:241-245.

Knobil E (1981a) Patterns of hormonal signals and hormone action. *N Engl J Med* **305**:1582-1583.

Knobil E (1981b) Patterns of hypophysiotropic signals and gonadotropin-secretion in the rhesus-monkey. *Biol of Reprod* **24**:44-49.

Kreke MR, Goldstein AS (2004) Hydrodynamic shear stimulates osteocalcin expression but not proliferation of bone marrow stromal cells. *Tissue Eng* **10**:780-788.

Kupzig S, Walker SA, Cullen PJ (2005) The frequencies of calcium oscillations are optimized for efficient calcium-mediated activation of Ras and the ERK/MAPK cascade. *Proc Natl Acad Sci USA* **102**:7577-7582.

Kurokawa K, Mochizuki N, Ohba Y, Mizuno H, Miyawaki A, Matsuda M (2001) A pair of fluorescent resonance energy transfer-based probes for tyrosine phosphorylation of the CrkII adaptor protein in vivo. *J Biol Chem* **276**: 31305-31310.

Lahav G, Rosenfeld N, Sigal A, Geva-Zatorsky N, Levine AJ, Elowitz MB, Alon U (2004) Dynamics of the p53-Mdm2 feedback loop in individual cells. *Nature Genetics* **36:** 147-150.

Laurent G (2002) Olfactory network dynamics and the coding of multidimensional signals. *Nature Rev Neurosci* 3:884-895.

Li YX, Goldbeter A (1992) Pulsatile signaling in intercellular signaling in intercellular communication-periodic stimuli are more efficient than random or chaotic signals in a model based on receptor desensitization. *Biophys J* **61**:161-171.

Li YX, Goldbeter A (1989) Frequency specificity in intercellular communication. *Biophys J* **55**:125-145.

Linderman JJ (2009) Modeling of G-protein-coupled receptor signaling pathways. *J Biol Chem* **284**:5427-5431.

Lotka AJ (1925) Elements of physical biology. Williams and Wilkins, Baltimore, MD, USA.

Lu H, Koo LY, Wang WCM, Lauffenburger DA, Griffith LG, Jensen KF (2004) Microfluidic shear devices for quantitative analysis of cell adhesion. *Anal Chem* **18**:5257:5264.

Maresca A, Supuran CT (2008) Muscarinic acetylcholine receptors as therapeutic targets for obesity. *Exp Opin Therap Targets* **9**:1167-1175.

Martiel JL, Goldbeter A (1987) A model based on receptor desensitization for cyclic-AMP signaling in dictyostelium cells. *Biophys J* **52**: 807-828.

Mehta G, Kiel MJ, Lee JW, Kotov N, Linderman JJ, Takayama S (2007) Polyelectrolyte-Clay-Protein Layer Films on Microfluidic PDMS Bioreactor Surfaces for Primary Murine Bone Marrow Cultures. *Adv Funct Mater* **17**:2701–2709.

Melin J, Quake SR (2007) Microfluidic large-scale integration: The evolution of design rules for biological automation. *Annu Rev Biophys Biomol Struct* **36**:213-231.

Mettetal JM, Muzzey D, Gomez-Uribe C, van Oudenaarden A (2008) The frequency dependence of osmo-adaptation in Saccharomyces cerevisiae. *Science* **319**:482:484.

Miyawaki A, Llopis J, Heim R, McCaffery JM, Adams JA, Ikura M, Tsien RY (1997) Fluorescent indicators for Ca2+ based on green fluorescent proteins and calmodulin. *Nature* **388**: 882-887.

Miyawaki A (2003) Visualization of the spatial and temporal dynamics of intracellular signaling. *Dev Cell* **4**: 295-305.

Mochizuki N, Yamashita S, Kurokawa K, Ohba Y, Nagai T, Miyawaki A, Matsuda M (2001) Spatio-temporal images of growth-factor-induced activation of Ras and Rap1. *Nature* **411**: 1065-1068.

Monod J (1942) Recherches sur la croissance des cultures bacteriennes. Hermann et Cie.

Morin JG, Hastings JW (1971) Energy transfer in a bioluminescent system. *J Cell Phys* **77**:313-318.

Nagai T, Ibata K, Park ES, Kubota M, Mikoshiba K, Miyawaki A (2002) A variant of yellow fluorescent protein with fast and efficient maturation for cell-biological applications. *Nat Biotechnol* **20**:87-90.

Nagai T, Yamada S, Tominaga T, Ichikawa M, Miyawaki A (2004) Expanded dynamic range of fluorescent indicators for Ca2+ by circularly permuted yellow fluorescent proteins. *Proc Natl Acad Sci U S A* **101:** 10554-10559.

Nikolaev VO, Bunemann M, Hein L, Hannawacker A, Lohse MJ (2004) Novel single chain cAMP sensors for receptor induced signal propagation. *J Biol Chem* **279**: 37215-37218.

Norstedt G, Palmiter R (1984) Secretory rhythm of growth hormone regulates sexual differentiation of mouse liver. *Cell* **36**:805-812.

Novak B, Tyson JJ (1993) Numerical analysis of a comprehensive model of m-phase control in xenopus oocyte extracts and intact embryos. *J Cell Sci* **106**:115-1168.

Ogawa S, Lozach J, Benner C, Pascual G, Tangirala RK, Westin S, Hoffmann A, Subramaniam S, David M, Rosenfeld MG, Glass CK (2005) Molecular determinants of crosstalk between nuclear receptors and toll-like receptors. *Cell* **122**:707-721.

Olofsson J, Pihl J, Sinclair J, Sahlin E, Karlsson K, Orwar O (2004) A microfluidics approach to the problem of creating separate solution environments accessible from macroscopic volumes. *Anal Chem* **76**:4968-4976.

Olofsson J, Bridle H, Sinclair J, Granfeldt D, Sahlin E, Orwar O (2005) A chemical waveform synthesizer. *Proc Natl Acad Sci USA* **102**: 8097-8102.

Paliwal S, Wang CJ, Levchenko A (2008) Pulsing cells: how fast is too fast?. *HFSP J* **2**:251-256.

Persidis A (1998) Signal transduction as a drug-discovery platform. *Nature Biotechnol* **16**:1082-1083.

Prentki M, Glennon MC, Thomas AP, Morris RL, Matschinsky FM, Corkey BE (1988) Cell-specific patterns of oscillating free Ca2+ in carbamylcholine-stimulated insulinoma cells. *J Biol Chem* **263:** 11044-11047.

Riddle RC, Taylor AF, Genetos DC, Donahue HJ (2006) MAP kinase and calcium signaling mediate fluid flow-induced human mesenchymal stem cell proliferation. *Am J Physiol Cell Physiol* **290**:776−784.

Robertson A, Drage DJ, Cohen MH (1972) Control of aggregation in dictyostelium discoideum by an external periodic pulse of cyclic adenosine monophosphate. *Science* **175**:333-335.

Saigusa T, Tero A, Nakagaki T, Kuramoto Y (2008) Amoebae anticipate periodic events. *Phys Rev Let* **100**: 018101.

Sanford KK, Earle WR, Likely GD (1948) The growth in-vitro of single isolate tissue cells. *J Natl Cancer Inst* **9**:229-246.

Sato M, Hida N, Ozawa T, Umezawa Y (2000) Fluorescent indicators for cyclic GMP based on cyclic GMP-dependent protein. *Anal Chem* **72**:5918-5924.

Sawano A, Takayama S, Matsuda M, Miyawaki A (2002) Lateral propagation of EGF signaling after local stimulation is dependent on receptor density. *Dev Cell* **3**:245-257.

Schmidt C, Mayer M, Vogel H (2000) A chip-based biosensor for the functional analysis of single ion channels. *Angew Chem* **39**:3137-3140.

Schofl C, Sanchez-Bueno A, Brabant G, Cobbold PH, Cuthbertson KS (1991) Frequency and amplitude enhancement of calcium transients by cyclic AMP in hepatocytes. *Biochem J* **273**:799-802.

Schofl C, Brabant G, Hesch RD, von zur Muhlen A, Cobbold PH, Cuthbertson KS (1993) Temporal patterns of alpha1-receptor stimulation regulate amplitude and frequency of calcium transients. *Am J Physiol* **265**:C1030-C1036.

Schofl C, Prank K, Brabant G (1994) Mechanisms of Cellular Processing. *Trends Endocrinol Met* **5**:53-59.

Shapiro L, Wagner N (1989) Transferrin is an autocrine growth factor secreted by reuber H-35 cells in serum-free culture. *In-vitro Cell Dev Biol* **25**:650-654.

Shim J, Bersano-Begey TF, Zhu X, Tkaczyk A, Linderman JJ, Takayama S (2003) Micro- and nanotechnologies for studying cellular function. *Curr Top Med Chem* **3**:687-703.

Shimomura O, Saiga Y, Johnson FH (1962) Purification and properties of aequorin, a bio-(chemi-) luminescent protein from jelly-fish, Aequorea aequorea. *Fed Proc* **21**:401.

Shimomura O, Johnson FH, Saiga Y (1962) Extraction, purification and properties of aequorin, a bioluminescent protein from luminous hydromedusan, Aequorea. *J Cell Comp Phys* **59**:223-239.

Sneyd J (2005) Modeling IP3-dependent calcium dynamics in non-excitable cells. *Tutor Math Biosci II* **1867:** 15-61.

Song PF, Sekhon HS, Jia YB, Keller JA, Blusztajn JK, Mark GP, Spindel ER (2003) Acetylcholine is synthesized by and acts as an autocrine growth factor for small cell lung carcinoma. *Cancer Res* **63**:214-221.

Steiner RA, Bremner WJ, Clifton DK (1982) Regulation of luteinizing-hormone pulse frequency and amplitude by testosterone in the adult male rat. *Endocrinol* **111**:2055-2061.

Tay LH, Griesbeck O, Yue DT (2007) Live cell transforms between calcium transients and FRET responses for a troponin C based calcium sensor. *Biophys J* **93**:4031-4040.

Terry SC, Jerman JH, Angell JB (1979) Gas-chromatographic air analyzer fabricated on a silicon wafer. *IEEE Trans Electron Devices* **26**:1880-1886.

Ting AY, Kain KH, Klemke RL, Tsien RY (2001) Genetically encoded fluorescent reporters of protein tyrosine kinase activities in living cells. *Proc Natl Acad Sci USA* **98**: 15003-15008.

Tolic IM, Moseklide E, Sturis J (2000) Modeling the insulin-glucose feedback system: The significance of pulsatile insulin secretion. *J Theor Biol* **207**:361-375.

Tourovskaia A, Figueroa-Masot X, Folch A (2005) Differentiation-on-a-chip: A microfluidic platform for long-term cell culture studies. *Lab Chip* **5**:14-19.

Tsang VL, Bhatia SN (2006) Fabrication of three-dimensional tissue. *Tissue Eng II: Basics Tissue Eng Tissue Appl* **103**:189-205.

Van Couter E, Refetoff S (1985) Evidence for 2 subtypes of Cushing's disease based on the analysis of episodic cortisol secretion. *N Eng J Med* **312**:1342-1349.

Verkman AS, Chao AC, Hartmann T (1992) Hormonal regulation of Cl transport in polar airway epithelia measured by a fluorescent indicator. *Am J Physiol* **262**:C23-C31.

Volterra V (1926) Variazioni e fluttuazioni del numero d'individui in specie animali conviventi. *Mem Acad Lineci Roma* **2**:31-113.

Walker GM, Zeringue HC, Beebe DJ (2004) Microenvironment design consideration for cellular scale studies. *Lab Chip* **4**:91-97.

Weigle DS, Koerker DJ, Goodner CJ (1984) Pulsatile glucagon delivery enhances glucose production by perifused rat hepatocytes. *Am J Physiol* **247**:E564-E568.

Whitesides GM, Ostuni E, Takayama S, Jiang XY, Ingber DE (2001) Soft lithography in biology and biochemistry. *Annu Rev Biomed Eng* **3**:335-373.

Wildt L, Hausler A, Marshall G, Hutchison JS, Plant TM, Belchetz PE, Knobil E (1981) Frequency and amplitude of gonadotropin-releasing hormone stimulation and gonadotropin-secretion in the rhesus monkey. *Endocrinol* **109**:376-385.

Woods NM, Cuthbertson KS, Cobbold PH (1986) Repetitive transient rises in cytoplasmic free calcium in hormone-stimulated hepatocytes. *Nature* **319:** 600-602.

Zhang J, Ma Y, Taylor SS, Tsien RY (2001) Genetically encoded reporters of protein kinase A activity reveal impact of substrate tethering. *Proc Natl Acad Sci USA* **98**:14997–15002.

Zhang J, Campbell RE, Ting AY, Tsien RY (2002) Creating new fluorescent probes for cell biology. *Nature Rev Mol Cell Biol* **3**:906-918.

Chapter II.

High fidelity intracellular calcium signal control using microfluidic-pulsed receptor stimulation

II.1 Introduction:

Faithful conversion of environmental chemical cues into intracellular signals is instrumental for cell survival. Physiologic chemical cues are often periodic, a biological manifestation of frequency-encoded information (Brabant *et al*, 1992; Goldbeter, 2008; Rapp, 1987). A regular intracellular messenger relaying extracellular information is calcium, whose information is also frequency-encoded (Boulware and Marchant, 2008). What would enhance scientific and clinical progress in this field is a deeper understanding of factors that affect the fidelity with which extracellular signals are translated to intracellular calcium signals, along with development of tools that enable user-defined control of intracellular signals frequencies.

Cellular calcium oscillation frequencies can be modulated by the concentration of chemical stimulant applied continuously, since increases in stimulant concentration result in increases in calcium oscillation frequency (Jacob *et al*, 1988; Prentki *et al*, 1988; Woods *et al*, 1986). However, this approach does not afford adequate control in terms of dictating specific frequencies in populations of cells because of cell-to-cell variability (Prank *et al*, 2005; Wood and Cadusch, 2005). A promising method for controlling the timing of intracellular signals of entire cell populations is to use periodic chemical stimulation, though the fidelity of signaling in this case has received only minimal attention (Prank *et al*, 2005).

Using a mathematical model of the calcium signaling pathway, we determined the periodic stimulation parameters that modulated the fidelity of a G-protein-mediated calcium signaling model. We tested our findings using periodic stimulation of HEK 293 cells with carbachol, the stable analog of the neurotransmitter acetylcholine, which is able

to activate the Gq protein-coupled M3 muscarinic receptor; activation of M3 receptors triggers a signal cascade eventually leading to biphasic or oscillatory calcium release (based upon stimulant concentration range) (Luo *et al*, 2001); biphasic calcium release signifies that the calcium levels rise to a peak and eventually plateau to a concentration higher than the initial resting levels. The experiments were performed using a microfluidic device that generated periodic chemical patterns of stimulation on the seconds to minutes scale, similar to previously observed frequencies of calcium oscillations in cells (Boulware *et al*, 2008) and also encompassing neurotransmitter release rates (Li *et al*, 2003). We believe this study opens new possibilities for mechanistic studies where precise regulation of intracellular calcium signaling is required and potentially provides insight into how information is encoded chemically in biological systems.

II.2 Results:

Cell-to-cell variability in calcium oscillation frequency during continuous stimulation:

Upon exposure to constant chemical stimulation with 25 nM carbachol (CCh), cells exhibited intracellular calcium oscillations of highly variable frequencies (Fig. II.1a). This variability in oscillation frequency under continuous stimulation could be reproduced, to a degree, by using the mathematical model of Chay et al. (Chay *et al*, 1995; Cuthbertson and Chay, 1991) to which we added receptor dynamics and varied the receptor number (Fig. II.1b; Appendix A). Similar results are obtained if other physiologically relevant quantities, such as G protein number, show cell-to-cell variation; while cell-to-cell variability in terms of protein and parameter values was explored in this study, previous studies have shown that stochasticity in signal pathways can also account for the variability in individual calcium oscillation frequencies (Prank *et al*, 2005; Wood and Cadusch, 2005). Ultimately, a consequence of cell-to-cell variability is a lack of control of the timing of intracellular calcium signals.

Cell-to-cell variability in calcium oscillation frequency during periodic stimulation:
We next examined whether calcium response timing could be improved with periodic, rather than continuous, stimulation of cells. Using our modified version of the Chay et al.

model, we simulated exposure of the same cells from Fig. II.1b to periodic stimulation (Fig. II.1c). As had been predicted by Chay et al. (Chay *et al*, 1995), it was noted in experiments that not every stimulation event led to a corresponding intracellular calcium signal. For example, one of the two cells stimulated responded to every other stimulation input (top calcium trace in Fig. II.1c), indicative of compromised fidelity.

We then explored whether specific periodic stimulation parameters could improve calcium signal fidelity. We focused on three stimulation parameters: stimulant concentration (C), stimulation duration (D), and rest period (R). Latin Hypercube Sampling (LHS) was utilized to sample the values of two model parameters (number of receptors/cell and number of G proteins/cell) in order to simulate cell-to-cell variability; each model cell resulting from LHS was exposed to periodic stimulation and the percentage of cells exhibiting complete fidelity to the periodic signal was calculated. We found that as C, D, or R was increased (keeping the other two parameters fixed), the calcium response fidelity increased (Fig. II.2); with C in the biphasic regime (C = 100 nM), the percentage of cells attaining complete fidelity was 98%, compared with 63% in the oscillatory regime (C = 5 nM) for the same periodic stimulation conditions, indicating that biphasic concentrations potentially provided an effective method for manipulation of calcium signaling. In the biphasic regime, our model predictions put limitations on D, because if D was too large, then multiple spikes per stimulation event could result, thereby diminishing fidelity. Collectively, these simulation results provided concrete strategies for modulation of C, D, or R to overcome the limitations of implementing periodic stimulation to control intracellular signaling in a population of cells.

Periodic chemical stimulation generated with microfluidics:
In order to test how the stimulation parameters C, D, and R affected intracellular calcium signal fidelity experimentally, we developed a programmable, Braille-actuated microfluidic device capable of generating square-wave pulses of chemical stimulant (Fig. II.3a, b; Appendix B). One reservoir of the device was filled with media while the other was filled with stimulant dissolved in media. Alternately pumping liquid from each reservoir, while valving-off the other, resulted in pulse generation (Fig. II.3c); the pulses

could be generated reliably over long periods of time (Fig. II.3b). A custom-made program directly controlled the duration of the pulses, as well as the rest period between pulses, meaning a user could control D and R (Fig. II.3d), while C was controlled by the amount of stimulant added to the inlet reservoir.

By producing brief periodic pulses of the agonist carbachol to stimulate M3 receptor on HEK293 cells, the microfluidic setup could eliminate the variability in the timing of intracellular calcium signals; in other words, calcium signals only resulted when a stimulation pulse was applied. In contrast, addressing cells with a constant concentration of carbachol resulted in calcium oscillations of varied frequencies and timing among cells (Fig. II.1a, Fig. II.3e- left-most panel); exposure to square-wave pulses controlled the timing and number of spikes per stimulation pulse (Fig. II.3e). Pulses of sufficiently short stimulation duration (16 seconds) resulted in one calcium spike being produced only when carbachol pulses were supplied (Fig. II.3e- right-most panel). The stimulation pulse rise time was less than 1 second, while washing out (time to reach 10% C from 90% C) took less than 2 seconds (Fig. II.3f; Appendix B).

Improving fidelity in the calcium response:
Although carbachol pulsing eliminated variability in the timing of calcium signals, pulsing led to a different challenge in controlling intracellular calcium signals. As expected based on our theoretical analysis (Fig. II.1c), some cells did not respond to every stimulation pulse; in Fig. II.4, the red trace represents a cell that responded to every periodic chemical stimulation event, whereas the blue trace represents a neighboring cell that responded to every other stimulation event.

We assessed experimentally how stimulation parameters could be modified to improve the calcium signaling fidelity of a cell population. To assess the fidelity, 9 pulses of carbachol were applied and the percentage of cells that responded to all 9 stimulation pulses was evaluated (Fig. II.5a-c). As stimulant concentration (C), stimulation duration (D), or rest period (R) was increased, fidelity increased, as expected based on our theoretical results (Fig. II.2). However, as depicted in Fig. II.3e, there were limitations to

the length of D, since more than one spike could result per stimulation event; therefore D should be fixed at a maximum of about 30 s, since the period of calcium oscillations are rarely smaller than this (for our cell type and stimulant). Values of R on the order of 60 s yielded the highest fidelity in a cell population (Fig. II.5c); R values on the order of 10 min produced similar fidelity. For the purposes of providing user-control over the timing of intracellular calcium signals, it would be useful to be able to overcome these limitations in D and R.

We therefore explored use of different values of the ligand concentration C. Whereas with continuous stimulation, C must be below a certain value for cells to exhibit intracellular calcium oscillations (~ 25 nM for the cells tested here), pulsed stimulations using microfluidics allow use of C above this threshold concentration to still generate "oscillations". Using the same periodic stimulation conditions as those from Fig. II.5b and c, but using concentrations in the higher biphasic calcium signaling regime (100 nM), fidelity of the cell populations was on average >= 85% for each condition (Fig. II.5d, e). For the D values tested (16 s and 32 s), we did not observe a statistically significant difference in response fidelity, which would favor the use of shorter D values to avoid depletion of calcium stores (Fig. II.5d). For the R values tested (8 s and 64 s), we noted a statistically significant difference, indicating that longer R values are still more favorable for improving fidelity (Fig. II.5e). The ability to control calcium responses in the biphasic regime with our microfluidic setup is depicted in Fig. II.5f.

II.3 Discussion:

Periodic signals are manifested in a variety of signaling axes and organs; the periodicity of chemical signals provides information to target cells with regard to how to respond (Brabant *et al*, 1992; Goldbeter, 2008). Therefore, it is imperative to understand what the limitations of such cellular interpretations are and how these limitations can be overcome to achieve maximum control over intracellular signaling.

To address these questions, we developed a microfluidic setup that could address cells with pulses of chemical stimulant, and used calcium as a readout of intracellular

signaling. Using this setup, we revealed that control of intracellular signaling was limited by both noise and cell-to-cell variability. If each cell in a population has a unique response upon exposure to a uniform stimulus, coordination of cellular or tissue operations might be confounded. As predicted by our mathematical model of calcium signaling, because of noise and variability, each cell in a population responded uniquely to continuous chemical stimulation in terms of the frequency and timing of its calcium signals (Fig. II.1a). While the variability in calcium signal timing of individual cells was eliminated with periodic stimulation, cells exhibited compromised fidelity, indicated by skipped beats during a stimulation event (Fig. II.4- blue trace). Presumably, these differences in the timing and fidelity of calcium signaling would lead to differential responses, such as gene expression, secretion, contraction, proliferation (Berridge *et al*, 2000), and so on, since this signaling information is frequency encoded. Physiologically, compromised response fidelity to periodic stimulation can result in arrhythmias in cardiac systems (Guevara *et al*, 1981). In addition, the limitations of cellular response fidelity observed in our study would not have been attainable with previous setups for calcium signal control (Dolmetsch *et al*, 1998; Kuczenski *et al*, 2009). With these setups, the extracellular calcium concentration was used to dictate the intracellular concentration, thereby bypassing cells' native calcium signaling machinery. Since these approaches bypassed the cells' native signaling processes, the limitations caused by the upstream calcium generating elements on response fidelity could never be characterized.

With our microfluidic setup, we found that despite improvements in response fidelity that can be attained by augmenting stimulant concentration (C), stimulation duration (D), or rest period (R), skipped beats still result (Fig. II.5a-c). We found that by using C values in the biphasic regime of calcium signaling, fidelity could reach close to 100% for a variety of periodic stimulation conditions (Fig. II.5d, e); this finding may provide insight into the body's strategy for achieving maximal control over the timing of intracellular signals to carry out certain operations. The caveat with using C values in the biphasic regime may be that the mechanisms for generating biphasic and oscillatory calcium signals differ to the point where downstream targets are differentially affected; in addition, calcium stores may deplete rapidly and the calcium levels may drop rapidly for each stimulation event,

although a small D can be used to potentially reduce this effect. Ultimately, our microfluidic setup would provide an effective means of investigating all these points.

II.4 Materials and Methods:

Cell Culture:

HEK293 cells were cultured in DMEM (Invitrogen) supplemented with 10% FBS (Gibco) and were maintained at 37°C with 5% CO2 in 24-well plates. Cells were detached from plates using 0.25% Trypsin/EDTA (Gibco), and the resulting cell suspensions were transferred to the microfluidic setup. Media was supplemented 0.4 mg/mL Geneticin (Gibco) to select for cells stably transfected with the M3 receptor. The calcium FRET probe YC3.60 (Nagai *et al*, 2004) was transiently transfected into cells. Transfections were carried out with Lipofectamine2000 (Invitrogen) using the manufacturer's protocol.

Microfluidics:

Microfluidic device molds were fabricated as follows: front-side photolithography (Xia and Whitesides, 1998) was used to construct the outlet channel where cells were cultured; the remaining channels (inlets and "Braille" channels) were constructed with backside photolithography (Futai *et al*, 2004). PDMS (1:10 ratio of curing agent to base) was cast upon the positive relief features of the resulting glass mold and allowed to cure in a 60°C oven for at least 2 hours. 30 s plasma oxidation irreversibly sealed the resulting PDMS device to a thin (~100 μm) PDMS sheet. The device was filled with PBS and sterilized for 2 hrs in a UV oven after sealing. The chip was subsequently filled with 500 μg/mL fibronectin (Invitrogen) and allowed to incubate at 37°C for two hours, to ensure proper cell adhesion in the device. DMEM supplemented with 10% FBS was used to flush out and refill the device. Transfected HEK293 cells were then seeded from the outlet port and were appropriately positioned in the outlet hydrodynamically. The cells were then allowed to attach overnight.

In order to control the dynamic pumping mediated by Braille-actuation (Gu *et al*, 2004) and create the various temporal stimulation patterns used in experiments (Fig. II.1a), a

custom program written in Visual Basic was written. The nearly square-wave shape and reproducibility of these patterns was confirmed by experiments with fluorescein solution (Fig. II.3b). Characterizations of the pumping and wash times are provided in Appendix B. Carbachol (CCh) dissolved in imaging media (Palmer and Tsien, 2006) was added to one of the inlet reservoirs, and the other reservoir was filled with stimulant-free imaging media. A transparent indium tin oxide heater (situated between the objective and the thin PDMS-sheet upon which the cells were cultured) was used maintain the temperature for cells at 37°C (Heo *et al*, 2007).

Imaging:

A TE2000-U Nikon inverted microscope was used to image cells, using a 20x objective, a 490 nm long pass dichroic mirror, and a standard 100W mercury lamp. Fluorescence images of YC3.60-transfected cells were captured with a CoolSnap HQ2 camera (Photometrics, Tucson, AZ). Cells were excited at 450 nm and the emission signals were captured at 490 and 535 nm (filters from Chroma Technology Corp, Rockingham, VT). Photo-bleaching was reduced with an ND4 neutral density filter. Lambda 10-3 Shutter Controller (Sutter Instruments, Novato, CA) was used to control the excitation and emission filter wheels. Images were acquired every 3 s, and an exposure time of 100 ms was used. The program MetaFluor (Molecular Devices, Downington, PA) was implemented for image acquisition and processing; the background was subtracted, ratiometric images were constructed (intensity at 535 nm divided by intensity at 490 nm), and calcium FRET ratios of individual cells were generated with this software, for each emission image (at 490 nm and 535 nm). These FRET ratios (I) were normalized by the minimum FRET ratio obtained in the experimental run (I_0), and, as has been done previously (Sawano *et al*, 2002), I/I_0 was plotted in our figures. The normalized ratio values of the calcium peaks fell between 1.2 and 7.5, which was in accord with previously obtained values using the same FRET indicator (Nagai *et al*, 2004). The resulting images were then analyzed to assess the percentage of cells that exhibited complete fidelity for a particular experimental condition.

Computation of Fidelity Percentages:

Cells were exposed to 9 stimulation inputs, and the calcium response traces for each experimental condition were analyzed to determine the percentage of cells that responded to all 9 inputs. Calcium spikes that did not reach an amplitude greater than 33% of the maximum calcium spike height in an experimental run were counted as a skipped beat. In addition, for instances where more than one calcium spike resulted per stimulation event, this was also perceived as a lack of fidelity because the goal was to have only one calcium spike per stimulation event; thus if a cell exhibited more than one spike per stimulation event, it was deemed that the cell did not exhibit complete fidelity. Percent fidelity averages and standard errors of the mean were computed for each experimental condition. Statistics were based upon three experiments (each of no less than 20 cells) for each experimental condition. Between 65-106 cells were examined for each experimental condition. The Student's t-test was used to statistically compare pairs of experimental conditions; $p < 0.05$ was used as a threshold of statistical significance.

Mathematical models:

The oscillatory calcium model used for this study was a slight variation of that by Chay et al. (Chay *et al*, 1995; Cuthbertson *et al*, 1991). Under constant stimulation, the Chay et al. model exhibits oscillatory calcium spikes, whose frequency increases as the stimulation input increases. Calcium oscillations are generated by virtue of a feedback loop where G-proteins activate PLC, PLC produces IP3, and IP3 both initiates calcium release and inhibits G-protein activity.

For this study, simple ligand-receptor dynamics were added to the Chay et al. model, using binding (0.004 1/(nM*s)) and dissociation constants (0.5 1/s) obtained from literature values of carbachol binding to muscarinic receptors (Schreiber *et al*, 1985); the ligand-receptor complex promoted G-protein activation. Subsequent dynamics were identical to the original model.

All original parameters were unchanged, except for 'kg' and the basal G-protein activation term. In our model, the parameter 'kg' was held constant at a value of $3.875*10^{-5}$ 1/(nM*s); this parameter represents the receptor-mediated G-protein

activation constant and in the original model had been used to control the calcium response. The basal G-protein activation term in our model was changed to 0.009 1/s (from the original value of 0.005 1/s) in order to ensure that the receptor dynamics did not alter the calcium dynamics. More details about the model are provided in Appendix A.

The model was coded in MATLAB version 7.8.0 (MathWorks Inc, Natick, MA) and the system of ODEs was solved with the stiff solver ode15s.

Latin hypercube sampling:

We used Latin Hypercube Sampling (LHS) to generate random model cells, to simulate experimentally observed cell-to-cell variability (Fig. II.1a). LHS is a highly effective method for exploring parameter spaces for mathematical models (Blower and Dowlatabadi, 1994; Kinzer-Ursem and Linderman, 2007; Marino *et al*, 2008; McKay *et al*, 1979). Using LHS code from Marino et al. (2008) (http://malthus.micro.med.umich.edu/lab/usadata/), we varied model parameter values by sampling from a normal distribution with a 75% standard deviation; original parameter values were used as the mean. For the Chay et al. model, we varied two parameters: receptor number/cell and G-protein number/cell. For each periodic stimulation condition, LHS was run for 500 iterations, thereby generating 500 model cells with different receptor and G-protein numbers. The percent response fidelity of the model cell population was assessed by hand for each periodic stimulation condition (Fig. II.2).
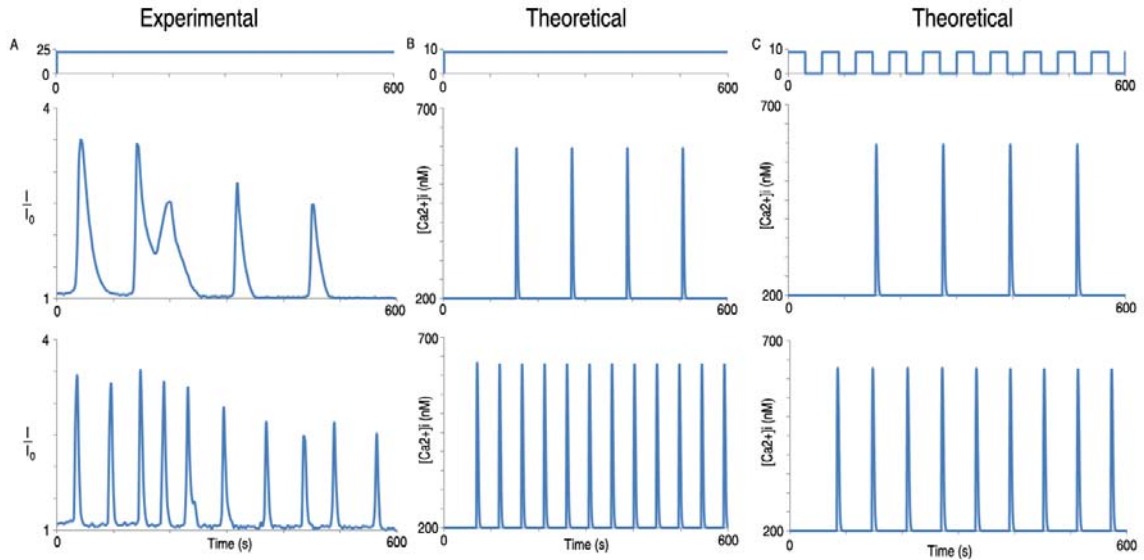
Fig. II.1 Control of the timting of intracellular calcium signaling is challenging due to cell-to-cell variability. a) Under continuous carbachol stimulation stimulation (25 nM), HEK293 cells exhibit intracellular calcium oscillations with differing periods due to cell-to-cell variability. b) Under continuous stimulation, a mathematical model of calcium signaling exhibits different oscillation periods by virtue of differences in receptor number ($\sim 8*10^4$ for top case vs $\sim 8*10^5$ for the bottom case). c) Under periodic stimulation (stimulant concentration = 10 nM, stimulation duration = 24 s, rest period = 24 s), the model cells from b) exhibit calcium oscillations only during stimulation events. However, as depicted in the top trace, not every stimulation event leads to a calcium response, indicative of skipped beats. This loss in fidelity is due to cell-to-cell variability.
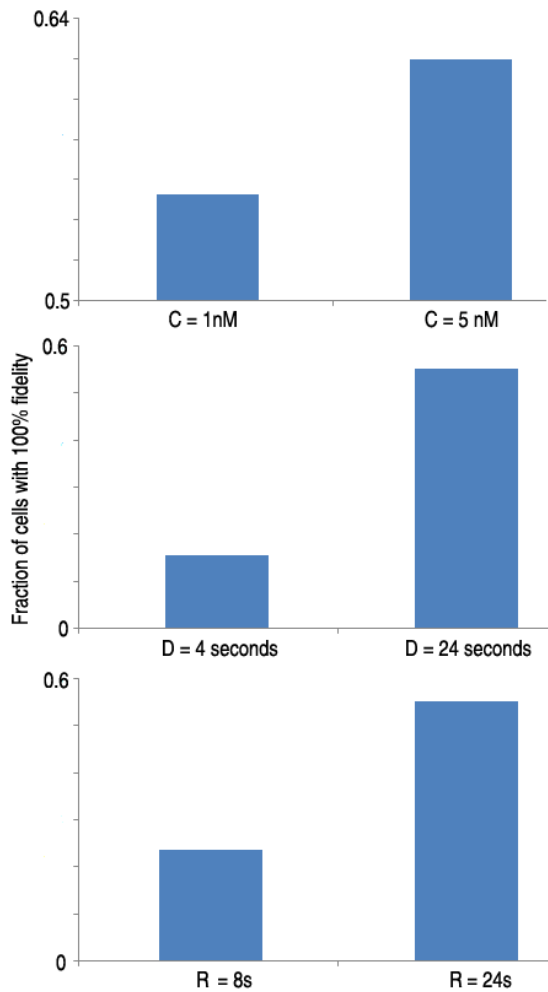
**Fig. II.2** Modulation of periodic stimulation parameters are predicted to improve fidelity of calcium responses despite cell-to-cell variability using mathematical models. As C, D, or R is increased, the fraction of model cells exhibiting 100% fidelity increased. 500 model cells were analyzed for each periodic stimulation condition, by varying receptor and G-protein number using Latin Hypercube Sampling.
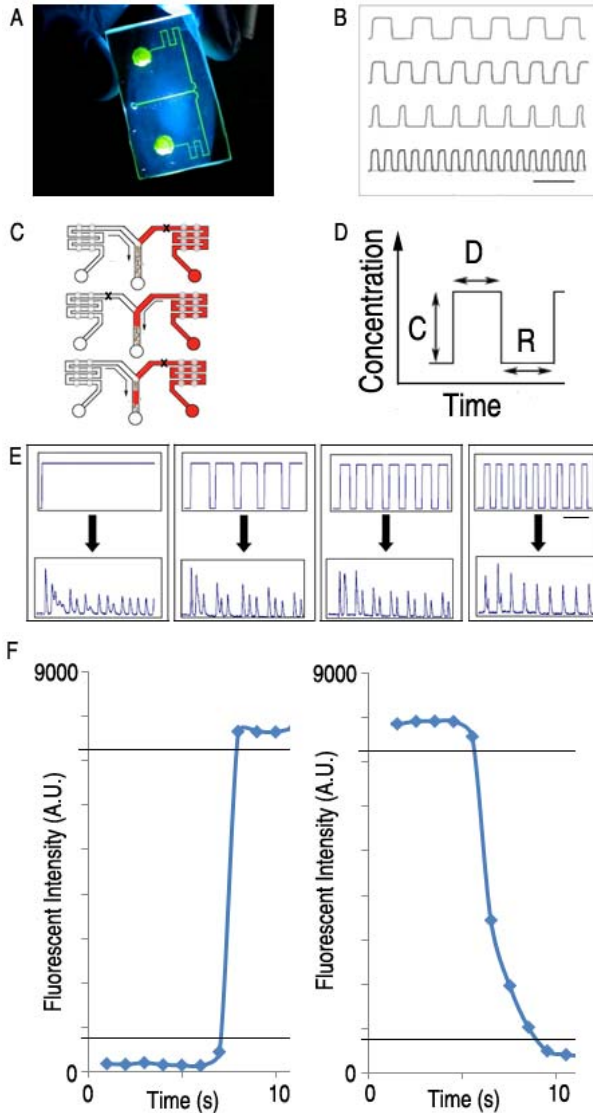
Fig. II.3 Experimental setup for periodic stimulation of cells. a) Braille-actuated microfluidic device filled with fluorescein solution. b) The microfluidic setup is able to produce stimulation pulses of varying duration and frequency, and high reproducibility, as assessed by experiments with fluorescein solution. (scale bar = seconds) c) Stimulation pulses are created alternately pumping from a reservoir with cell media and a reservoir with the chemical stimulant, while valving off the reservoir not in use (designated by an 'x'). d) With the microfluidic setup, a user can control D and R, while C is the concentration of chemical stimulant directly added to the reservoir. e) Demonstration of direct control of oscillatory intracellular calcium signals; under continuous stimulation, cells exhibit calcium oscillations (leftmost panel). Under periodic stimulation, the duration of stimulation determines the number of spikes per stimulation event. As the stimulation duration was diminished, the number of spikes was decreased from three, to two, to one, per stimulation event. (scale bar = 64 seconds) f) Rise (< 1 s) and wash time (< 2 s) of stimulation pulses generated by the microfluidic device, assessed by experiments with fluorescein. The horizontal black lines represent the 10% and 90% concentration levels.
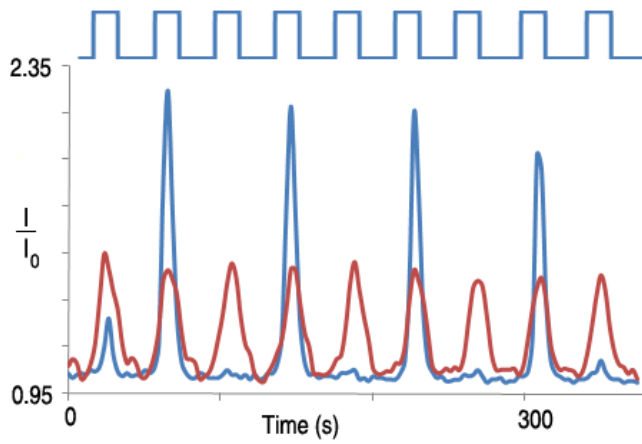
Fig. II.4 Calcium response fidelity to periodic stimulation is compromised by cell-to-cell variability, as predicted in Fig. II.1c. With C = 10 nM, D = 16 s, and R = 24 s, one cell in the experimental population (red trace) responded to every periodic stimulation event, while another cell (blue trace) responded to every other stimulation event.
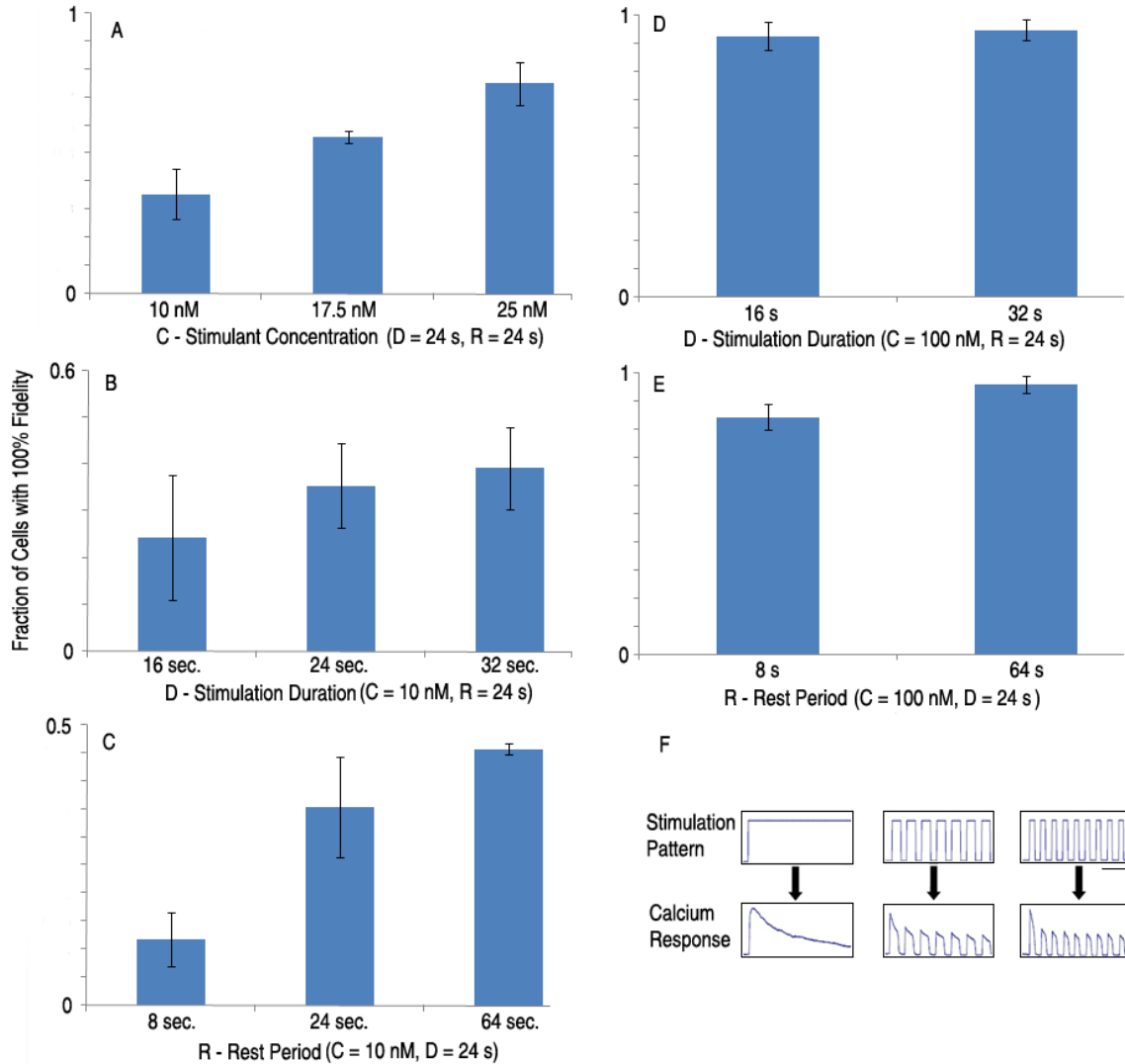
Fig. II.5 Modulation of periodic stimulation parameters can improve calcium signal response fidelity. a)-c) As C, D, or R are increased, the percentage of cells in the population exhibiting 100% fidelity increased. For a), D and R were both fixed at 24 s; for b), C and R were fixed at 10 nM and 24 s respectively; for c) C and D were fixed at 10 nM and 24 s respectively. d)-e) Using stimulant concentrations in the biphasic regime of calcium signaling (100 nM) improved signal fidelity to levels close to 100%, demonstrating that despite cell-to-cell variability, the timing of intracellular signaling of entire cell populations could be controlled. For d), C and R were fixed at 100 nM and 24 s respectively; for e), C and D were fixed at 100 nM and 24 s respectively. f) Control of calcium signals with carbachol concentrations in the biphasic regime (100 nM) (scale bar = 64 s). For a)-e), between 65-106 cells were examined for each experimental condition. Bars represent the S.E.M and the Student's t-test was used to statistically compare pairs of experimental conditions; $p < 0.05$ was used as a threshold of statistical significance.

II.5 References:

Berridge MJ, Lipp P, Bootman MD (2000) The versatility and universality of calcium signalling. *Nat Rev Mol Cell Biol* **1:** 11-21.

Blower SM, Dowlatabadi H (1994) Sensitivity and uncertainty analysis of complex-models of disease transmission- an HIV model, as an example. *Int Stat Rev* **62:** 229-243.

Boulware MJ, Marchant JS (2008) Timing in cellular Ca2+ signaling. *Curr Biol* **18:** R769-R776.

Brabant G, Prank K, Schofl C (1992) Pulsatile patterns in hormone-secretion. *Trends Endocrinol Metab* **3:** 183-190.

Chay TR, Lee YS, Fan YS (1995) Appearance of phase-locked Wenckebach-like rhythms, devil's staircase and unviersality in intracellular calcium spikes in nonexcitable cell models. *J Theor Biol* **174:** 21-44.

Cuthbertson KSR, Chay TR (1991) Modeling receptor-controlled intracellular calcium oscillators. *Cell Calcium* **12:** 97-109.

Dolmetsch RE, Xu KL, Lewis RS (1998) Calcium oscillations increase the efficiency and specificity of gene expression. *Nature* **392:** 933-936.

Futai N, Gu W, Takayama S (2004) Rapid prototyping of microstructures with bell-shaped cross-sections and its application to deformation-based microfluidic valves. *Adv Mater* **16:** 1320-1323.

Goldbeter A (2008) Biological rhythms: Clocks for all times. *Curr Biol* **18:** R751-R753.

Gu W, Zhu XY, Futai N, Cho BS, Takayama S (2004) Computerized microfluidic cell culture using elastomeric channels and Braille displays. *Proc Natl Acad Sci U S A* **101:** 15861-15866.

Guevara MR, Glass L, Shrier A (1981) Phase Locking, Period-Doubling Bifurcations, and Irregular Dynamics in Periodically Stimulated Cardiac-Cells. *Science* **214:** 1350-1353.

Heo YS, Cabrera LM, Song JW, Futai N, Tung YC, Smith GD, Takayama S (2007) Characterization and resolution of evaporation-mediated osmolality shifts that constrain microfluidic cell culture in poly(dimethylsiloxane) devices. *Anal Chem* **79:** 1126-1134.

Jacob R, Merritt JE, Hallam TJ, Rink TJ (1988) Repetitive spikes in cytoplasmic calcium evoked by histamine in human endothelial cells. *Nature* **335:** 40-45.

Kinzer-Ursem TL, Linderman JJ (2007) Both ligand- and cell-specific parameters control ligand agonism in a kinetic model of G protein-coupled receptor signaling. *PLoS Comput Biol* **3:** 84-94.

Kuczenski B, Ruder WC, Messner WC, LeDuc PR (2009) Probing Cellular Dynamics with a Chemical Signal Generator. *PLoS One* **4:** 8.

Li Y, Wu XY, Zhu JX, Yan J, Owyang C (2003) Hypothalamic regulation of pancreatic secretion is mediated by central cholinergic pathways in the rat. *J Physiol-London* **552:** 571-587.

Luo D, Broad LM, Bird GSJ, Putney JW (2001) Signaling pathways underlying muscarinic receptor-induced [Ca2+](i) oscillations in HEK293 cells. *J Biol Chem* **276:** 5613-5621.

Marino S, Hogue IB, Ray CJ, Kirschner DE (2008) A methodology for performing global uncertainty and sensitivity analysis in systems biology. *J Theor Biol* **254:** 178-196.

McKay MD, Beckman RJ, Conover WJ (1979) Comparison of 3 methods for selecting values of input variables in the analysis of output from a computer code. *Technometrics* **21:** 239-245.

Nagai T, Yamada S, Tominaga T, Ichikawa M, Miyawaki A (2004) Expanded dynamic range of fluorescent indicators for Ca2+ by circularly permuted yellow fluorescent proteins. *Proc Natl Acad Sci U S A* **101:** 10554-10559.

Palmer AE, Tsien RY (2006) Measuring calcium signaling using genetically targetable fluorescent indicators. *Nat Protoc* **1:** 1057-1065.

Prank K, Waring M, Ahlvers U, Bader A, Penner E, Moller M, Brabant G, Schofl C (2005) Precision of intracellular calcium spike timing in primary rat hepatocytes. *Syst Biol* **2:** 31-34.

Prentki M, Glennon MC, Thomas AP, Morris RL, Matschinsky FM, Corkey BE (1988) Cell-specific patterns of oscillating free Ca2+ in carbamylcholine-stimulated insulinoma cells. *J Biol Chem* **263:** 11044-11047.

Rapp PE (1987) Why are so many biological systems periodic. *Prog Neurobiol* **29:** 261-273.

Sawano A, Takayama S, Matsuda M, Miyawaki A (2002) Lateral propagation of EGF signaling after local stimulation is dependent on receptor density. *Dev Cell* **3:** 245-257.

Schreiber G, Henis YI, Sokolovsky M (1985) Rate constants of agonist binding to muscarinic receptors in rat-brain medulla- Evaluation by competition kinetics. *J Biol Chem* **260:** 8795-8802.

Wood AW, Cadusch PJ (2005) Cell calcium oscillations: the origin of their variability. *Med Biol Eng Comput* **43:** 200-205.

Woods NM, Cuthbertson KS, Cobbold PH (1986) Repetitive transient rises in cytoplasmic free calcium in hormone-stimulated hepatocytes. *Nature* **319:** 600-602.

Xia YN, Whitesides GM (1998) Soft lithography. *Annu Rev Mater Sci* **28:** 153-184.

51

Chapter III.

Large-scale modulation of cellular response fidelity through changes in protein levels

III.1 Introduction:

Proper decoding of time-varying second messenger signals, such as calcium signaling, by corresponding downstream targets is critical for a variety of processes, including gene expression, cell death or survival, differentiation, and secretion (Berridge *et al*, 2003; 2008). To ensure efficient execution of these cellular operations, messengers must accurately transmit information from activated receptors to intracellular protein machinery. In the previous chapter, it was delineated that periodic stimulation parameters (stimulant concentration, stimulation duration, and rest period) had a profound effect upon calcium response fidelity. In this chapter, the effects of intrinsic parameters, such as cellular protein levels, on calcium response fidelity under periodic stimulation are assessed.

For this study, the levels of M3 muscarinic receptor and Regulator of G-protein Signaling (RGS) proteins were modified; these proteins have garnered a great deal of attention as therapeutic targets (Felder *et al*, 2000; Neubig and Siderovski, 2002), and as such may play a crucial role in terms of intracellular signaling fidelity. RGS proteins simulate the rapid hydrolysis of GTP bound to activated G-proteins, have been implicated as mediators of calcium signaling (Luo *et al*, 2001b), and play a crucial role in a variety of cardiac and neuronal capacities (Gold *et al*, 1997; Hendriks-Balk *et al*, 2008). M3 receptors are in the G-protein-coupled receptor (GPCR) family and are also highly expressed in the brain, lungs, muscle, and heart (Caulfield, 1993), and have recently been found to play a critical role in pancreas function (Gautam *et al*, 2006). Upon activation, these receptors engage a signaling cascade that eventually results in oscillatory or biphasic intracellular calcium signaling (depending upon the concentration of stimulant

used to activate the receptor) (Luo *et al*, 2001a). While it was seemingly obvious that increasing the concentration of RGS proteins and decreasing the M3 receptor density would decrease calcium response fidelity, it was uncertain how sensitive fidelity was to changes in these intrinsic factors under fixed periodic stimulation conditions; in other words: are small changes in receptor number or RGS protein concentration sufficient to precipitously alter calcium response fidelity?

To provide insight into this facet, the mathematical model of calcium signaling from the previous chapter was used. The calcium model system was subjected to periodic stimulation with fixed stimulant concentration, stimulation duration, and rest period, while the number of receptors or Regulator of G-protein Signaling (RGS) protein concentration was varied. These theoretical results showed that under some periodic stimulation conditions, a < 5% change in receptor density or RGS concentration could dramatically reduce the calcium response fidelity such that only half of the stimulation events were transmitted successfully into calcium responses. These dramatic fidelity modulations resulting from small changes in intrinsic parameters suggest that fidelity could be quite sensitive in this context. Based upon these theoretical predictions, the role of M3 receptor density and RGS proteins in altering calcium response fidelity was investigated experimentally.

To evaluate the effect of receptor density and RGS proteins on calcium response fidelity, the cellular system and microfluidic platform from the previous chapter were used. For this study, mammalian cells were subjected to identical periodic stimulation patterns in the presence and absence of atropine, an antagonist of muscarinic receptors, thereby mimicking changes in muscarinic receptor density. To modulate the levels of RGS, a doxycycline-inducible system was implemented; upon exposure to doxycycline, cells upregulated the level of the protein RGS4. Fidelity was significantly reduced with a decrease in muscarinic receptor density and an increase in RGS4 concentration, signifying that these are crucial intrinsic parameters to consider in this context, as had been predicted theoretically.

Since calcium signaling is intimately linked with a variety of other cellular transduction pathways, low calcium response fidelity is predicted to have consequences on a number

of signaling systems. A prominent intracellular component intimately linked to calcium signaling is cAMP, which has been found to oscillate in phase with calcium (Gorbunova and Spitzer, 2002) and is prominently associated with orchestrating gene expression (Montminy, 1997). Reduced fidelity is predicted to not only have an effect on the timing of cAMP signals but also on the average amplitude, suggesting that this mode of calcium signaling can have a significant effect on this pathway. In this regard, the results presented in this chapter show that intrinsic components like the M3 receptor and RGS proteins might be viable targets for improving calcium response fidelity in situations where low fidelity is detrimental.

III.2 Results and Discussion:

Mathematical modeling of effect of receptor density on calcium response fidelity to periodic stimulation:

A modified version of the intracellular calcium model by Chay et al. (Chay *et al*, 1995; Cuthbertson and Chay, 1991) was used to understand the effect that receptor density has on the fidelity of calcium signals (Appendix A). The Chay et al. model was altered such that receptor dynamics were added, with binding and dissociation kinetics representative of carbachol binding to M3, as was done in the previous chapter. Fidelity was measured by computing the phase-locking ratio: the number of calcium responses was divided by the number of stimulation pulses; a phase-locking ratio with value one would represent a cell that responded to every stimulation pulse, whereas a cell that responded to every other stimulation pulse would have a phase-locking ratio of 0.5. This metric was chosen in order to easily discern not only the effects that intrinsic cellular parameters had on fidelity, but how precipitously these changes in fidelity occurred.

With the mathematical model of calcium signaling, periodic stimulation parameters (stimulant concentration, stimulation duration, and rest period) were fixed and the receptor number was varied in a physiologically relevant range (Fig. III.1- right graph); for this figure, the periodic stimulation patterns used was: stimulant concentration = 30 nM, stimulation duration = 10 s, and rest period = 70 s. For each receptor density, the

phase-locking ratio was assessed. As the receptor number was increased, the phase-locking ratio correspondingly increased as had been expected.

However, upon closer inspection, it was found that small differences in receptor density (< 5% difference) could determine the difference between high (Fig. III.1- top) and low fidelity (Fig. III.1- bottom). The latter case has potentially detrimental physiological consequences, as has been shown in cardiac systems (Guevara *et al*, 1981). Based upon the results depicted in Fig. III.1, noise inherent in the signal pathway could render control of calcium response fidelity extremely challenging under these conditions since the cell could easily jump between two fidelity states (low and high). Ultimately, this would suggest that receptor number is a substantial parameter to consider when determining the optimal periodic stimulation pattern for signal transmission.

Mathematical modeling of effect of RGS concentration on calcium response fidelity to periodic stimulation:

The modified Chay et al. model (Chay *et al*, 1995; Cuthbertson *et al*, 1991) was used to predict the role of RGS proteins in dictating the calcium response fidelity. Upon exposure to a fixed periodic stimulation pattern (the same used above), the RGS concentration was varied and the corresponding phase-locking ratio for each concentration was plotted. As expected, as the RGS concentration was increased, the phase-locking ratio decreased.

However, it was discovered that (as had been the case for receptor density) small differences in RGS concentration could result in large differences in fidelity (Fig. III.1- left graph). As discussed above, noise may play a prominent role in how the cell responds to periodic chemical stimulation. Furthermore, the phase-locking graphs depicted in Fig. III.1 illustrate how a cell may be able to actively tune its degree of responsiveness: with a phase-locking ratio of 0.5, a cell may have a feedback mechanism that could slightly increase the number of receptors or decrease the concentration of RGS, enabling the cell to reach complete fidelity, making the cell more robust against noise effects. This type of feedback system would be similar to a phase-locked loop, an implement used in electronics to synchronize a circuit to an oscillatory signal where negative feedback is proportional to the error between the input and output frequencies (Hsieh and Hung,

1996); instances where cells display low calcium response fidelity and switch to high fidelity have been observed on occasion experimentally (Fig. III.2). Collectively, our theoretical results predict that receptor density and RGS concentration are potent modulators of calcium signaling fidelity, and are perhaps crucial elements to consider when determining optimal periodic stimulation conditions.

Experimental alteration of receptor density modulates calcium response fidelity:

The microfluidic platform described in the previous chapter was used to expose mammalian (HEK293) cells to periodic stimulation with the acetylcholine analog carbachol (CCh), which resulted in M3 activation and oscillatory calcium release; cells were exposed to 25 nM CCh for 24 seconds and washed for 24 seconds in the presence and absence of 1 nM atropine. Atropine is an antagonist for muscarinic receptors, and mimicked a reduction in the average M3 receptor density. Comparison of the average phase-locking ratios for the two cases revealed that the treated cells exhibited a phase-locking ratio which was nearly half of the untreated case (Fig. III.3- top). These results confirmed theoretical predictions of the prodigious effect of receptor density upon calcium response fidelity, indicating that the model was accurate in this capacity and also portraying that M3 is a potential pharmacological target for modulating calcium response fidelity.

Experimental alteration of RGS concentration modulates calcium response fidelity:

To analyze the effect of RGS concentration on calcium response fidelity, HEK293 cells in the microfluidic device were exposed to doxycycline, which augmented the RGS concentration and were then exposed to the same periodic stimulation pattern as above. The resulting average phase-locking ratio was again lower than that of the untreated case (Fig. III.3- bottom), although not as dramatically compared with application of 1 nM atropine. These results again confirmed theoretical predictions that RGS concentration could have a significant effect upon calcium response fidelity, indicated model accuracy in this facet, and demonstrated that RGS proteins are a potential pharmacological target for altering calcium response fidelity.

Downstream consequences of compromised calcium response fidelity:

To demonstrate that low calcium response fidelity can have a potentially detrimental downstream effect, a mathematical model of cAMP signaling was used to show that this prominent signaling pathway would be adversely affected as well. cAMP has been found to oscillate in phase with calcium signals (Gorbunova *et al*, 2002), and therefore figures to be profoundly affected by calcium response fidelity. Using the model developed by Gorbunova et al. (2002), the system was exposed to periodic stimulation with the same stimulation duration and rest period as those used in Fig. III.1. Two stimulation strength values (parameter α_2) that differed by 10% were used, where the higher concentration led to high calcium response fidelity, with phase-locking ratio of 1 (Fig. III.4- top), and the lower concentration showed a low calcium response fidelity, with phase-locking ratio of 0.5 (Fig. III.4- bottom). Compared to the case exhibiting complete fidelity, the skipping case showed not only half the cAMP frequency, but the average cAMP level was about half as well (Fig. III.4- middle). These results therefore predict that cAMP frequencies and amplitudes are affected by calcium response fidelity, suggesting that cAMP-mediated cell operations would be drastically effected as well. These results provide further motivation for taking intrinsic parameters, such as receptor density and RGS concentration, into account for determining optimal periodic stimulation conditions.

III.3 Conclusions:

In this chapter, the sensitivity of calcium response fidelity to changes in intrinsic parameters was tested theoretically using the mathematical model from Chapter II. Under some periodic stimulation conditions, very small changes in receptor number and RGS concentration were able to reduce the number of calcium signals transmitted by half, as assessed by the phase-locking ratio. To gain insight into these theoretical observations, the microfluidic setup from Chapter II was used to periodically stimulate cells with reduced receptor density or upregulated RGS concentration. In both cases, the calcium response fidelity was significantly reduced compared to untreated cells, demonstrating that these two intrinsic parameters are important to consider, in addition to the stimulation parameters themselves. Should low calcium response fidelity prove to be deleterious in a clinical context, these results suggest that receptor number or RGS concentration are parameters that are potentially alterable to improve signal transmission.

Since calcium signaling is intimately linked with a number of pathways, the potential downstream consequences of low calcium response fidelity were explored with a previously-published mathematical model of calcium/cAMP signaling. Strikingly, these results portrayed that both cAMP frequency and amplitude were affected by low calcium response fidelity, which suggests a harmful, amplified effect upon cellular function. In sum, the results presented here portray that while low calcium response fidelity can be potentially harmful, the sensitivity of this fidelity can be adjusted by altering the number of receptors and RGS proteins.

III.4 Materials and Methods:

Cell Culture:

HEK293 cells were cultured in DMEM supplemented with 10% FBS (Gibco) and were maintained at 37°C with 5% CO2 in 24-well plates. Cells were detached from plates using 0.25% Trypsin/EDTA (Gibco), and the resulting cell suspensions were transferred to the microfluidic setup. Media was supplemented 0.4 mg/mL Geneticin (Gibco) to select for cells stably transfected with the M3 receptor, and 0.2 mg/mL Hygromycin (Invitrogen) and 15 μg/mL Blasticidin was used to select for cells transfected with the Flp-In/T-REx system for doxycyline-inducible RGS4 expression. In order to induce increased RGS4 expression, media with 1 μg/mL doxycycline was added to cells for approximately 48 hrs. The calcium FRET probe YC3.60 (Nagai *et al*, 2004) was transiently transfected into cells. Transfections were carried out with Lipofectamine2000 using the manufacturer's protocol. All reagents were purchased from Invitrogen, unless otherwise noted.

Microfluidics:

Fabrication and operation of the microfluidic device were identical to the protocol presented in Chapter II. Briefly, a combination of soft photolithography (Xia and Whitesides, 1998) and backside photolithography (Futai *et al*, 2004) were used to create the mold for the microfluidic device. PDMS was cast upon these positive relief features and allowed to cure. The device was then bonded to a thin PDMS sheet and transfected HEK293 cells were seeded and allowed to adhere overnight. Periodic stimulation of cells

with carbachol was mediated by Braille-actuated pumping (Gu *et al*, 2004), and temperature was maintained at 37°C using an indium tin oxide heater (Heo *et al*, 2007). For experiments, cells were cultured in imaging media (Palmer and Tsien, 2006) to reduce the background. Details about the pumping and washing characteristics are provided in Appendix B.

Imaging:

A TE2000-U Nikon inverted microscope was used to image cells, using a 20x objective, a 490 nm long pass dichroic mirror, and a standard 100W mercury lamp. Fluorescence images of YC3.60-transfected cells were captured with a CoolSnap HQ2 camera (Photometrics, Tucson, AZ). Cells were excited at 450 nm and the emission signals were captured at 490 and 535 nm (filters from Chroma Technology Corp, Rockingham, VT). Photo-bleaching was reduced with an ND4 neutral density filter. Lambda 10-3 Shutter Controller (Sutter Instruments, Novato, CA) was used to control the excitation and emission filter wheels. Images were acquired every 3 s, and an exposure time of 100 ms was used. The program MetaFluor (Molecular Devices, Downington, PA) was implemented for image acquisition and processing; the background was subtracted, ratiometric images were constructed (intensity at 535 nm divided by intensity at 490 nm), and calcium FRET ratios of individual cells were generated with this software, for each emission image (at 490 nm and 535 nm). These FRET ratios (I) were normalized by the minimum FRET ratio obtained in the experimental run (I_0), and, as has been done previously (Sawano *et al*, 2002), I/I_0 was plotted in our figures. The normalized ratio values of the calcium peaks fell between 1.2 and 7.5, which was in accord with previously obtained values using the same FRET indicator (Nagai *et al*, 2004). The resulting images were then analyzed to assess the percentage of cells that exhibited complete fidelity for a particular experimental condition.

Computation of phase-locking ratios:

Cells were exposed to 9 stimulation inputs, and the number of calcium responses for each run was recorded. For instance, for a cell that had been exposed to 9 CCh stimulation pulses and responded with 6 calcium spikes, the phase-locking ratio was computed as

0.67. Calcium spikes that did not reach an amplitude greater than 33% of the maximum calcium spike height in an experimental run were not counted as true calcium spikes, and were deemed sub-threshold calcium spikes. Phase-locking ratios were computed for individual cells, and averages and standard errors of the mean were computed for each experimental condition. Statistics were based upon three experiments (each of no less than 20 cells) for each experimental condition. Between 85-106 cells were examined for each experimental condition. To monitor the effect of atropine upon the calcium phase-locking ratio, cells were stimulated with 25 nM CCh for 24 s and washed for 24 s in the presence and absence of 1 nM atropine. Similarly, the same periodic stimulation patterns was used with cells that had upregulated RGS4 expression, in order to observe the effect that RGS had upon the phase-locking ratio. The student t-test was used to statistically compare pairs of experimental conditions; $p < 0.05$ was used as a threshold of statistical significance.

Mathematical models:

The oscillatory calcium model used for this study was a slight variation of that by Chay et al. (Chay *et al*, 1995; Cuthbertson *et al*, 1991). Under constant stimulation, the Chay et al. model exhibits oscillatory calcium spikes, whose frequency increases as the stimulation input increases. Calcium oscillations are generated by virtue of a feedback loop where G-proteins activate PLC, PLC produces IP3, and IP3 both initiates calcium release and inhibits G-protein activity. For this study, simple ligand-receptor dynamics were added to the Chay et al. model, using binding (0.004 1/(nM*s) and dissociation constants (0.5 1/s) obtained from literature values of carbachol binding to muscarinic receptors (Schreiber *et al*, 1985); the ligand-receptor complex promoted G-protein activation. Subsequent dynamics were identical to the original model. All original parameters were unchanged, except for 'kg' and the basal G-protein activation term. In our model, the parameter 'kg' was held constant at a value of 0.017 1/(nM*s); this parameter represents the receptor-mediated G-protein activation constant and in the original model had been used to control the calcium response. The basal G-protein activation term in our model was changed to 0.009 1/s (from the original value of 0.005 1/s) in order to ensure that the receptor dynamics did not alter the calcium dynamics.

To predict the effect of changes in receptor density on the phase-locking ratio, model cells were exposed to the same stimulation pattern while the receptor density was varied (Fig. III.1- right side). Receptor protein concentrations were converted into receptor number by assuming that cells were spherical and had a radius of 2.5 μm; multiplying the resulting volume by the receptor protein concentration yielded the corresponding receptor number, which was in the range of previously measured values (Pinkaskramarski *et al*, 1988). The same periodic stimulation pattern was used as the RGS concentration was varied (Fig. III.1- left side). Hydrolysis rates were converted into RGS concentrations by using the linear relationship for G-protein hydrolysis rate vs. RGS4 concentration obtained by Lan et al. (2000); it must be noted that for this case, the G-proteins in question were his-tagged Gi-proteins, and not Gq-proteins that are associated with M3 receptor signaling. It was found that oscillations could not be produced in the model using experimentally measured RGS-mediated Gq-protein hydrolysis rates (Mukhopadhyay and Ross, 1999), because the values were too high. More details about the mathematical model is provided in Appendix A.

For the calcium-cAMP model developed by Gorbunova et al. (2002), all original parameters were used. The parameter α_2 represented the amplitude of periodic stimulation for this study. All models were coded in MATLAB version 7.8.0 (MathWorks Inc, Natick, MA) and the system of ODEs was solved with the stiff solver ode15s.
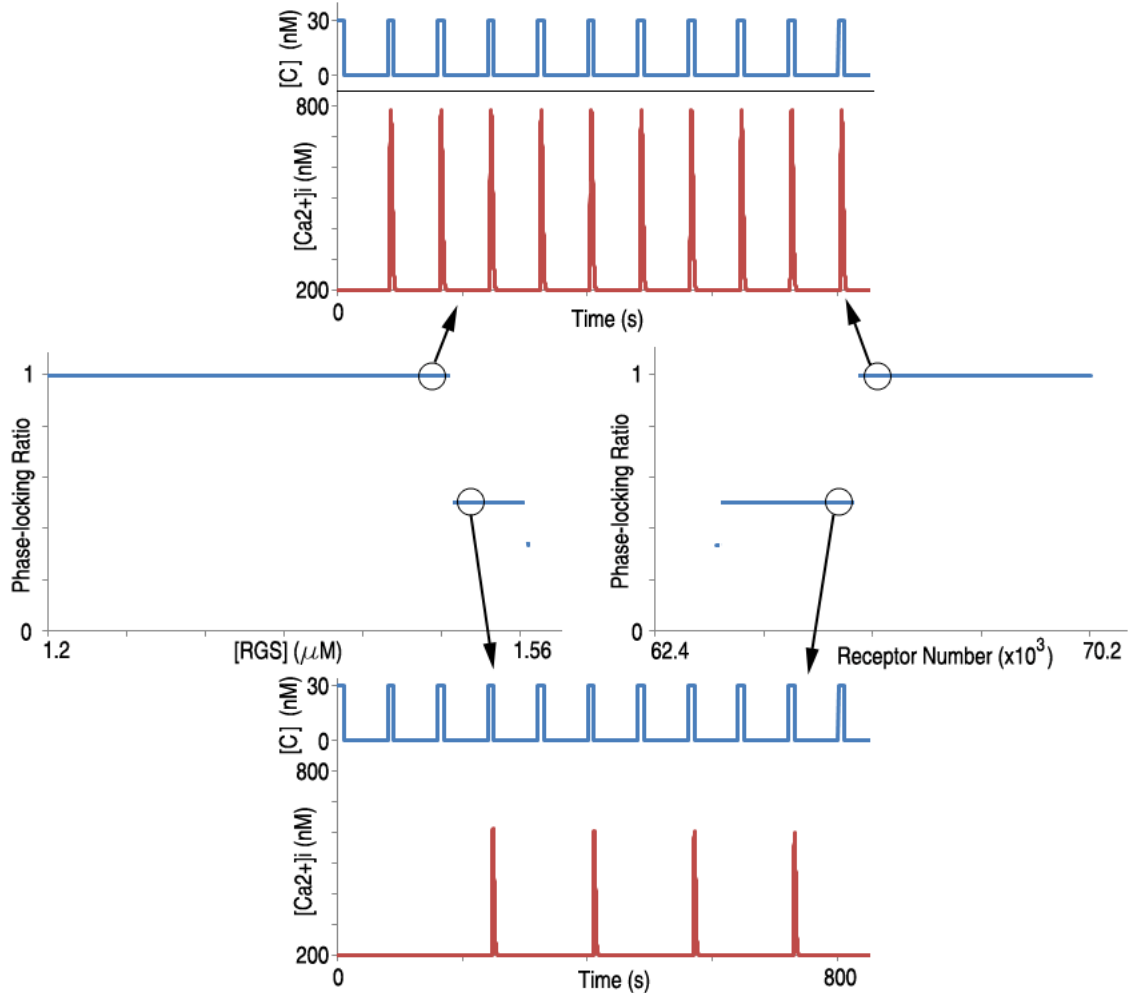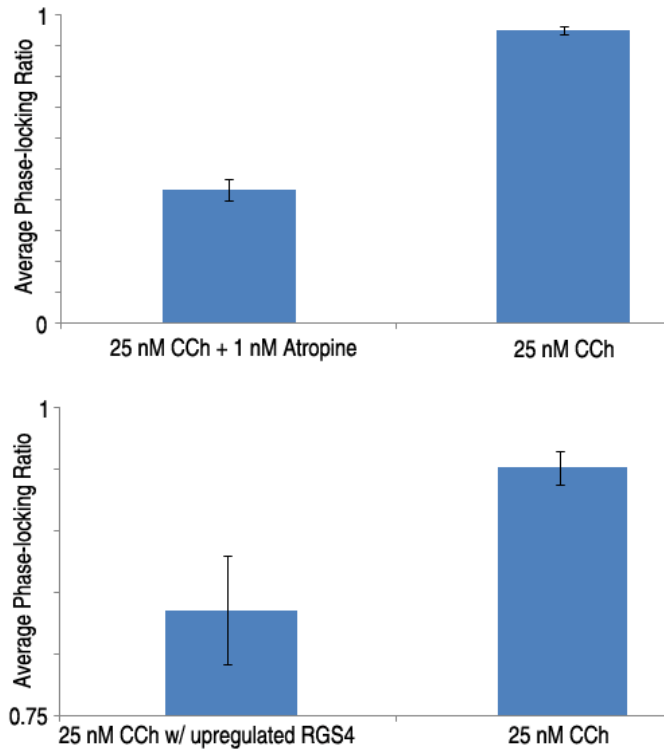
Fig. III.1 Drastic shifts in calcium response fidelity caused by small changes in receptor number and RGS concentration predicted by mathematical models of oscillatory calcium signaling. The modified Chay et al. model predicts that as RGS concentration increases (left graph), the phase-locking ratio decreases, reflecting a decrease in fidelity (compare upper and lower graphs). The circles on the graph show that a 5% change in concentration can result in a change of phase-locking ratio from 1 to 0.5, under these periodic stimulation conditions. As the receptor number increases, the phase-locking ratio increases. Under these periodic stimulation conditions, if the receptor number is changed by 5%, the phase-locking ratio decreases from 1 to 0.5 (right graph). The periodic stimulation pattern used here was: stimulant concentration = 30 nM, stimulation duration = 10 s, and rest period = 70 s. Computation of RGS concentration and receptor number are explained in the methods section.
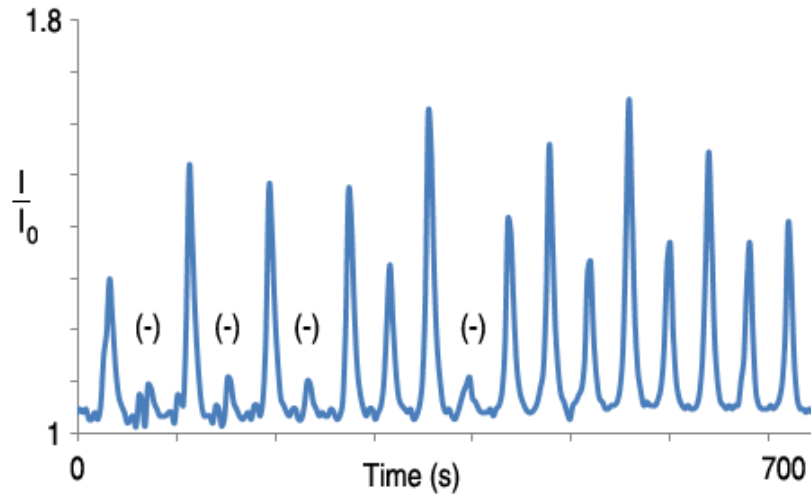
Fig 2 Experimental calcium response vs. time graph depicting potential phase-locked loop mechanism under periodic stimulation. The cell initially exhibits a phase-locking ratio of 0.5 until about 300 s, and subsequently displays a phase-locking ratio of 1 after 400 s. The periodic stimulation conditions for this case were: stimulant concentration = 10 nM, stimulation duration = 16 s, and rest period = 24 s. The '(-)' symbols represent sub-threshold calcium spikes.

Fig. III.3 Intrinsic parameters have a drastic effect upon calcium response fidelity. Experimental results showing a decrease in average phase-locking ratio when M3 receptor density is decreased by 1 nM atropine (top), and upregulation of RGS4 concentration (bottom). The periodic stimulation pattern used for experiments was: stimulant concentration = 25 nM, stimulation duration = 24 s, and rest period = 24 s. Between 85-106 cells were examined for each experimental condition. Bars represent the S.E.M and the Student's t-test was used to statistically compare pairs of experimental conditions; $p < 0.05$ was used as a threshold of statistical significance. Both pairs of experimental conditions were statistically significant.
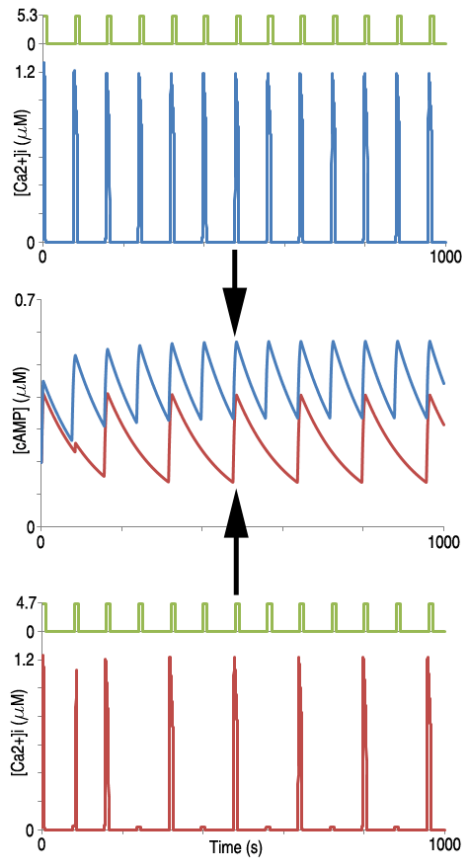
Fig. III.4 Downstream consequences of low fidelity calcium signaling on cAMP signaling, using the mathematical model developed by Gorbunova and Spitzer (2002). For the top graph, calcium signaling demonstrates high fidelity to the periodic stimulation input, resulting in cAMP dynamics that follow the frequency of the stimulation input (middle graph in blue). A 10% change in stimulation strength resulted in low fidelity calcium signaling with respect to the same periodic input (bottom graph). A consequence of this low fidelity is that cAMP levels demonstrate a lower frequency compared to the stimulation input, and their average concentration is lower than that of the high fidelity case (middle graph in red). The periodic stimulation pattern used was: stimulant concentration 4.7 and 5.3 1/(μM*s) for the bottom and top graphs respectively, stimulation duration = 10 s, and rest period = 70 s.

III.5 References:

Berridge MJ, Bootman MD, Roderick HL (2003) Calcium signalling: Dynamics, homeostasis and remodelling. *Nat Rev Mol Cell Biol* **4:** 517-529.

Boulware MJ, Marchant JS (2008) Timing in cellular Ca2+ signaling. *Curr Biol* **18:** R769-R776.

Caulfield MP (1993) Muscarinic Receptors - Characterization, Coupling and Function. *Pharmacol Therapeutics* **58:** 319-379.

Chay TR, Lee YS, Fan YS (1995) Appearance of phase-locked Wenckebach-like rhythms, devil's staircase and unviersality in intracellular calcium spikes in nonexcitable cell models. *J Theor Biol* **174:** 21-44.

Cuthbertson KSR, Chay TR (1991) Modeling receptor-controlled intracellular calcium oscillators. *Cell Calcium* **12:** 97-109.

Felder CC, Bymaster FP, Ward J, DeLapp N (2000) Therapeutic opportunities for muscarinic receptors in the central nervous system. *J Med Chem* **43:** 4333-4353.

Futai N, Gu W, Takayama S (2004) Rapid prototyping of microstructures with bell-shaped cross-sections and its application to deformation-based microfluidic valves. *Adv Mater* **16:** 1320-1323.

Gautam D, Han SJ, Hamdan FF, Jeon J, Li B, Li JH, Cui YH, Mears D, Lu HY, Deng CX, Heard T, Wess J (2006) A critical role for beta cell M-3 muscarinic acetylcholine receptors in regulating insulin release and blood glucose homeostasis in vivo. *Cell Metabol* **3:** 449-461.

Gold SJ, Ni YG, Dohlman HG, Nestler EJ (1997) Regulators of G-protein signaling (RGS) proteins: Region-specific expression of nine subtypes in rat brain. *J Neurosci* **17:** 8024-8037.

Gorbunova YV, Spitzer NC (2002) Dynamic interactions of cyclic AMP transients and spontaneous Ca2+ spikes. *Nature* **418:** 93-96.

Gu W, Zhu XY, Futai N, Cho BS, Takayama S (2004) Computerized microfluidic cell culture using elastomeric channels and Braille displays. *Proc Natl Acad Sci U S A* **101:** 15861-15866.

Guevara MR, Glass L, Shrier A (1981) Phase Locking, Period-Doubling Bifurcations, and Irregular Dynamics in Periodically Stimulated Cardiac-Cells. *Science* **214:** 1350-1353.

Hendriks-Balk MC, Peters SLM, Michel MC, Alewijnse AE (2008) Regulation of G protein-coupled receptor signalling: Focus on the cardiovascular system and regulator of G protein signalling proteins. *Euro J Pharmacol* **585:** 278-291.

Heo YS, Cabrera LM, Song JW, Futai N, Tung YC, Smith GD, Takayama S (2007) Characterization and resolution of evaporation-mediated osmolality shifts that constrain microfluidic cell culture in poly(dimethylsiloxane) devices. *Anal Chem* **79:** 1126-1134.

Hsieh GC, Hung JC (1996) Phase-locked loop techniques - A survey. *IEEE Trans Ind Electr* **43:** 609-615.

Lan KL, Zhong HL, Nanamori M, Neubig RR (2000) Rapid kinetics of regulator of G-protein signaling (RGS)-mediated G alpha(i) and G alpha(o) deactivation - G alpha specificity of RGS4 and RGS7. *J Biol Chem* **275:** 33497-33503.

Luo D, Broad LM, Bird GSJ, Putney JW (2001a) Signaling pathways underlying muscarinic receptor-induced [Ca2+](i) oscillations in HEK293 cells. *J Biol Chem* **276:** 5613-5621.

Luo X, Popov S, Bera AK, Wilkie TM, Muallem S (2001b) RGS proteins provide biochemical control of agonist-evoked [Ca2+](i) oscillations. *Mol Cell* **7:** 651-660.

Montminy M (1997) Transcriptional regulation by cyclic AMP. *Annu Rev Biochem* **66:** 807-822.

Mukhopadhyay S, Ross EM (1999) Rapid GTP binding and hydrolysis by G(q) promoted by receptor and GTPase-activating proteins. *Proc Natl Acad Sci U S A* **96:** 9539-9544.

Nagai T, Yamada S, Tominaga T, Ichikawa M, Miyawaki A (2004) Expanded dynamic range of fluorescent indicators for Ca2+ by circularly permuted yellow fluorescent proteins. *Proc Natl Acad Sci U S A* **101:** 10554-10559.

Neubig RR, Siderovski DR (2002) Regulators of G-protein signalling as new central nervous system drug targets. *Nat Rev Drug Discov* **1:** 187-197.

Palmer AE, Tsien RY (2006) Measuring calcium signaling using genetically targetable fluorescent indicators. *Nat Protoc* **1:** 1057-1065.

Pinkaskramarski R, Stein R, Zimmer Y, Sokolovsky M (1988) Cloned rat M3 muscarinic receptors mediate phosphoinositide hydrolysis but not adenylate-cyclase inhibition. *FEBS Lett* **239:** 174-178.

Sawano A, Takayama S, Matsuda M, Miyawaki A (2002) Lateral propagation of EGF signaling after local stimulation is dependent on receptor density. *Dev Cell* **3:** 245-257.

Schreiber G, Henis YI, Sokolovsky M (1985) Rate constants of agonist binding to muscarinic receptors in rat-brain medulla- Evaluation by competition kinetics. *J Biol Chem* **260:** 8795-8802.

Xia YN, Whitesides GM (1998) Soft lithography. *Annu Rev Mater Sci* **28:** 153-184.

Chapter IV.

Phase-locked signals elucidate circuit architecture of an oscillatory pathway

IV.1 Introduction:

Determining the circuit architecture of cellular signaling pathways is challenging. Although a variety of plausible models can often be constructed using conventional genetic tools, such as siRNA (Brandman *et al*, 2007; Liou *et al*, 2005) and protein over-expression (Berridge *et al*, 2003), and chemical perturbations, such as inhibitors (Putney and Bird, 1993) and caged compounds (Sneyd *et al*, 2006), further elucidation of molecular mechanisms is often not possible. This process would benefit from additional readouts that shed light on system architecture in a robustly discriminating manner.

While continuous stimulation of cellular systems provides a simple means of assessing pathway properties, it cannot simultaneously reveal information on system recovery dynamics (Guevara *et al*, 1981). We hypothesized that use of periodic chemical stimulation would better reveal both the activation and recovery properties of crucial biological oscillators to enable elucidation of molecular mechanisms. Here we demonstrate and validate this concept for the oscillatory calcium pathway of the G-protein coupled receptor (GPCR) M3 muscarinic system.

The recovery properties of this system were evaluated by reducing the rest period between pulses of the M3 ligand, carbachol (CCh), and observing the resulting calcium responses. We noted the emergence of phase-locked system responses upon periodic stimulation. Phase-locking describes the phenomenon whereby an oscillatory system becomes synchronized to a periodic stimulation input. As the rest period was decreased, the number of system responses generally became less than the number of stimulatory inputs, indicative of skipped beats, thereby revealing recovery properties not attainable by continuous stimulation. Furthermore, the skipped beats often were not completely

absent, but instead appeared as small calcium transients that we here term "sub-threshold". The sub-threshold spikes provided insight into the activation properties of the signaling system: the complete absence of a sub-threshold spike would suggest that a switch-like mechanism produced calcium spikes; their presence, however, would suggest that a graded mechanism was more plausible.

Experimental observations of phase-locking properties were compared to the activation and recovery properties of two models of calcium signaling, the Chay et al. model (Chay *et al*, 1995; Cuthbertson and Chay, 1991), and the positive feedback Politi et al. model (2006). In the former model, the activation properties are characterized by switch-like activation of PLC by G-protein, and it also features basal IP3 production, which represents a recovery mechanism that ensures that IP3 returns to its pre-stimulus levels. The latter model does not have such a recovery mechanism, and features graded PLC activation. To produce oscillations in the Chay et al. model, the products of the switch-like activation of PLC (IP3 and diacylglycerol) negatively feedback on upstream pathway components (G-proteins). In the Politi et al. model, IP3, produced by graded activation of PLC, feeds back on downstream elements (IP3 receptor) along with calcium to make oscillations.

Under continuous stimulation, both models exhibit calcium oscillations with increasing frequencies upon increasing stimulation concentration, as seen in a host of experimental data (Jacob *et al*, 1988; Prentki *et al*, 1988; Woods *et al*, 1986). Both models were thus appropriate but indistinguishable by conventional stimulation methods. The discriminating features provided by phase-locking analysis, however, revealed that neither of the calcium models correctly predicted all the experimental behaviors based upon their activation and recovery dynamics. Furthermore, by analyzing the sources of discrepancy between the predictions and experiments, we were able to propose a mechanism modification to account for all the experimental observations of phase-locking.

Although phase-locking can be thought of as a general property of biological oscillators (Machlup and Sluckin, 1980), it has not been previously explored experimentally in the context of chemical stimulations. Here, we demonstrate that phase-locking, which can

only be observed using temporally patterned stimulation, complements conventional chemical and genetic tools for elucidating pathways.

IV.2 Results and Discussion:

We assessed cellular responses to square-wave stimulation through use of a microfluidic platform (from Chapters II and III), which enabled exploration of phase-locked rhythms induced by chemical input signals (Fig. IV.1a-c). With fixed stimulant concentration (C) and stimulation duration (D), increases in the rest period (R) resulted in increases in the phase-locking ratio (Fig. IV.1d), where phase-locking ratios were calculated by dividing the number of system responses by the number of chemical inputs. Analysis of the phase-locking rhythms also uncovered the existence of sub-threshold calcium spikes in individual cellular calcium responses (Fig. IV.1b). In addition, we explored the phase-locking trends induced by varying C and D (Fig. IV.2a, b; Appendix C). These observations collectively provided robust discrimination markers for rigorous evaluation of mathematical models of oscillatory calcium signaling in order to elucidate molecular mechanisms.

Two existing oscillatory calcium models (Fig. IV.3) were chosen as a test set against the experimental results, based upon the inability to discriminate their behavior upon continuous stimulation (Fig. IV.4a-c) despite significant differences in their activation and recovery mechanisms. We demonstrate that phase-locking analysis is able to effectively dissect these differences between the models (Fig. IV.4d-i). We first analyzed the Chay et al. model (Chay *et al*, 1995; Cuthbertson *et al*, 1991) (Fig. IV.3a; Appendix A). Despite the agreement of the model with the effects of R on phase-locking ratio observed in the system (compare Fig. IV.1d with Fig. IV.4d), it could not account for the presence of sub-threshold calcium spikes (Fig. IV.4g), suggesting inaccuracies in its activation properties. We attributed the lack of sub-threshold spikes to the model mechanisms, and not model parameter values, as we used a sampling algorithm (Latin Hypercube Sampling (LHS)) to survey a range of parameter values and found no parameter set able to result in sub-threshold calcium spikes (Fig. IV.5). The Chay et al. model assumes that G-protein activation of PLC is a switch-like response with a Hill Coefficient of 4. Therefore if activated G-protein levels are not sufficiently high to

surpass the threshold for PLC activation, a calcium spike will not result. However, the presence of sub-threshold calcium spikes in these experiments suggested that such a sharp activation threshold does not exist. We know of no data to support a switch-like mechanism; in fact, recent experiments suggest that G-protein activation of PLC is graded (Nash *et al*, 2001). When the Hill coefficient of the G-protein/PLC interaction was reduced in the Chay et al. model, calcium oscillations could not be obtained under continuous stimulation; this finding shows that these reaction mechanisms and model parameters need to be re-evaluated.

Our experimental observations were then used to evaluate the Politi et al. model (Fig. IV.3b; Appendix A). Individual calcium graphs portrayed sub-threshold calcium spikes upon exposure to square-wave stimulation pulses (Fig. IV.4h). However, the model incorrectly predicted that larger R resulted in smaller phase-locking ratios (Fig. IV.4e), suggesting that the recovery properties of the model are not accurate. LHS analysis indicated that the choice of model parameter values alone could not explain these inaccuracies, suggesting that reaction mechanisms used to formulate the model need revision.

Thus, neither of the calcium models tested was able to account for all of the experimental observations. We noted that the Politi et al. model showed continued IP3 decay between stimulation pulses, while in the Chay et al. model, IP3 levels exhibited a slow recovery between stimulation pulses (Fig. IV.6). In the latter model, IP3 recovery between stimulation pulses is due to a mechanism for basal IP3 production. Addition of basal IP3 production to the Politi et al. model was able to correct its deficiencies in recovery dynamics (Fig. IV.3 right column). This model revision may provide crucial insight into physiological systems where cells or tissues require fidelity of its calcium signals to periodic chemical stimulation in order to carry out their function (Fendler *et al*, 2009). We note that other mechanisms may be found that can account for the experimental observations, but basal IP3 production provides the simplest explanation and is supported by the literature (Hwa *et al*, 1997). Collectively, this would suggest that the activation and recovery mechanisms reflected in the revised Politi et al. model (positive feedback

mechanism of calcium upon PLC activity, graded PLC activation by G-proteins, and basal IP3 production) are the best fit for the pathway studied here.

In sum, we employed a combination of microfluidics, real-time imaging, and mathematical modeling in order to probe the circuit architecture of an oscillatory signaling pathway in mammalian cells. Here chemical-induced phase-locking was explored and analysis of its properties was used to test mathematical models and elucidate molecular mechanisms. As microfluidic setups become more elaborate in their ability to generate temporal stimulation patterns, we can expect even more discriminating markers for signaling studies (Ingolia and Weissman, 2008). While a single optical readout was employed for this study, the setup is amenable to the use of multiple real-time readouts of cellular signaling, thereby further enhancing the number of discriminating markers for elucidation of signaling pathways. Finally, although this paper focused on calcium oscillations, we believe this approach would be well-suited for studies on various biological oscillators such as ERK (Shankaran *et al*, 2009), NFκB (Nelson *et al*, 2004), and components involved in circadian (Dunlap, 1999) and ultradian (Stavreva *et al*, 2009) rhythms. For example, phase-locking analysis of a circadian oscillator model (Tyson *et al*, 1999) shows that when S is large, the phase-locking ratio increased for increasing R (Fig. IV.7a), and when S is small, the phase-locking ratio increased for increasing R, then decreased (Fig. IV.7b); we also noted the presence of sub-threshold spikes (Fig. IV.8). Thus, these types of phase-locking analyses provide experimentally testable hypotheses for elucidating molecular mechanisms of a range of oscillatory pathways.

IV.3 Materials and Methods:

Cell Culture:

HEK293 cells were cultured in DMEM (Invitrogen) supplemented with 10% FBS (Gibco) and were maintained at 37°C with 5% CO2 in 24-well plates. 0.25% Trypsin/EDTA (Gibco) was used to detach cells from plates and transfer them to the microfluidic setup. These cells were stably transfected with the M3 muscarinic receptor (selected with 0.4 mg/mL Geneticin (Gibco)). Cells were transiently transfected with the

calcium FRET probe YC3.60 (Nagai *et al*, 2004). Transfections were carried out with Lipofectamine2000 (Invitrogen) using the manufacturer's protocol.

Microfluidics:

Microfluidic device molds were fabricated based upon the ones described in Futai et al (2006). Front-side photolithography (Xia and Whitesides, 1998) was used to construct the outlet channel where cells were cultured; the remaining channels (inlets and "Braille" channels) were constructed with backside photolithography (Futai *et al*, 2004). With the resulting glass mold, PDMS (1:10 ratio of curing agent to base) was cast upon the positive relief features and allowed to cure for at least 2 hours in a 60°C oven. The resulting device was then irreversibly sealed against a thin (~100 μm) PDMS sheet through 30 s plasma oxidation. Once sealed, the device was filled with PBS and sterilized for 2 hrs in a UV oven. To ensure cell adhesion, the chip was subsequently filled with 100 μg/mL laminin (Invitrogen) and allowed to incubate at 37°C for two hours. After this, the chip was flushed and refilled with DMEM supplemented with 10% FBS. Transfected HEK293 cells were then seeded from the outlet port and were appropriately positioned in the outlet hydrodynamically. The cells were then allowed to attach overnight.

A custom program written in Visual Basic was used to control the dynamic pumping mediated by Braille-actuation (Gu *et al*, 2004), and thereby create the various temporal stimulation patterns used in experiments (Fig. IV.1a); experiments with fluorescein solution confirmed the nearly square-wave shape and reproducibility of these patterns. Carbachol (CCh) dissolved in imaging media (Palmer and Tsien, 2006) was added to one of the inlet reservoirs, and the other reservoir was filled with stimulant-free imaging media. Cells in the devices were maintained at 37°C via a transparent indium tin oxide heater (Heo *et al*, 2007), situated between the objective and the thin PDMS-sheet upon which the cells were cultured. Details about the pumping and washing characteristics of the device are provided in Appendix B.

Imaging:

Cells were imaged with a TE2000-U Nikon inverted microscope, using a 20x objective, a standard 100W mercury lamp, and a 490 nm long pass dichroic mirror. A CoolSnap HQ2 camera (Photometrics, Tucson, AZ) was used to capture fluorescence images of YC3.60-transfected cells. Cells were excited at 450 nm and the emission signals were captured at 490 and 535 nm (filters from Chroma Technology Corp, Rockingham, VT). An ND4 neutral density filter was used to reduce photo-bleaching. The excitation and emission filter wheels were controlled by the Lambda 10-3 Shutter Controller (Sutter Instruments, Novato, CA). Images were acquired every 3 s, and an exposure time of 100 ms was used. The program MetaFluor (Molecular Devices, Downington, PA) was used for image acquisition and processing; for each emission image (at 490 nm and 535 nm) the background was subtracted, ratiometric images were constructed (intensity at 535 nm/intensity at 490 nm), and calcium FRET ratios of individual cells were generated with this software. These FRET ratios (I) were normalized by the minimum FRET ratio obtained in the experimental run (I_0), and accordingly I/I_0 was plotted in the figures, as has been done previously (Sawano *et al*, 2002).The normalized ratio values of the calcium peaks fell between 1.2 and 7.5, which was in accord with previously obtained values using the same FRET indicator (Nagai *et al*, 2004).

The resulting images were then analyzed to calculate the phase-locking ratios by dividing the number of calcium spike events by the number of CCh stimulation inputs. Since at least several cells always responded to a particular stimulation pulse, we concluded that when cells did not respond, it was due to phase-locking and not a malfunction with the microfluidic setup. We also concluded that lack of cellular response was not due to slow image acquisition, since results could be reproduced with image acquisition every 2 s. Lastly, we found that the cells did not exhibit a calcium response due to fluid flow alone.

Computation of Phase-locking Ratios:

Cells were exposed to 9-18 stimulation inputs, and the number of calcium responses for each run was recorded. For instance, for a cell that had been exposed to 12 CCh stimulation pulses and responded with 6 calcium spikes, the phase-locking ratio was computed as 0.5. Calcium spikes that did not reach an amplitude greater than 33% of the maximum calcium spike height in an experimental run were not counted as true calcium

spikes, and were deemed sub-threshold calcium spikes. Phase-locking ratios were computed for individual cells, and averages and standard errors of the mean were computed for each experimental condition. Statistics were based upon three experiments (each of no less than 20 cells) for each experimental condition. Between 85-106 cells were examined for each experimental condition. Phase-locking ratios of individual cells can be observed in Appendix C. The unpaired Student t-test was used to statistically compare pairs of experimental conditions; $p < 0.05$ was used as a threshold of statistical significance.

Mathematical models:

Two mathematical models of oscillatory calcium signaling were evaluated in this study: the Chay et al. model (Chay *et al*, 1995; Cuthbertson *et al*, 1991) (Fig. IV.3a), and the positive feedback Politi et al. model (2006) (Fig. IV.3b). For these two mathematical models, we used the equations and initial conditions defined in the original publications. For the Chay et al. model, it was assumed that receptor-mediated G-protein activation was proportional to stimulant concentration. For the Politi et al. model, it was assumed that the maximal rate of PLC-mediated IP3 production was proportional to stimulant concentration. These assumptions are based upon those from the original publications. For the Politi et al. model, we used calcium flux strength $\varepsilon = 5$, instead of $\varepsilon = 0$ as was presented in the original paper; this modification was introduced to reflect the role of extracellular flux in calcium oscillations (Luo *et al*, 2001). In addition, we found that calcium phase-locking could not be achieved with this model with $\varepsilon = 0$, using original parameters and adjustment of ER calcium dynamics (as was used in the original publication). The mathematical systems were exposed to 12 square-wave stimulation pulses and the corresponding number of calcium spike responses was counted in order to compute phase-locking ratios. Calcium spikes which did not reach an amplitude of greater than 33% of the maximum spike height for a model run were not counted as a calcium response, and were deemed sub-threshold spikes. To assess the effect of rest period on the phase-locking ratio, this parameter was varied, while stimulant concentration and stimulation duration were fixed; we then plotted the resulting phase-locking ratio against the rest period (Fig. IV.4- middle row). The same procedure was

applied to assess the effects of stimulant concentration and stimulation duration on the phase-locking ratio, respectively (Fig. IV.2).

For phase-locking analysis of the circadian oscillator model developed by Tyson et al. (1999), the same criteria was used as above to evaluate phase-locking ratios (Fig. IV.8). Original parameters were used and square-wave stimulation of the model system was achieved through variation of the parameter 'vm', which represents the rate of mRNA synthesis (Fig. IV.7a).

All models were coded in MATLAB version 7.8.0 (MathWorks Inc, Natick, MA) and the system of ODEs was solved with the stiff solver ode15s. Details for both models are provided in Appendix A.

Latin hypercube sampling:

We used Latin Hypercube Sampling (LHS) to check if inaccuracies in model parameter values alone could account for differences between experimental results and model predictions. LHS is a highly effective method for exploring parameter spaces for mathematical models (Blower and Dowlatabadi, 1994; Kinzer-Ursem and Linderman, 2007; Marino *et al*, 2008; McKay *et al*, 1979). Using LHS code from Marino et al. (2008) (http://malthus.micro.med.umich.edu/lab/usadata/), we varied model parameter values by sampling from a normal distribution with a 25% standard deviation; original parameter values were used as the mean. Larger standard deviations (100%) did not yield results different from those at 25% standard deviation. For the Chay et al. model, we varied all twelve independent parameters; for the Politi et al. model, we varied all 17 independent parameters, except for β, which represented the ratio of ER to cytoplasm volume. LHS was run for 500 iterations on each model, and each model output was analyzed to decipher whether the results matched experimental observations (either by constructing 'phase-locking vs. rest period' graphs for the Politi et al. model or by looking at individual model runs for the Chay et al. model, as depicted in Fig. IV.5).
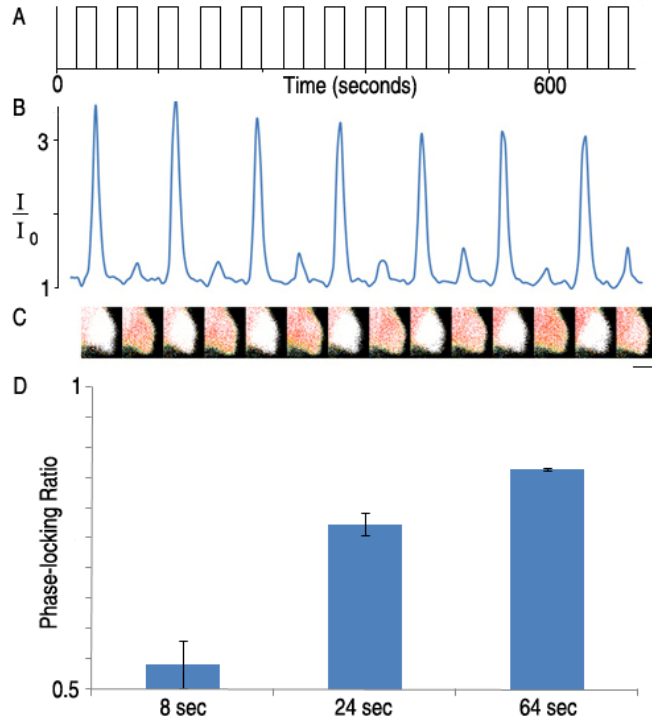
Fig. IV.1 Individual HEK293 cell exhibiting a calcium phase-locking ratio of 0.5 upon square-wave carbachol (CCh) stimulation. a) Temporal pattern of CCh stimulation; the cell was addressed with 25 nM CCh for 24 s, followed by a rest period of 24 s. b) Phase-locked calcium response monitored by normalized FRET ratio (I/I_0); I_0 is the minimum FRET ratio obtained during an experimental run to which the remaining ratios (I) were normalized. c) FRET images of the cellular calcium responses. (scale bar = 10 microns) d) Effect of rest period (R) on average phase-locking ratio; cells were exposed to three different rest period values, while the stimulant concentration (C) was fixed at 10 nM CCh and stimulation duration (D) was fixed at 24 s. Bars indicate the S.E.M., representative of three experiments for each experimental condition; for each experiment, the responses of least 20 cells were recorded, resulting in totals between 85 and 106 cells for each experimental condition. All pairs of experimental conditions were statistically significant as determined by the unpaired Student's t-test ($p<0.05$).
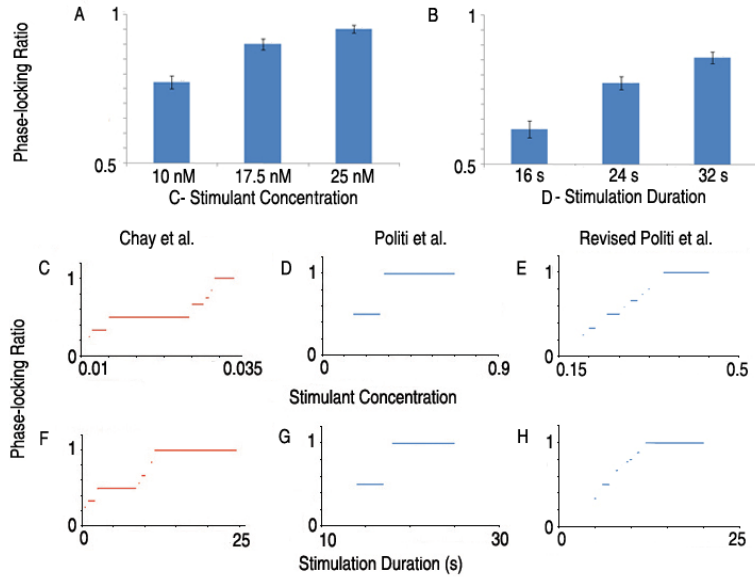
Fig. IV.2 Phase-locking behaviors: experimental (a, b) and theoretical (c-h) for the Chay et al. model (c, f), the positive feedback Politi et. al. (d, f) (middle column) and the revised Politi et al. model (basal PLC activity = 0.3 µM/s) (e, g) when stimulant concentration (C) and stimulation duration (D) were varied. a) Phase-locking ratio vs. C, with D and R = 24 s. b) Phase-locking ratio vs. D, with C = 10 nM and R = 24 s. c)-e) Phase-locking Ratio vs. Stimulant Concentration. In c) the stimulant concentration has units of 1/s and represents the rate of receptor-mediated G-protein activation. For d) and e) the stimulant concentrations have units of µM/s and represent the maximal rate of IP3 production. For c)-e), D = 10 s and R = 50 s. f)-h) Phase-locking ratio vs. D with R fixed at 60 s. For f) C = 0.03 1/s, for g) C = 0.8 µM/s, and for h) C = 0.3 µM/s. Bars indicate the S.E.M., representative of three experiments for each experimental condition; for each experiment, the responses of least 20 cells were recorded. All pairs of experimental conditions were statistically significant as determined by the unpaired Student's t-test (p<0.05).
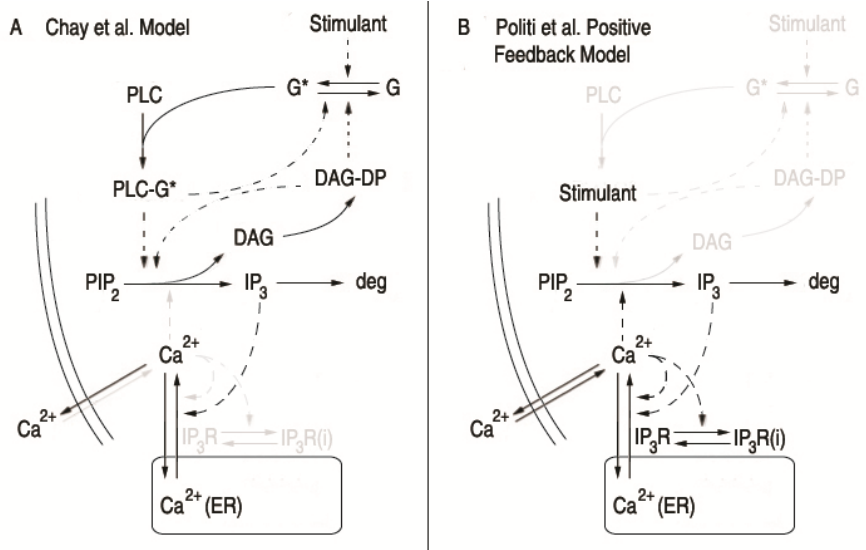
Fig. IV.3 Mathematical model schematics. a) Mathematical model developed by Chay et al. (Chay *et al*, 1995; Cuthbertson *et al*, 1991) b) Mathematical model developed by Politi et al. (2006). Dashed arrows indicate positive feedback. DAG = diacylglycerol; DAG-DP = DAG-dependent protein; IP3R = IP3 Receptor; IP3R(i) = inactivated IP3R; Ca2+(ER) = Endoplasmic Reticulum calcium.
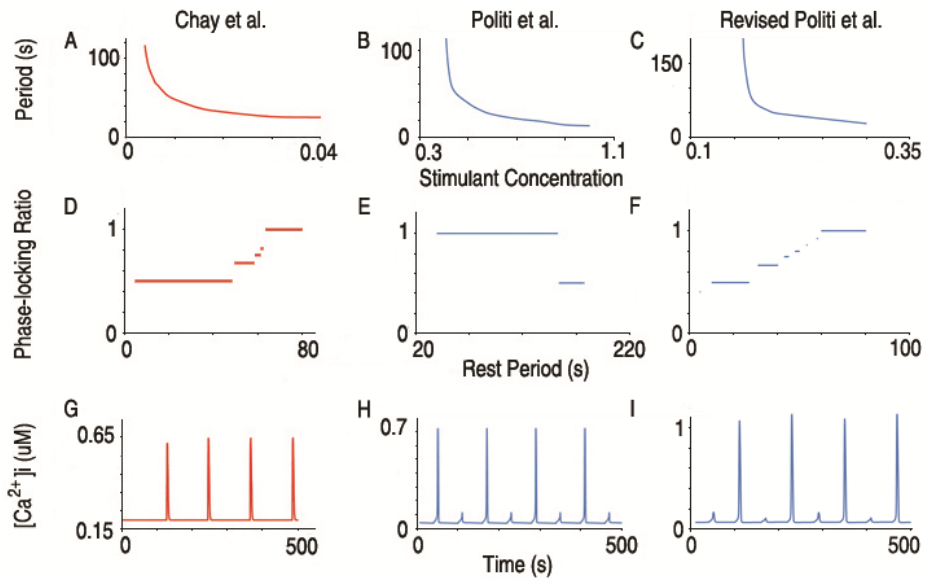
Fig. IV.4 Behaviors of the Chay et al. model (left column), the Politi et. al. model (middle column), and revised Politi et al. model (basal IP3 production = 0.3 µM/s) (right column) under continuous and square-wave stimulation. a)-c) Oscillation period vs. continuous stimulant concentration for all three models. In a) stimulant concentration has units of 1/s and represents the rate of receptor-mediated G-protein activation. For b) and c) the stimulant concentrations have units of µM/s and represent the maximal rates of IP3 production. d) Phase-locking ratio vs. Rest Period (R) (Concentration (C) = 0.03 1/s, Stimulation Duration (D) = 10 s). e) Phase-locking ratio vs. R (C = 0.8 µM/s D = 10 s). f) Phase-locking ratio vs. R (C = 0.3 µM/s D = 10 s). g) Intracellular calcium vs. time, C = 0.03 1/s, D = 10 s, R = 50 s. h) Intracellular calcium vs. time, C = 0.8 µM/s, D = 30 s, R = 50 s. i) Intracellular calcium concentration vs. time, with C = 0.3 µM/s, D = 10 s, R = 50 s.
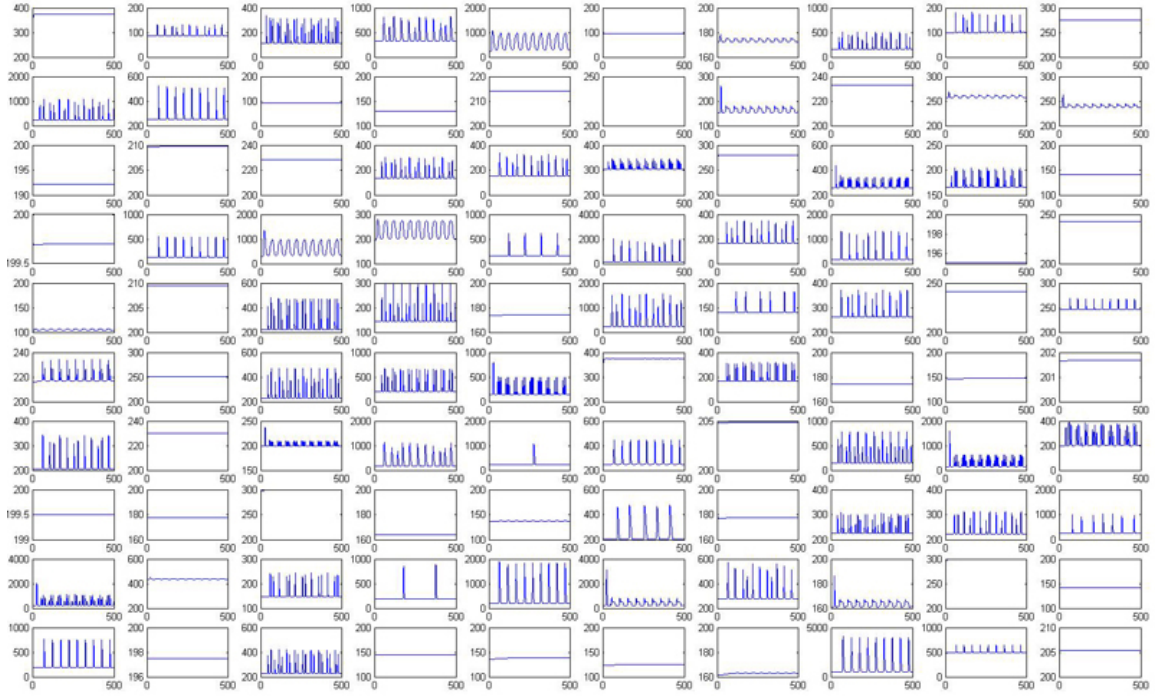
Fig. IV.5 Results of Latin Hypercube Sampling (LHS) for the Chay et al. model. Intracellular cellular calcium (nM) vs. time (s) is plotted for 100 different parameter sets (out of 500 total generated), with stimulant concentration = 0.01 1/s, stimulation duration = 25 s, and rest period = 50 s.
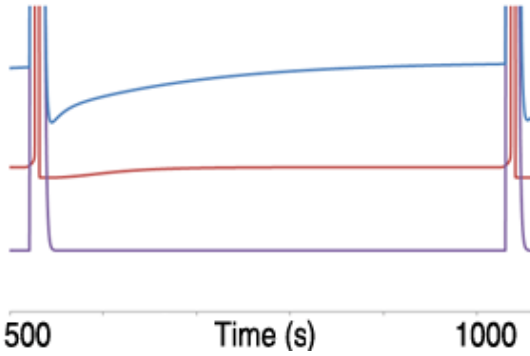
Fig. IV.6 IP3 recovery dynamics for the positive feedback Politi et al. model (purple), for the Chay et al. model (red), and the former model with basal PLC activity (blue). The times and magnitudes of the IP3 curves have been offset for easier comparison. For each curve, the stimulation duration was 10 s and the rest period was 500 s. The stimulant concentration was 0.05 1/s for the Chay et al. model, 1.2 µM/s for the positive feedback model, and 0.3 µM/s for the latter model with basal IP3 production. Basal IP3 production was set at 0.3 µM/s.
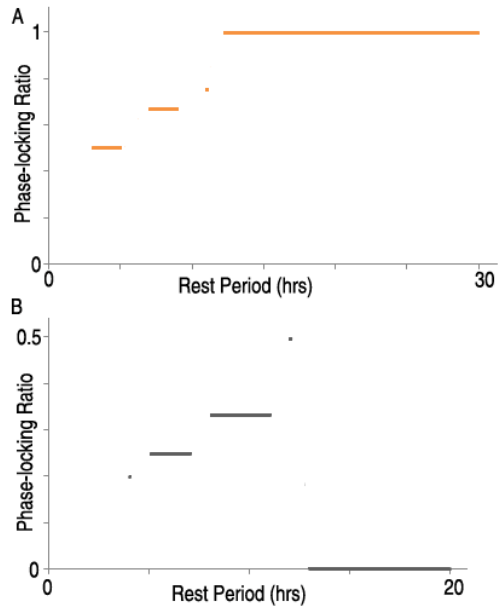
Fig. IV.7 Phase-locking ratio vs. rest period for circadian oscillator model, with fixed stimulant concentration (C) = 1 unit, and stimulation duration (D) = 10 hrs (for a) and D = 2 hrs (for b).
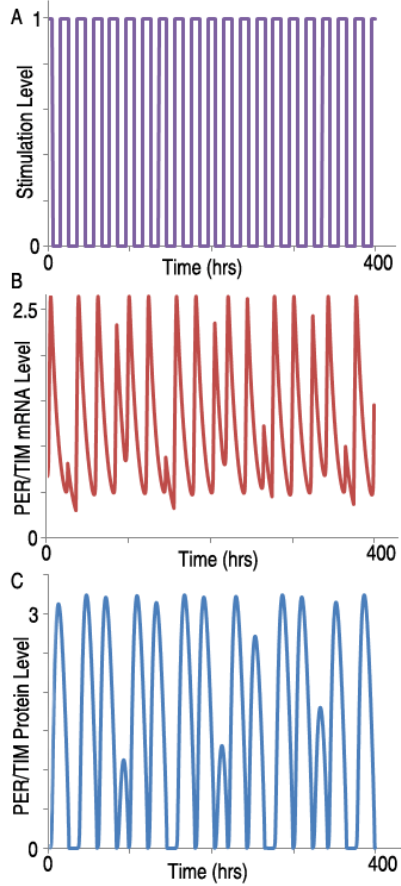
Fig. IV.8 Periodic stimulation of circadian oscillator model with C = 1 unit, D = 10 hrs, and R = 10 hrs. a) Periodic stimulation pattern b) PER/Tim mRNA levels vs. time c) PER/Tim Protein levels vs. time. Sub-threshold spikes can be seen in both b) and c).

IV.4 References:

Berridge MJ, Bootman MD, Roderick HL (2003) Calcium signalling: Dynamics, homeostasis and remodelling. *Nat Rev Mol Cell Biol* **4:** 517-529.

Blower SM, Dowlatabadi H (1994) Sensitivity and uncertainty analysis of complex-models of disease transmission- an HIV model, as an example. *Int Stat Rev* **62:** 229-243.

Brandman O, Liou J, Park WS, Meyer T (2007) STIM2 is a feedback regulator that stabilizes basal cytosolic and endoplasmic reticulum Ca2+ levels. *Cell* **131:** 1327-1339.

Chay TR, Lee YS, Fan YS (1995) Appearance of phase-locked Wenckebach-like rhythms, devil's staircase and unviersality in intracellular calcium spikes in nonexcitable cell models. *J Theor Biol* **174:** 21-44.

Cuthbertson KSR, Chay TR (1991) Modeling receptor-controlled intracellular calcium oscillators. *Cell Calcium* **12:** 97-109.

Dunlap JC (1999) Molecular bases for circadian clocks. *Cell* **96:** 271-290.

Fendler B, Zhang M, Satin L, Bertram R (2009) Synchronization of pancreatic islet oscillations by intrapancreatic ganglia: a modeling study. *Biophys J* **97:** 722-729.

Futai N, Gu W, Song JW, Takayama S (2006) Handheld recirculation system and customized media for microfluidic cell culture. *Lab Chip* **6:** 149-154.

Futai N, Gu W, Takayama S (2004) Rapid prototyping of microstructures with bell-shaped cross-sections and its application to deformation-based microfluidic valves. *Adv Mater* **16:** 1320-1323.

Gu W, Zhu XY, Futai N, Cho BS, Takayama S (2004) Computerized microfluidic cell culture using elastomeric channels and Braille displays. *Proc Natl Acad Sci U S A* **101:** 15861-15866.

Guevara MR, Glass L, Shrier A (1981) Phase Locking, Period-Doubling Bifurcations, and Irregular Dynamics in Periodically Stimulated Cardiac-Cells. *Science* **214:** 1350-1353.

Heo YS, Cabrera LM, Song JW, Futai N, Tung YC, Smith GD, Takayama S (2007) Characterization and resolution of evaporation-mediated osmolality shifts that constrain microfluidic cell culture in poly(dimethylsiloxane) devices. *Anal Chem* **79:** 1126-1134.

Hwa J, Gaivin R, Porter JE, Perez DM (1997) Synergism of constitutive activity in alpha(1)-adrenergic receptor activation. *Biochem* **36:** 633-639.

Ingolia NT, Weissman JS (2008) Systems biology - Reverse engineering the cell. *Nature* **454:** 1059-1062.

Jacob R, Merritt JE, Hallam TJ, Rink TJ (1988) Repetitive spikes in cytoplasmic calcium evoked by histamine in human endothelial cells. *Nature* **335:** 40-45.

Kinzer-Ursem TL, Linderman JJ (2007) Both ligand- and cell-specific parameters control ligand agonism in a kinetic model of G protein-coupled receptor signaling. *PLoS Comput Biol* **3:** 84-94.

Liou J, Kim ML, Heo WD, Jones JT, Myers JW, Ferrell JE, Meyer T (2005) STIM is a Ca2+ sensor essential for Ca2+-store-depletion-triggered Ca2+ influx. *Curr Biol* **15:** 1235-1241.

Luo D, Broad LM, Bird GSJ, Putney JW (2001) Signaling pathways underlying muscarinic receptor-induced [Ca2+](i) oscillations in HEK293 cells. *J Biol Chem* **276:** 5613-5621.

Machlup S, Sluckin TJ (1980) Driven Oscillations of a Limit-Cycle Oscillator. *J Theor Biol* **84:** 119-134.

Marino S, Hogue IB, Ray CJ, Kirschner DE (2008) A methodology for performing global uncertainty and sensitivity analysis in systems biology. *J Theor Biol* **254:** 178-196.

McKay MD, Beckman RJ, Conover WJ (1979) Comparison of 3 methods for selecting values of input variables in the analysis of output from a computer code. *Technometrics* **21:** 239-245.

Nagai T, Yamada S, Tominaga T, Ichikawa M, Miyawaki A (2004) Expanded dynamic range of fluorescent indicators for Ca2+ by circularly permuted yellow fluorescent proteins. *Proc Natl Acad Sci U S A* **101:** 10554-10559.

Nash MS, Young KW, Willars GB, Challiss RAJ, Nahorski SR (2001) Single-cell imaging of graded Ins(1,4,5)P-3 production following G-protein-coupled-receptor activation. *Biochem J* **356:** 137-142.

Nelson DE, Ihekwaba AEC, Elliott M, Johnson JR, Gibney CA, Foreman BE, Nelson G, See V, Horton CA, Spiller DG, Edwards SW, McDowell HP, Unitt JF, Sullivan E, Grimley R, Benson N, Broomhead D, Kell DB, White MRH (2004) Oscillations in NF-kappa B signaling control the dynamics of gene expression. *Science* **306:** 704-708.

Palmer AE, Tsien RY (2006) Measuring calcium signaling using genetically targetable fluorescent indicators. *Nat Protoc* **1:** 1057-1065.

Politi A, Gaspers LD, Thomas AP, Hofer T (2006) Models of IP3 and Ca2+ oscillations: Frequency encoding and identification of underlying feedbacks. *Biophys J* **90:** 3120-3133.

Prentki M, Glennon MC, Thomas AP, Morris RL, Matschinsky FM, Corkey BE (1988) Cell-specific patterns of oscillating free Ca2+ in carbamylcholine-stimulated insulinoma cells. *J Biol Chem* **263:** 11044-11047.

Putney JW, Bird GS (1993) The Inositol Phosphate-Calcium Signaling System in Nonexcitable Cells. *Endocr Rev* **14:** 610-631.

Sawano A, Takayama S, Matsuda M, Miyawaki A (2002) Lateral propagation of EGF signaling after local stimulation is dependent on receptor density. *Dev Cell* **3:** 245-257.

Shankaran H, Ippolito DL, Chrisler WB, Resat H, Bollinger N, Opresko LK, Wiley HS (2009) Rapid and sustained nuclear-cytoplasmic ERK oscillations induced by epidermal growth factor. *Mol Syst Biol* **5:** 332.

Sneyd J, Tsaneva-Atanasova K, Reznikov V, Bai Y, Sanderson MJ, Yule DI (2006) A method for determining the dependence of calcium oscillations on inositol trisphosphate oscillations. *Proc Natl Acad Sci U S A* **103:** 1675-1680.

Stavreva DA, Wiench M, John S, Conway-Campbell BL, McKenna MA, Pooley JR, Johnson TA, Voss TC, Lightman SL, Hager GL (2009) Ultradian hormone stimulation induces glucocorticoid receptor-mediated pulses of gene transcription. *Nat Cell Biol* **11:** 1093-U1111.

Tyson JJ, Hong CI, Thron CD, Novak B (1999) A simple model of circadian rhythms based on dimerization and proteolysis of PER and TIM. *Biophys J* **77:** 2411-2417.

Woods NM, Cuthbertson KS, Cobbold PH (1986) Repetitive transient rises in cytoplasmic free calcium in hormone-stimulated hepatocytes. *Nature* **319:** 600-602.

Xia YN, Whitesides GM (1998) Soft lithography. *Annu Rev Mater Sci* **28:** 153-184.

Chapter V.

Conclusions and Future Directions

V.1 Conclusions:

The highly dynamic nature of biological systems is manifested in part in the myriad of rhythms that control behaviors from the cellular level to the tissue level to the whole-organism level. In this regard, information is often encoded in the periodicity of the rhythms and cells use their protein machinery to appropriately interpret these signals (Brabant *et al*, 1992; Goldbeter, 2008). It is therefore crucial to understand the mechanisms that convert these periodic rhythms into messages that cells decode to carry out vital operations. This phenomenon is, however, vastly understudied, due in part, to the scarcity of experimental setups available to aptly control and analyze cellular signaling under dynamic stimulation (Bennett and Hasty, 2009). In order to surmount these limitations, a microfluidic device was developed, able to deliver periodic chemical stimulation to mammalian cells and facilitating real-time imaging of the resulting cellular responses. For this thesis research, periodic chemical stimulation was used to both manipulate and elucidate the mechanisms of intracellular signaling of calcium, an immensely important intracellular messenger of extracellular signals (Berridge *et al*, 2003; Berridge *et al*, 2000; Boulware and Marchant, 2008).

Under continuous chemical stimulation, cells exhibited intracellular calcium signals of highly variable periodicities, rendering control of these signals unattainable under these stimulation conditions. On the other hand, periodic stimulation was found to effectively control the timing of intracellular calcium signals; in addition, increasing the stimulant concentration, stimulation duration, or rest period improved the fidelity of the calcium responses, providing concrete strategies for manipulation of intracellular calcium signaling. In this regard, the results of this study are going to enable effective study of the downstream targets and cellular operations controlled by calcium signaling, such as

secretion, gene expression, and cell growth and death (Berridge *et al*, 2003; Boulware *et al*, 2008).

While the conjecture that intrinsic parameters, such as protein levels, could modulate calcium response fidelity was obvious, it was not immediately apparent how sensitive fidelity was to small changes in these values. Receptor levels, for instance, are always fluctuating due to internalization, recycling, and down-regulation (Bohm *et al*, 1997), and thus it was worthwhile to ascertain how sensitive fidelity was to such a parameter. Strikingly, theoretical predictions demonstrated that small changes in receptor density or Regulator of G-protein Signaling (RGS) protein concentration had a prodigious effect upon calcium response fidelity, under certain periodic stimulation conditions. Experimentally, decreasing the receptor density or increasing the RGS protein concentration resulted in diminished calcium response fidelity quite drastically. These results are substantial because they provide insight into how dramatic shifts in protein levels can alter fidelity; in addition, the fact that receptor and RGS proteins are pharmacologically-targetable components (Felder *et al*, 2000; Neubig and Siderovski, 2002) presents potentially a clinically-relevant means of correcting any detrimental effects of compromised calcium response fidelity. At this juncture, it is uncertain whether chemical signals of compromised fidelity are manifested in the body; however, there is ample reason to believe in its existence due to the phase-locking phenomenon observed in cardiac systems (Guevara *et al*, 1981).

While compromised calcium fidelity presents a potentially undesirable physiological situation, analysis of this limitation provided valuable insight into signaling mechanisms. Existing mathematical models were evaluated for the ability to predict these limitations; none of the models tested was able to account for all experimental observations of calcium response fidelity, suggesting that model mechanisms needed to be adjusted. Upon simple alteration of the mechanisms, the models were able to account for all experimental observations. Ultimately, this approach provides further insight into cellular signaling mechanisms, unattainable by conventional methods. The potential power of the method was demonstrated theoretically on models of circadian rhythm, uncovering previously unreported behaviors. By harnessing the properties of the limitations

uncovered by dynamic chemical stimulation, elucidation of molecular mechanisms was achieved.

V.2 Future Directions:

For future studies involving manipulation and elucidation of mechanisms of cellular signaling, the setup and results presented here provide tremendous opportunities. In particular, the ability to manipulate calcium signals through periodic stimulation enables could provide a means of manipulating crucial cellular operations such as gene expression, differentiation, and secretion. It can be envisioned that through precise delivery of periodic stimulation, for instance, a cell can be induced to differentiate into another cell type. An appropriate cell system to begin such studies would be with monocytes and macrophages, which upon RANKL stimulation, exhibit calcium oscillations, which are believed to be necessary for differentiation into osteoclasts (Takayanagi *et al,* 2002). Control of calcium oscillations may reveal the relationship between the frequency and the degree of osteoclast differentiation.

While the link between intracellular calcium signaling and gene expression has been established, there exist a great deal of intriguing questions regarding the specificity of calcium signaling. Specifically, it is unclear whether different stimulation sources producing the same calcium signal elicit the same genes (Berridge *et al*, 2000). It is envisioned that this point could be addressed with the setup presented here through periodic stimulation of cells with two different chemical stimulants, to observe whether the same genes are expressed in the same proportion. In addition, it would be valuable to evaluate how gene expression, elicited in this manner, differs from cell type to cell type, and how pharmacological drugs could modulate this cellular operation. Ultimately, this research would provide great insight into how cell populations could be programmed genetically without elaborate biochemical manipulations, and with simple chemical stimulation patterns.

Temporal patterns of chemical stimulation revealed limitations of calcium signaling fidelity, which uncovered an interesting parallel with cardiac signaling. Under periodic electronic stimulation, it was found that the heart's electronic impulses exhibited skipped

beats, signifying a loss of fidelity to the input signal. This loss of fidelity is manifested as arrhythmia and AV block (Shrier *et al,* 1987). The existence of skipped beats induced by periodic chemical stimulation has not been established, but it could imaginably lead to detrimental consequences for the body, as demonstrated by the predictions made in Chapter III. The development of cell-based sensors may be able to provide key insight into this issue; Nguyen *et al* (2010) developed such a sensor for *in vivo* monitoring of acetylcholine signaling in the brains of mice. Due to the high frequency chemical stimulation occurring in the brain, it might be an appropriate location to study initially. Another candidate in this context would be the pancreas, since it has been theorized that synchronization of insulin secretion of islets is mediated by periodic release of acetylcholine (Fendler *et al,* 2009). Interestingly, the main receptor mediating insulin secretion is the M3 muscarinic receptor (Gautam *et al,* 2006), and another important protein component in this process is RGS4 (Ruiz de Azua *et al,* 2010), both studied in Chapter III. Therefore, with advances in *in vivo* real-time imaging of cellular signaling, the existence chemically-induced loss of signaling fidelity can be definitely addressed and perhaps even may provide insight into various pathologies, including diabetes.

Simple periodic stimulation patterns were also used in this study to also elucidate mechanisms of calcium signaling. As microfluidic setups become more elaborate in the type of temporal patterns achievable for cellular stimulation, even further elucidation of molecular mechanisms can be attained. In this regard, each type of temporal stimulation pattern can serve as a unique readout of the cellular signaling system, based upon the dynamics of a single imaging probe; by combining this approach with analysis of multiple cellular signaling probes and comparing the results to mathematical models, a very detailed picture of cell signaling architecture can emerge. The recent work by Muzzey et al. (Muzzey *et al*, 2009) provides a glimpse of this concept. The authors analyzed cellular responses to a ramped stimulatory chemical signal, which aided in eliminating putative mathematical models of the pathway studied. Ideally, if the highly diverse stimulation patterns achieved by the setup developed by Olofsson et al. (Olofsson *et al*, 2005) could be combined with the high throughput capabilities of the "flow-encoded" microfluidic setup (King *et al*, 2008), this would result in remarkable progress in the field of signal transduction. In all, use of dynamic stimulation for manipulation and

elucidation of cellular signaling mechanisms is certain to have a tremendous impact upon systems biology, the development of therapeutic drugs, and the rapidly emerging field of synthetic biology (Benner and Sismour, 2005).

V.3 References:

Benner SA, Sismour AM (2005) Synthetic biology. *Nat Rev Genet* **6:** 533-543.

Bennett MR, Hasty J (2009) Microfluidic devices for measuring gene network dynamics in single cells. *Nat Rev Genet* **10:** 628-638.

Berridge MJ, Bootman MD, Roderick HL (2003) Calcium signalling: Dynamics, homeostasis and remodelling. *Nat Rev Mol Cell Biol* **4:** 517-529.

Berridge MJ, Lipp P, Bootman MD (2000) The versatility and universality of calcium signalling. *Nat Rev Mol Cell Biol* **1:** 11-21.

Bohm SK, Grady EF, Bunnett NW (1997) Regulatory mechanisms that modulate signalling by G-protein-coupled receptors. *Biochem J* **322:** 1-18.

Boulware MJ, Marchant JS (2008) Timing in cellular Ca2+ signaling. *Curr Biol* **18:** R769-R776.

Brabant G, Prank K, Schofl C (1992) Pulsatile patterns in hormone-secretion. *Trends Endocrinol Metab* **3:** 183-190.

Felder CC, Bymaster FP, Ward J, DeLapp N (2000) Therapeutic opportunities for muscarinic receptors in the central nervous system. *J Med Chem* **43:** 4333-4353.

Fendler B, Zhang M, Satin L, Bertram R (2009) Synchronization of pancreatic islet oscillations by intrapancreatic ganglia: a modeling study. *Biophys J* **97:** 722-729.

Gautam D, Han SJ, Hamdan FF, Jeon J, Li B, Li JH, Cui YH, Mears D, Lu HY, Deng CX, Heard T, Wess J (2006) A critical role for beta cell M-3 muscarinic acetylcholine receptors in regulating insulin release and blood glucose homeostasis in vivo. *Cell Metabol* **3:** 449-461.

Goldbeter A (2008) Biological rhythms: Clocks for all times. *Curr Biol* **18:** R751-R753.

Guevara MR, Glass L, Shrier A (1981) Phase Locking, Period-Doubling Bifurcations, and Irregular Dynamics in Periodically Stimulated Cardiac-Cells. *Science* **214:** 1350-1353.

King KR, Wang S, Jayaraman A, Yarmush ML, Toner M (2008) Microfluidic flow-encoded switching for parallel control of dynamic cellular microenvironments. *Lab Chip* **8:** 107-116.

Muzzey D, Gomez-Uribe CA, Mettetal JT, van Oudenaarden A (2009) A Systems-Level Analysis of Perfect Adaptation in Yeast Osmoregulation. *Cell* **138:** 160-171.

Neubig RR, Siderovski DR (2002) Regulators of G-protein signalling as new central nervous system drug targets. *Nat Rev Drug Discov* **1:** 187-197.

Nguyen QT, Schroeder LF, Mank M, Muller A, Taylor P, Griesbeck O, Kleinfeld D (2010) An in vivo biosensor for neurotransmitter release and in situ receptor activity. *Nat Neurosci* **13:** 127-132.

Olofsson J, Bridle H, Sinclair J, Granfeldt D, Sahlin E, Orwar O (2005) A chemical waveform synthesizer. *Proc Natl Acad Sci U S A* **102:** 8097-8102.

Ruiz de Azua I, Scarselli M, Rosemond E, Gautam D, Jou W, Gavrilova O, Ebert PJ, Levitt P, Wess J (2010) RGS4 is a negative regulator of insulin release from pancreatic beta-cells in vitro and in vivo. *Proc Natl Acad Sci U S A* **107:** 7999-8004.

Shrier A, Dubarsky H, Rosengarten M, Guevara MR, Nattel S, Glass L (1987) Prediction of Complex Atrioventricular-Conduction Rhythms in Humans with Use of the Atrioventricular Nodal Recovery Curve. *Circulation* **76:** 1196-1205.

Takayanagi H, Kim S, Koga T, Nishina H, Isshiki M, Yoshida H, Saiura A, Isobe M, Yokochi T, Inoue J, Wagner EF, Mak TW, Kodama T, Taniguchi T (2002) Induction and activation of the transcription factor NFATc1 (NFAT2) integrate RANKL signaling in terminal differentiation of osteoclasts. *Dev Cell* **3:** 889-901.

Appendix A

Intracellular calcium signaling models

Rate equations for the Chay et al. model:

$$\frac{d[R]}{dt} = kr * [LR] - hr * (R0 - [LR]) * L$$

$$\frac{d[LR]}{dt} = hr * (R0 - [LR]) * L - kr * [LR]$$

$$\frac{d[G \propto -GTP]}{dt} = kg * ([LR] + basal) * (G0 - [G \propto -GTP] - 4 * [PLC]) - 4 * kp$$
$$* [G \propto -GTP]^4 * (P0 - PLC) - hg * [G \propto -GTP]$$

$$\frac{d[IP3]}{dt} = kd * [PLC] - hd * [IP3] + ld$$

$$\frac{d[Ca2 +]}{dt} = \rho kc * \left(\frac{[IP3]^3}{Ks^3 + [IP3]^3}\right) - \rho hc * [Ca2 +] + \rho lc$$

$$\frac{d[PLC]}{dt} = kp * [G \propto -GTP]^4 * (P0 - PLC) - hp * [PLC]$$

$$kn = knprime * \left(\frac{[IP3]^2}{Kd^2 + [IP3]^2}\right); \quad where\ kn = kp, hp, kd$$

Variables: R = free receptor, L = ligand, LR = ligand receptor complex, Gα-GTP = activated G-protein, PLC = Phospholipase C, IP3 = inositol triphosphate, Ca2+ = intracellular calcium

Parameter	Value	Parameter	Value
hg	0 1/s	^Kg	$3.875*10^{-5}$ 1/(nM*s) (0.035 1/s)
hd	100 1/s	^Basal	129 nM (0.005 1/s)
ld	250 nM/s	G0	200 nM
ρkc	$9*10^4$ nM/s	P0	10 nM
ρhc	1 1/s	°#R0	2000 nM
ρlc	200 nM/s	kdprime	700 1/s
Ks	300 nM	kpprime	$2*10^{-7}$ 1/(nM^4*s)
Kd	25 nM	hpprime	0.5 1/s
#hr	0.004 1/(nM*s)	#kr	0.5 1/s

Table A.2: Parameter Table for the Chay et al. model:

^ signifies that the value was changed from its original value

signifies that the value was not in the original model

° signifies that the value was converted into number/cell

Rate equations for the Politi et al. model:

$$vplc = (Vplc + basal) * \left(\frac{[Ca2 +]^2}{Kplc^2 + [Ca2 +]^2} \right)$$

$$v\,deg = (k5p + k3k * \left(\frac{[Ca2 +]^2}{K3k^2 + [Ca2 +]^2} \right)) * [IP3]$$

$$\frac{d[IP3]}{dt} = vplc - vdeg$$

$$vrel = \left(k1 * \left([IP3r] * \frac{[Ca2 +]}{Ka + [Ca2 +]} * \frac{[IP3]}{Kp + [IP3]} \right)^3 + k2 \right) * ([Ca2 + (ER)]$$
$$- [Ca2 +])$$

$$vserca = Vserca * \left(\frac{[Ca2 +]^2}{Kserca^2 + [Ca2 +]^2} \right)$$

$$vin = v0 + \emptyset * Vplc * (\frac{1}{k3k + k5p})$$

$$vout = Vpm * \left(\frac{[Ca2 +]^2}{Kpm^2 + [Ca2 +]^2} \right)$$

$$\frac{d[Ca2+]}{dt} = vrel - vserca + \varepsilon * (vin - vout)$$

$$\frac{d[Ca2 + (ER)]}{dt} = \left(\frac{1}{\beta} \right) * (vserca - vrel)$$

$$\frac{d[IP3r]}{dt} = \left(\frac{1}{Taur} \right) * (1 - [IP3r] * \frac{Ki + [Ca2 +]}{Ki})$$

Variables: Ca2+ = intracellular calcium, Ca2+(ER) = endoplasmic reticulum calcium, IP3 = inositol triphosphate, IP3r = IP3 receptor

| Parameter	Value	Parameter	Value
K3k	0.4 μM	k3k	0
k5p	0.66 1/s	Kplc	0.2 μM
β	0.185	Vserca	0.9 μM/s
Kserca	0.1 μM	Vpm	0.01 μM/s
Kpm	0.12 μM	v0	0.0004 μM/s
	0.0047 1/s	^ε	5 (0)
Ctot	2 μM	k1	1.11 1/s
k2	0.0203 1/s	Ka	0.08 μM
Ki	0.4 μM	Kp	0.13 μM
Taur	12.5 s	#basal	0.3 μM/s

Table A.2 Parameter Table for the Politi et al. model

^ signifies that the value was changed from its original value in parentheses

signifies that the value was not in the original model

Microfluidic device characteristics
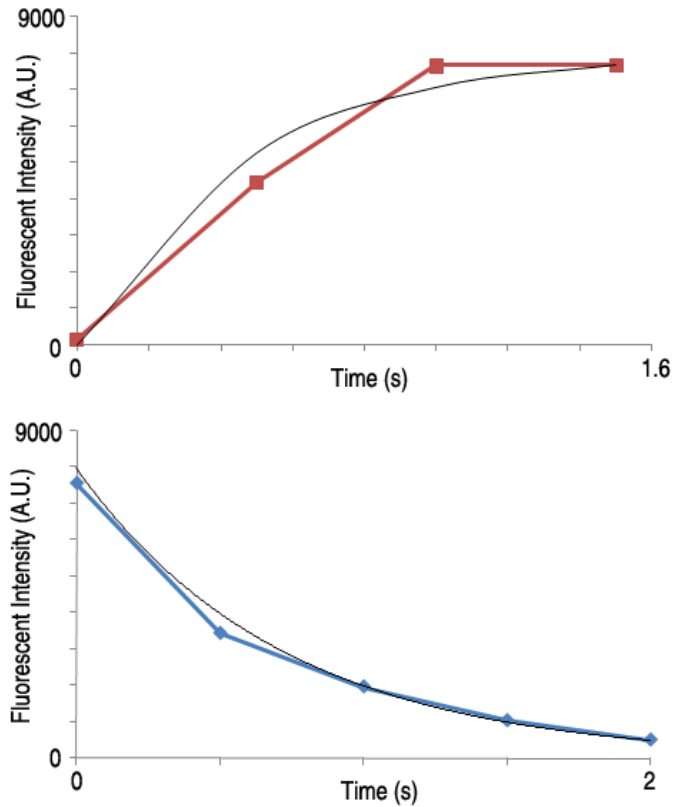
Fig. B.1 Pumping of fluorescein solution (top, red) and washing away of fluorescein solution (bottom, blue), with thin black traces representing fitting with the following equations and the corresponding time constants:

Pumping: $y1 = 8000 * (1 - e^{-2.1t})$; τ (pump) $= 0.48$ s

Washing: $y2 = 8000 * e^{-1.38t}$; τ (wash) $= 0.72$ s

Appendix C

Variability in phase-locking ratios of individual HEK293 cells
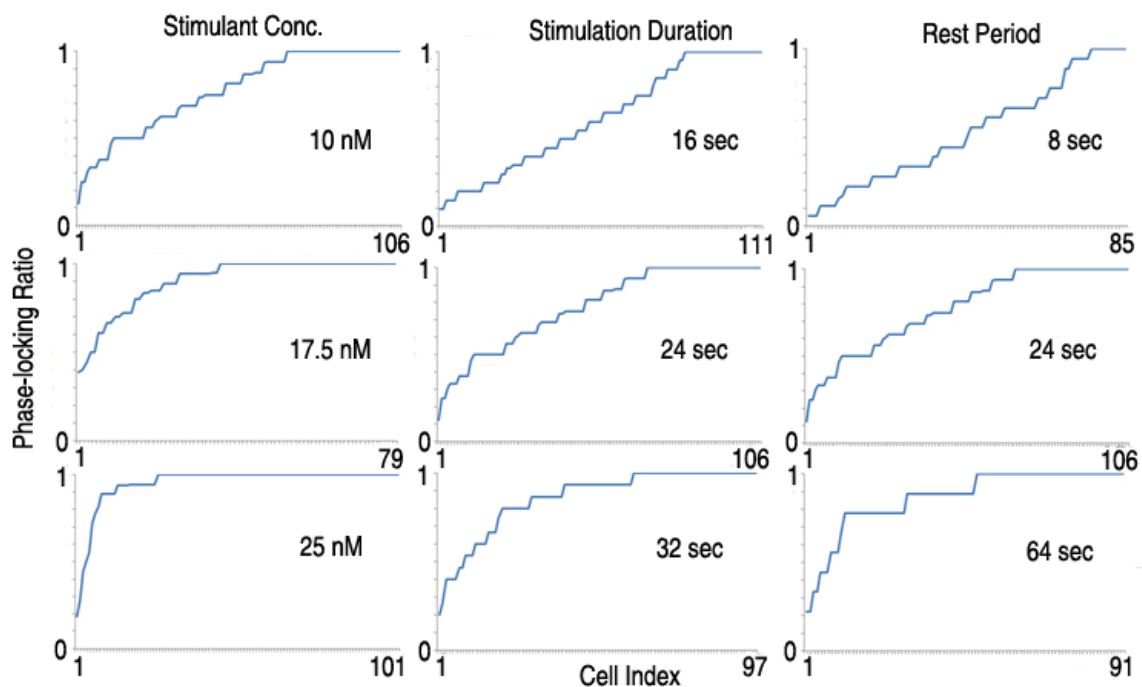
Fig. C.1 Individual cellular phase-locking ratios for each experimental condition tested in Chapter IV. The x-axis represents the cell index and the y-axis represents the phase-locking ratios of each individual cell from a total of three experiments; the periodic stimulation parameter that was varied is listed at the top of each column.